

Diurnal Mountain Wind Systems

Dino Zardi¹ and C. David Whiteman²

¹Atmospheric Physics Group,
Department of Civil and Environmental Engineering
University of Trento,
Trento, Italy

²Atmospheric Sciences Department
University of Utah
Salt Lake City, Utah, USA

Submitted as Chapter 2
in “Mountain weather research and forecasting”
(Chow, F. K., S. F. J. DeWekker, and B. Snyder (Eds.))
Springer, Berlin

June 2012

Corresponding Author:
Dr. Dino Zardi
Atmospheric Physics Group,
Department of Civil and Environmental Engineering
University of Trento
Via Mesiano, 77
Trento, Italy I-38123
E-mail: dino.zardi@ing.unitn.it
Office: +39 0461 28 2682
Cell phone: +39 347 4469 347
Fax: +39 0461 28 2672

Abstract

Diurnal mountain wind systems are local thermally driven wind systems that form over mountainous terrain and are produced by the buoyancy effects associated with the diurnal cycle of heating and cooling of the lower atmospheric layers. This chapter reviews the present scientific understanding of diurnal mountain wind systems, focusing on research findings published since 1988. Slope flows are examined first, as they provide a good introduction to the many factors affecting diurnal mountain wind systems. The energy budgets governing slope flows; the effects of turbulence, slope angle, ambient stability, background flows and slope inhomogeneities on slope flows; and the methods used to simulate slope flows are examined. Then, valley winds are reviewed in a similar manner and the diurnal phases of valley and slope winds and their interactions are summarized. Recent research on large-scale mountain-plain wind systems is reviewed, with an emphasis on the Rocky Mountains and the Alps. Winds occurring in closed basins and over plateaus are then discussed, and analogies between the two wind systems are outlined. This is followed by a discussion of forecasting considerations for diurnal mountain wind systems. Finally, the chapter concludes with a summary of open questions and productive areas for further research.

TABLE OF CONTENTS

1. Introduction

2. The slope wind system

2.1. *Slope flow models*

2.1.1 Reynolds-averaged Navier-Stokes equations

2.1.2 Large-eddy simulation (LES) models

2.1.3 Analytical models

2.1.3.1 Profile models

2.1.3.2 Hydraulic flow models

2.1.4 Laboratory tank models

2.2. *Surface radiative and energy budgets – the driving force for slope flows*

2.2.1 Radiative flux divergence, $\nabla \cdot R$

2.2.2 Turbulent sensible heat fluxes and their divergence, $\nabla \cdot H$

2.3. *Role of turbulence in slope flows*

2.4. *Upslope flows*

2.5. *Downslope flows*

2.5.1 Impact of slope angle on downslope flows

2.5.2 Impact of ambient stability on downslope flows

2.5.3 Impact of background flow on downslope flows

2.5.4 The effects of slope inhomogeneity on downslope flows

2.5.5 Drainage flow oscillations

2.5.6 Glacier winds

3. The valley wind system

3.1 *The effects of boundary layer processes and turbulence on valley flows*

3.2. *The effects of other winds on valley flows*

3.3. *Topographic effects on valley flows*

3.3.1 Tributary valleys

3.3.2 Canyons

3.4. *Modeling of the valley flows*

3.5. *Exceptions and anomalies*

4. Phases of and interactions between the slope and valley winds

4.1 *Daytime phase*

4.2 *Evening transition phase*

4.3 *Nighttime phase*

4.4. *Morning transition phase*

5. The mountain-plain wind system

5.1. *Mountain-plain winds in the Alps*

5.2. *Mountain-plain winds in the Rocky Mountains*

6. Diurnal wind systems in basins and over plateaus

6.1 *Diurnal wind systems in basins*

6.1.1 The diurnal cycle in basins

6.1.2 Persistent wintertime inversions in basins

6.2 *Diurnal wind systems over plateaus*

7. Forecasting

8. Past progress, future objectives

Acknowledgments

References

Tables

Figure captions

Figures

1. Introduction

Diurnal mountain winds develop, typically under fair weather conditions, over complex topography of all scales, from small hills to large mountain massifs, and are characterized by a reversal of wind direction twice per day. As a rule, *upslope*, *up-valley* and *plain-to-mountain* flows occur during daytime and *downslope*, *down-valley* and *mountain-to-plain* flows occur during nighttime.

Because diurnal mountain winds are produced by heating of atmospheric layers during daytime and cooling during nighttime, they are also called *thermally driven winds*. Horizontal temperature differences develop daily in complex terrain when cold or warm boundary layers form immediately above sloping surfaces. Air at a given point in the sloping boundary layer is colder or warmer than the air just outside the boundary layer at the same elevation. These temperature differences result in pressure differences and thus winds that blow from areas with lower temperatures and higher pressures toward areas with higher temperatures and lower pressures. The boundary layer flows and *return*, or *compensation*, flows higher in the atmosphere form closed circulations.

The atmosphere above and around a mountain massif is composed of three distinct regions or sloping layers in which the thermal structure undergoes diurnal variations and in which diurnal winds develop: the slope atmosphere, the valley atmosphere and the mountain atmosphere (Ekhardt 1948; **Fig. 1**). The slope atmosphere is the domain of the slope flows, the valley atmosphere is the domain of the valley flows and the mountain atmosphere is the domain of the mountain-plain flows. It is difficult to observe any one component of the diurnal mountain wind system in its pure form, because each interacts with the others and each can be affected by larger scale flows aloft.

Indeed well-organized thermally driven flows can be identified over a broad spectrum of spatial scales, ranging from the dimension of the largest mountain chains to the smallest local landforms, such as, for instance, “farm-scale” topographic features (Dixit and Chen 2011; Bodine et al. 2009). All of these flows are induced by local factors, and in particular by the combination of landforms and surface energy budgets, under synoptic scale situations allowing for their development, and eventually conditioning them “top-down” by acting as boundary conditions. On the other hand the same flows may in turn affect large-scale phenomena. This is the case, for instance, of diurnal flows over sloping terrain forcing the Great Plains low-level jet (cf. Holton 1966; Parish and Oolman 2010) and of some organized convective systems triggered by thermally induced flows in the southern part of the Himalayas (Egger 1987; Yang et al. 2004; Bhatt and Nakamura 2006; Liu et al. 2009).

The regular evolution of the diurnal mountain wind systems exhibits four phases that are closely connected to the formation and dissipation of temperature inversions. The nighttime phase, characterized by the presence of a ground-based temperature inversion, or stable layer, and winds flowing down the terrain, is followed by a morning transition phase in which the inversion is destroyed and the winds undergo a reversal to the daytime winds flowing up the terrain. The evening transition phase completes the cycle as the inversion rebuilds and the winds once again reverse to the nighttime direction.

Diurnal mountain winds are a key feature of the climatology of mountainous regions (Whiteman 1990, 2000; Sturman et al. 1999). In fact, they are so consistent that they often appear prominently in long-term climatic averages (Martínez et al. 2008). They are particularly prevalent in anticyclonic synoptic weather conditions where background winds are weak and skies are clear, allowing maximum incoming solar radiation during daytime and maximum outgoing longwave emission from the ground during nighttime. Diurnal wind systems are usually better developed in summer than in winter, because of the stronger day-night heating contrasts. The local wind field patterns and their timing are usually quite similar from day to day under anticyclonic weather conditions (see, e.g., Guardans and Palomino 1995). The characteristic diurnal reversal of the slope, valley, and mountain-plain wind systems is also seen under partly cloudy or wind-disturbed conditions, though it is sometimes weakened by the reduced energy input or modified by winds aloft.

The speed, depth, duration and onset times of diurnal wind systems vary from place to place, depending on many factors including terrain characteristics, ground cover, soil moisture, exposure to insolation, local shading and surface energy budget (Zängl 2004). Many of these factors have a strong seasonal dependence. Indeed, the amplitude of horizontal pressure gradients driving valley winds displays appreciable seasonal variations (see e.g. Cogliati and Mazzeo 2005).

The scientific study of diurnal mountain winds has important practical applications, ranging from operational weather forecasting in the mountains, to the climatological characterization of mountain areas (e. g. for agricultural purposes), to the impact assessments of proposed new settlements or infrastructures. Indeed diurnal winds affect the distribution of air temperature in complex terrain (Lindkvist and Lindkvist 1997; Gustavsson et al. 1998; Lindkvist et al. 2000; Mahrt 2006), the transport and diffusion of smoke and other air pollutants, the formation and dissipation of fogs (Cuxart and Jiménez 2011) and low clouds, frost damage in vineyards and orchards, surface transportation safety from risks due to frost and fog, flight assistance (e. g. through the issuance of Terminal Aerodrome Forecasts and the evaluation of flying conditions for soaring or motorized flights), long-term weathering of structures, and the behavior of wildland and prescribed fires.

Diurnal mountain winds have been studied scientifically since the 19th century. Wagner (1938) laid the foundation for our current understanding of diurnal mountain wind systems. He provided a systematic overview and synthesis of the findings from field measurements and theoretical investigations gained at that time. Indeed much of the early research was published in German or French. This is evident in the first comprehensive English-language review of early research provided by Hawkes (1947). Whiteman and Dreiseitl (1984) published English translations of seminal papers by Wagner, Ekhardt and F. Defant. Additional reviews of research on diurnal mountain wind systems include those of Defant (1951), Vergeiner and Dreiseitl (1987), Whiteman (1990), Egger (1990), Simpson (1999), and Poulos and Zhong (2008). Additionally, chapters on diurnal mountain wind systems are available in textbooks by Yoshino (1975), Atkinson (1981), Stull (1988), Whiteman (2000), Barry (2008), and Geiger et al. (2009).

A fundamental obstacle to rapid progress in mountain meteorology is that there are almost infinitely many possible terrain configurations. So, any field measurement or numerical experiment that is valid for a specific situation does not automatically have greater significance beyond that case. Nonetheless, significant progress has been achieved by gathering real cases into groups according to similar landforms, and generalizing results from these groups with respect to the inherent important physical processes or mechanisms. The organization of this chapter benefits from this approach, with a special section on basin and plateau circulations. Another useful approach has been to focus conceptual or numerical simulations on simple or idealized topographies to investigate the essential meteorological processes. Other obstacles to progress should also be mentioned. Because most studies of diurnal mountain wind systems have been conducted on fine weather days with weak synoptic forcing, relatively little is known about other conditions. Further, the effects of forest canopies and other types of varying and patchy surface cover on diurnal wind systems have been largely neglected in much of the experimental and modeling work to date. Finally, while diurnal mountain wind systems are thought to be complete or closed circulations, little experimental evidence has been accumulated on the difficult-to-measure 'return' or upper-branch circulations.

This review aims to provide information on the basic physics of diurnal mountain wind systems and to summarize new research findings since the American Meteorological Society's 1988 workshop on mountain meteorology, as later published in an AMS monograph (Blumen 1990). Priority in the referenced material is given to peer-reviewed papers published in English since 1988. Other chapters in the present monograph also deal peripherally with diurnal mountain wind systems. **Chapters 3 and 4** discuss the effects on valley winds of dynamically induced channeling from larger scale flows. **Chapter 5** treats atmospheric boundary layer phenomena in mountain areas that affect pollutant transport. **Chapters 6 and 7** deal with orographic precipitation, including triggering from thermally forced flows. **Chapter 8** treats observational resources and strategies for mountain atmosphere processes, including diurnal mountain winds. **Chapters 9, 10, and 11** discuss numerical model simulations and operational weather forecasting.

2. The slope wind system

The slope wind system is a diurnal thermally driven wind system that blows up or down the slopes of a valley sidewall or an isolated hill or mountain, with upslope flows during daytime and downslope flows during nighttime. The up- and downslope flows are the lower branch of a closed circulation produced by inclined cold or warm boundary layers that form above the slopes. During daytime, the heated air in the boundary layer above a slope rises up the slope while continuing to gain heat from the underlying surface. During nighttime, air in the cooled boundary layer flows down the slope while continuing to lose heat to the underlying surface. Upslope and downslope winds are alternatively called *anabatic* and *katabatic* winds, respectively. These terms, however, are also used more comprehensively to refer to any flows that run up or down the terrain. Further, the term katabatic is typically used to describe the large-scale slope flows on the

ice domes of Antarctica and Greenland. The term *drainage wind* may be used to refer collectively to downslope and down-valley winds, and may also include mountain-to-plain flows. To reduce confusion, we will use the terms upslope and downslope, and will omit from consideration the flows over extensive ice surfaces which, in contrast to the smaller-scale mid-latitude flows discussed here, are affected by Coriolis forces (see, e.g., Kavčič and Grisogono 2007; Shapiro and Fedorovich 2008). An example of typical nighttime and daytime wind and temperature profiles through the slope flow layer is given in **Fig. 2**. The biggest daytime temperature excesses and nighttime temperature deficits occur near the ground, where radiative processes heat and cool the surface. It is here that the buoyancy forces that drive the slope flows are strongest. The wind profiles, however, have their peak speeds above the surface, since surface friction causes the speeds to decrease to zero at the ground. This gives both the daytime and nighttime wind speed profiles their characteristic jet-like shape in which the peak wind speed occurs above the surface.

Typical characteristics of the equilibrium steady-state wind and temperature profiles for mid-latitude downslope winds (**Fig. 2a**) include the strength (3 to 7°C) and depth (1 to 20 m) of the temperature deficit layer, the maximum wind speed (1 to 4 m s⁻¹), its height above ground (1 to 15 m), and the depth of the downslope flow layer (3 to 100 m). Downslope flows on uniform slopes often increase in both depth and strength with distance down the slope. A useful guideline for field studies is that the depth of the temperature deficit layer at a point on a slope is about 5% of the vertical drop from the top of the slope (Horst and Doran 1986). Characteristic values for upslope flows (**Fig. 2b**) include the strength (2 to 7°C) and depth (10 to 100 m) of the temperature excess layer, the maximum wind speed (1 to 5 m s⁻¹), its height above ground (10 to 50 m), and the depth of the upslope flow layer (20 to 200 m). Upslope flows on uniform slopes often increase in both depth and speed with distance up the slope.

Not covered in this review are mid-latitude ‘skin flows’ (Manins and Sawford 1979a) – shallow (< 1 or 2 m), weak (perhaps < 1 m s⁻¹), non-turbulent katabatic flows that have been reported by several investigators (Thompson 1986; Manins 1992; Mahrt et al. 2001; Soler et al. 2002; Clements et al. 2003). These have not yet been studied systematically.

Our discussion of slope flows begins with a simplified set of Reynolds-averaged Navier-Stokes (RANS) equations to guide understanding. Then different approaches to modeling slope flows are discussed and the state of scientific knowledge on upslope and downslope flows, as supported by both field and modeling investigations, are summarized.

2.1 Slope flow models

2.1.1 Reynolds-averaged Navier-Stokes equations

A reduced set of RANS equations can be used heuristically to gain an understanding of the key physics of slope flows. This is conveniently done using a coordinate system that is oriented along (s) and perpendicular (n) to an infinitely extended slope of uniform inclination angle α . n is perpendicular to the slope and increases upwards; s is parallel to the slope and increases in the downslope direction. Slope flows result from the cooling or heating of an air layer over the slope relative to air at the same elevation away from the slope. The potential temperature profile over the slope is expressed as

$$\theta = \theta_0 + \gamma z + d(s, n, t) \quad (1)$$

where θ_0 is a reference value for the potential temperature at the ground in the absence of surface cooling or heating, γ is the ambient vertical gradient of potential temperature, z is the vertical coordinate ($z = n \cos \alpha - s \sin \alpha$), and d is the potential temperature perturbation in the vicinity of the slope, negative when the air is colder than in the unperturbed state. The along-slope and slope perpendicular equations of motion, the thermodynamic energy equation, and the continuity equation are then written as

$$\frac{\partial u}{\partial t} + u \frac{\partial u}{\partial s} + w \frac{\partial u}{\partial n} = - \frac{1}{\rho_0} \frac{\partial (p - p_a)}{\partial s} - g \frac{d}{\theta_0} \sin \alpha - \frac{\partial \overline{u'w'}}{\partial n} \quad (2)$$

$$\frac{\partial w}{\partial t} + u \frac{\partial w}{\partial s} + w \frac{\partial w}{\partial n} = -\frac{1}{\rho_0} \frac{\partial(p - p_a)}{\partial n} + g \frac{d}{\theta_0} \cos \alpha \quad (3)$$

$$\frac{\partial \theta}{\partial t} + u \frac{\partial \theta}{\partial s} + w \frac{\partial \theta}{\partial n} = -\frac{1}{\rho_0 c_p} \frac{\partial R}{\partial n} - \frac{\overline{w' \theta'}}{\partial n} \quad (4)$$

and

$$\frac{\partial u}{\partial s} + \frac{\partial w}{\partial n} = 0 \quad (5)$$

where u and w are the velocity components parallel to s and n , respectively. These equations, from Horst and Doran (1986), were derived by Manins and Sawford (1979b) using the Boussinesq approximation. They considered the flow to be 2-dimensional, with wind and temperature independent of the cross-slope direction, with the ambient air at rest, and with negligible Coriolis force. ρ_0 is a reference value of density in the absence of surface cooling, g is the gravitational acceleration, c_p is the specific heat of air at constant pressure, R is the upward radiative flux, and $\overline{u'w'}$ and $\overline{w'\theta'}$ are the kinematic turbulent Reynolds fluxes of momentum and heat. Note that, consistent with the assumption of a shallow layer, this set of reduced equations includes only the slope-normal turbulent fluxes in (2) and (4); other turbulent fluxes are ignored. For simplicity, latent heat fluxes are not included here, although they can sometimes play a crucial role in the overall energy budgets. The ambient pressure p_a is determined from hydrostatic balance $\partial p_a / \partial z = -\rho_a g$, and, through the ideal gas law and the definition of potential temperature, is a function of the ambient potential temperature distribution $\theta_a = \theta_0 + \gamma z$. Accelerations normal to the slope are generally considered negligible so that the atmosphere normal to the slope is in quasi-hydrostatic balance and the RHS of (3) is practically zero. The coordinate system rotation needed to get to this set of equations can lead to interpretation errors if not done properly, as explained by Haiden (2003). Mahrt (1982) provided further details on the coordinate system and an overview of the classification of gravity flows in terms of the relative magnitudes of the individual terms of the along-slope momentum equation (2).

This system of equations can be solved numerically after the turbulent fluxes are parameterized in terms of mean flow variables. The parameterization of the momentum flux normal to the slope is usually expressed in terms of the wind shear and turbulence length and velocity scales. This type of parameterization was originally developed using knowledge of turbulence profiles over flat ground in flows that were driven by large-scale pressure gradients that changed little with height outside the surface layer. In contrast, slope flows are shallow flows in which the largest forcing is at the ground. The suitability of such parameterizations is thus called into question (Grisogono et al. 2007).

It is instructive to consider which terms in these equations are most important for understanding slope flow physics. The key term that drives slope flows is the buoyancy force caused by the temperature excess or deficit that forms over the slope (second term on the right hand side of (2)). The temperature excess or deficit itself is produced by radiative and sensible heat flux convergences or divergences (the first and second terms on the RHS of (4)) that warm or heat a layer of air above the slope. Considering the along-slope momentum equation (2) for the downslope flow situation, a steady state flow may be retarded by advection of slower moving air into the flow (two advection terms on the LHS), by the thickening or cooling of the layer with downslope distance which causes an adverse pressure gradient (first term on the RHS, see Princevac et al. 2008), and by the divergence of turbulent momentum flux (last term on the RHS).

Mesoscale numerical models that use the full set of RANS equations (see Chapter 4) have been used to simulate a variety of meteorological phenomena. These models, where turbulence is parameterized with closure assumptions, have been applied to complex terrain and have proven very useful in gaining an understanding of diurnal mountain wind systems (see, e.g., Luhar and Rao 1993; Denby 1999). Extensive experience with mesoscale models of this type, however, has shown that shallow slope flows cannot be

resolved adequately in a mesoscale setting for which the turbulence parameterizations are most appropriate. Simulated downslope flows are often too deep and strong, temperature deficits over the slope are too deep and weak, and it has been a challenge to get both the wind and temperature fields to agree with observations (see Chapter 10). In instances where the wind and temperature fields are in rough agreement with observations, these models have been used to investigate the relative roles of individual terms in the momentum and heat budget equations. Comparisons of slope flow simulations with multiple mesoscale models have provided valuable information on the effects of different parameterizations, resolutions, coordinate systems, and boundary conditions on model outputs. Zhong and Fast (2003) compared simulations of flows in Utah's Salt Lake Valley using the RAMS, MM5 and Meso-Eta models and compared the simulations to slope flow data. Forecast errors with these models were surprisingly similar, despite different coordinate systems, numerical algorithms and physical parameterizations. The models exhibited a cold bias, with weaker than observed inversion strengths, especially near the surface. All models successfully simulated the diurnally reversing slope flows but there were significant discrepancies in depths and strengths of wind circulations and temperature structure. Surprisingly, it is only recently that mesoscale numerical models have added parameterizations of slope shadowing from surrounding topography (Colette et al. 2003; Hauge and Hole 2003).

2.1.2 Large-eddy simulation (LES) models

Large-eddy simulation (LES) of turbulent flows is a numerical alternative to the RANS equations. It builds on the observation that most of the turbulence energy is contained in the largest eddies which, as they break down, cascade their energy into the smaller isotropic turbulent eddies where energy is dissipated. Accordingly, the LES approach explicitly resolves the larger energy-containing eddies and uses turbulence theory to parameterize the effects on the turbulent flow of the smallest scale eddies in the inertial sub-range of atmospheric motions. Because energy-containing eddies are much smaller in size in stable boundary layers than in convective boundary layers, the first LES simulations for inclined slopes were made for upslope flows (Schumann 1990). A more detailed account on these findings will be given in section 2.4 below. LES simulations of downslope flows in the stable boundary layer, with its much smaller turbulence length scales, requires finer grids and more extensive computational resources. Thus, numerical simulations of downslope flows have only recently become possible on highly idealized slopes with recent increases in computer power (Skylingstad 2003; Axelsen and van Dop 2008, 2009). Research in this area looks very promising, but is still at an early stage. Some applications of LES in complex terrain are provided in Chapter 10.

2.1.3 Analytical models

Useful slope flow models can sometimes be developed by further simplifying the reduced set of RANS equations (1) through (5), retaining only the key terms, and solving the simplified set analytically. Such analytical models are of two types – *profile* and *hydraulic flow* models.

2.1.3.1 Profile models

Profile models consider local equilibria in the buoyancy and momentum equations and obtain analytical solutions for equilibrium vertical profiles of velocity and temperature in the slope flow layer by neglecting or simplifying some of the terms in the equations. The classical Prandtl (1942) model is an equilibrium gravity flow solution in which constant eddy diffusivities are used for the friction term and a simple thermodynamic relationship balances the diffusion of heat with the temperature advection associated with the basic state stratification. The Prandtl model agreed qualitatively with observations of both upslope and downslope flows, successfully producing the typical jet-like wind profiles and temperature deficit profiles seen in slope flows (**Fig. 3**). Prandtl's model was modified by Grisogono and Oerlemans (2001a, b) to allow eddy diffusivities to vary with height, improving its agreement with observations. Extension of Prandtl's (1942) approach to reproduce nonstationary flows was accomplished by Defant (1949) and Grisogono (2003). Other investigators have developed alternative models of slope flows by finding analytical solutions to reduced sets of equations (Zammett and Fowler 2007; Shapiro and Fedorovich 2009; see also in Barry 2008).

2.1.3.2 Hydraulic flow models

Hydraulic models start from the RANS equations, average the terms over the slope flow depth and treat the drainage flow as a single layer interacting with an overlying stationary fluid. They focus on layer-averaged

quantities such as mass and momentum fluxes and can be used to determine how bulk quantities vary with distance up or down the slope. Manins and Sawford (1979a, b), Brehm (1986), and Horst and Doran (1986) were early developers of this approach for slope flows. They, Papadopoulos et al. (1997), Papadopoulos and Helmis (1999), Haiden and Whiteman (2005) and Martinez and Cuxart (2009) have used observations from lines of instrumented towers or tethersondes running down a slope, or the output of numerical model simulations, to estimate the magnitudes of the different terms in the hydraulic flow equations.

2.1.4 Laboratory tank models

Laboratory water tanks have been used to investigate both up- and downslope flows on sloping surfaces in basins containing stratified fluid. A bottom-heated, salt-stratified water tank over a slope with adjacent plain and plateau was used by Reuten et al. (2007) and Reuten (2008) to investigate layering, venting and trapping of pollutants that are carried in upslope flows. Conditions conducive to trapping include weak large-scale flows, strong sensible heat flux, weak stratification, a short or no plateau, symmetric geometry, a low ridge, and inhomogeneities in surface heat flux. Reuten et al. (2007) speculate that inhomogeneities in slope angle and surface roughness can also produce trapping. In a similar laboratory experiment by Princevac and Fernando (2008), but this time with a V-shaped tank containing thermally stratified water that was heated uniformly on the sloping surfaces, upslope flows were found to leave the sidewalls under certain conditions, intruding horizontally into the stratified fluid over the valley center.

Upslope winds flow up the slope as a bent-over plume rather than rising vertically, even in a neutral environment. These flows become turbulent when the heat flux becomes large enough. Laboratory simulations by Princevac and Fernando (2007) show that, for a certain range of Prandtl numbers¹, there is a minimum slope angle above which upslope flows can be sustained. For average atmospheric conditions the critical angle is only 0.1°. Princevac and Fernando (2007) used this result to explain Hunt et al.'s (2003) observations of a dominant upslope flow on a 0.18° slope in the Phoenix valley.

Downslope flows into a stratified environment have been studied in laboratory tanks, as well, by introducing a continuous source of negatively buoyant fluid at the top of a constant-angle slope (Baines 2001). In this case, the flow maintains a uniform thickness, with a distinct boundary at its top, until it approaches its level of neutral buoyancy, where it leaves the slope. Turbulent transfers of mass and momentum occur across the interface, causing a continuous loss of fluid (detrainment) from the downslope flow. Flows of negatively buoyant fluid over steep slopes, on the other hand, are in the form of entraining plumes (Baines 2005). It should be mentioned that realistic downslope flows over valley sidewalls are not produced by a continuous source of negatively buoyant fluid at the top of the slope. Rather, they must lose heat continuously to the underlying surface to maintain their negative buoyancy. Nonetheless, this laboratory tank analog provides important information on interactions that occur at the top of the downslope flow layer.

2.2 Surface radiative and energy budgets – the driving force for slope flows

Thermally driven winds in complex terrain are produced by the formation of inclined layers of temperature excess or deficit (relative to the ambient environment) along terrain slopes of different scale. It is thus of paramount importance to understand the physical processes that produce temperature changes above slopes. The key principle is that of energy conservation, which relates local changes in potential air temperature at any point to the budget of heat fluxes at that point. The potential temperature tendency equation, neglecting thermal conduction and latent heat release, can be written as

$$\frac{\partial}{\partial t}(\rho c_p \theta) = -\nabla \cdot \mathbf{A} - \nabla \cdot \mathbf{H} - \frac{\theta}{T} \nabla \cdot \mathbf{R} \quad (6)$$

where $\mathbf{A} = \rho c_p \mathbf{u} \theta$ is the sensible heat flux associated with local advection of warmer or colder air by the mean three-dimensional wind velocity \mathbf{u} , $\mathbf{H} = \rho c_p \overline{\mathbf{u}' \theta'}$ is the turbulent sensible heat flux produced by the coupling between turbulent fluctuations of wind velocity and potential temperature, \mathbf{R} is the radiative heat

¹ The Prandtl number Pr is a nondimensional number defined, for any fluid, as the ratio of the kinematic viscosity ν to the thermal diffusivity κ , i. e. $Pr = \nu/\kappa$. As an extension, for turbulent flows the turbulent Prandtl number Pr_t is defined as the ratio of the eddy viscosity K_m to the eddy heat diffusivity K_h : $Pr_t = K_m/K_h$. Both of these numbers provide, for laminar and turbulent flows respectively, an estimate of the relative importance of convection vs. diffusion in heat transfer processes involved with the flow.

flux (including both the shortwave and longwave spectra). In the absence of mean wind, as for instance over flat terrain under anticyclonic synoptic-scale conditions, the mean advection term \mathbf{A} is negligible. In contrast, over complex terrain identical weather conditions produce thermally driven flows, and thus the advection term is usually a relevant one. While latent heat release is not included in (6), it may be very important over vegetated areas and in mountainous regions adjacent to large water bodies, and even in some arid environments where condensation of moisture advected from elsewhere produces dew or fog (cf. Khodayar et al. 2008). Also not considered explicitly in (6) is local heat storage in forest canopies and other materials. During the course of a day all of the terms in (6) undergo changes with time, and display strongly varying distributions in space.

Slope flows, the smallest-scale diurnal wind system, respond rapidly to temporal and spatial variations in sensible heat fluxes caused by variations in the surface energy budget. The surface energy budget is affected by changes in net radiation, ground heat flux, soil moisture and its influence on the partitioning of energy between sensible and latent heat fluxes, by changes in surface cover or vegetation, cloud cover (Ye et al. 1989), break-in of background winds or turbulent episodes, advection, etc. Surface radiation and energy budget principles, measurements in mountain valleys, and examples of spatial variations across sample topographies have been discussed by Whiteman (1990), Matzinger et al. (2003) and Oncley et al. (2007).

Radiative and turbulent sensible heat flux divergences (convergences) cool (heat) a layer of air above a slope (see Eq. 4), creating a buoyancy force that has an along-slope gravitational component (Eq. 2) that is the basic driving force for downslope (upslope) flows. In this section we will consider topographic effects on radiative and sensible heat flux divergences, a topic that has received increasing attention in the last 20 years.

2.2.1 Radiative flux divergence, $\nabla \cdot R$

Radiative flux divergence contributes significantly to the cooling of clear air in the nocturnal boundary layer over flat terrain (Garratt and Brost 1981; André and Mahrt 1982; Ha and Mahrt 2003) and can be expected to play an important role in producing the cooling over sloping surfaces that drives downslope flows. Despite this expectation, slope flow models are generally driven by assumed or measured rates of surface sensible heat flux or prescribed surface temperatures, with radiative flux divergence in the atmosphere above the slope assumed negligible. While no direct measurements of radiative flux divergence have yet been made over slopes, simple radiative transfer (RT) models (e.g., Manins 1992) suggest that radiative flux divergence cannot be neglected as a source of cooling or heating of the slope boundary layer.

Because of recent improvements in RT models and increases in computer speeds, it is now possible to treat both long- and shortwave RT in a realistic way for complex terrain areas for clear sky conditions using Monte Carlo simulations (Mayer 2009). Monte Carlo RT models track the paths of individual photons, accounting in a stochastic way for emission, scattering, reflection and absorption interactions between photons and air molecules, aerosols and ground surfaces. The simulations, which often involve the tracking of millions of individual photons, can be accomplished for situations where required input data are available, including a digital terrain model, vertical atmospheric profiles of temperature, radiatively active gases (e.g. water vapor and carbon dioxide) and aerosols, and spatially resolved albedos and surface radiating temperatures. Improvements in complex terrain RT modeling will come from the further development of these models to handle key 3-dimensional aspects of complex terrain atmospheres including the existence of shallow cold and warm air layers on the slopes. Monte Carlo models can, in principle, be used to simulate not only radiative fluxes (see, e.g., Chen et al. 2006) but also radiative flux divergences, even over shallow slope layers. In the future, such simulations can perhaps be tested against measurements and used to develop better parameterizations for simpler models.

The MYSTIC Monte Carlo RT model (Mayer and Kylling 2005) has recently been applied to the complex terrain of Arizona's Meteor Crater and successfully evaluated against longwave and shortwave irradiance measurements made on slope-parallel broadband radiometers on the floor, sidewalls and rim of the crater on one October day (Mayer et al. 2010). **Figure 4** shows Monte Carlo simulations of direct and diffuse irradiance at noon over the entire crater domain for the same day. Following this successful evaluation of the model performance, further simulations were performed to determine the cooling rates caused by radiative flux divergence in idealized valley and basin atmospheres and in a realistic simulation of the Meteor Crater (Hoch et al. 2011). In this parameteric study the radiative flux divergence-induced cooling rates for different temperature profiles representative of different times of day were compared to those over

flat terrain for valleys and basins of different widths. Longwave radiative cooling in topographic depressions is generally weaker than over flat terrain because of the counter-radiation from surrounding terrain, but strong temperature gradients near the surface associated with nighttime inversions and temperature deficit layers over slopes significantly increase longwave cooling rates. The effects of the near-surface temperature gradients extend tens of meters into the overlying atmosphere and can produce cooling rates on the order of 30 K day^{-1} that play an important role in the in-situ cooling which produces and maintains drainage flows. Hoch et al. (2011) attributed nearly 30% of the total nighttime cooling observed in the Meteor Crater on a calm October night to radiative flux divergence. They approximated near-slope temperature gradients by specifying the ground radiating temperature and the air temperature at the first model level at 5 m. Since model results for flat terrain show that radiative flux divergence depends strongly on the detailed air temperature profile in the lowest meters above a surface (Räsänen 1996), it will be important in future RT work to gain better resolution of slope temperature structure profiles.

2.2.2 Turbulent sensible heat fluxes and their divergence, $\nabla \cdot H$

Several field experiments (e.g., Manins and Sawford 1979a; Horst and Doran 1988; Doran et al. 1989, 1990) have measured turbulent sensible heat fluxes at multiple heights on slope towers, but vertical gradients of these fluxes (i.e., the vertical divergence of sensible heat fluxes) have generally not been reported because of concerns regarding accuracy, with radiative flux divergence being the small difference between two large quantities. An accurate measurement of the total divergence through the slope flow layer would require a measurement very close to the surface and a measurement at the top of the slope flow layer. Both measurements are problematic: the upper measurement would have to be at the top of the slope flow - which depends on background weather conditions, varies with time during the day, and is not easily detected - and the lower measurement would suffer from underreporting of fluxes caused by instrumental errors associated with near-ground eddies being smaller than the sonic anemometer sampling volume (Kaimal and Finnigan 1994). Moreover, many slopes are inhomogeneous, covered with patches of forest, bushes, rocks, or uneven ground making it difficult to find representative measurement sites (Van Gorsel et al. 2003a). Further requirements regarding the appropriate coordinate system for the measurements, the representativeness of the measurement location in terms of the homogeneity of the surface flux in the upwind direction (i.e., flux footprint), and the post-processing of turbulence data collected over sloping surfaces make turbulence measurements in slope flows prone to errors. The reader will find further detailed discussions on these issues in papers by Andretta et al. (2002), de Franceschi and Zardi (2003), Hiller et al. (2008) and de Franceschi et al. (2009).

A surprising finding from evidence that has accumulated since the mid 1990's is that significant inaccuracies are occurring with the measurement of surface heat fluxes with existing research equipment. When individual terms of the surface energy budget (see Eqn. (7) below) are measured independently, an imbalance is often found. This finding comes primarily from field experiments over flat, homogeneous terrain in a variety of climate settings (see e.g., Oncley et al. 2007). The surface energy budget imbalance during daytime is characterized by a sum of ground, sensible and latent heat fluxes that is too small to balance the measured net radiation, undershooting this value by 10-40%. Imbalances have also been found during nighttime, again with the sum of the ground, sensible and latent heat flux terms being smaller than the nighttime longwave loss. Since the Law of Conservation of Energy must be satisfied, this suggests that experimental errors are the culprit. In complex terrain, additional sources of error may arise because of the neglect of budget terms under assumptions of shallow flows and horizontal homogeneity. Ground heat flux is often poorly measured, but is expected to be relatively small and thus incapable of explaining the error magnitude. Net radiation, on the other hand, is relatively well measured, especially when individual components of net radiation are measured with high-quality broadband radiometers. This suggests that the turbulent heat fluxes are being underestimated, and attention has been focused on advective effects, the differing flux footprints at different measurement heights, and unmeasured flux convergences/divergences below the typical 5- to 10-m eddy correlation measurement heights. Recent complex terrain research programs have also encountered these measurement problems (e.g., Rotach et al. 2008).

Because sensible heat flux divergence measurements are unavailable over slopes, most slope flow models have been driven by an assumed value of surface sensible heat flux. Most models additionally assume that sensible heat flux is constant along a slope, a useful approximation for a uniform slope on an isolated mountainside, but questionable on valley sidewalls. For simple surfaces with uniform surface cover, the surface heat flux Q_H can be expressed in terms of the surface energy and radiation budgets as follows

$$Q_H = \rho c_p \overline{w' \theta'_s} = -(S + D + K \uparrow + L \downarrow + L \uparrow + Q_G + Q_E) \quad (7)$$

where S is the incoming direct radiation, D is the incoming diffuse radiation, $K \uparrow$ is the reflected shortwave radiation, $L \downarrow$ is the incoming longwave radiation, $L \uparrow$ is the outgoing longwave radiation, Q_G is the ground heat flux, and Q_E is the latent heat flux. The individual terms represent the transfer of energy per unit time through a sloping unit surface area, as measured in W m^{-2} . In this equation, the sign convention is that fluxes toward the surface are considered positive and fluxes away from the surface are considered negative. Eq. (7) illustrates the large number of processes on which sensible heat flux depends.

During daytime, in complex, three-dimensional valley topography, the time varying sensible heat flux is driven primarily by the input of direct radiation on a slope (S in (7)). This input depends on the path of the sun's movement through the sky, on the azimuth and inclination angles of the slopes, the surface albedo (Pielke et al. 1993), the physical and vegetative properties of the surface, and especially near sunrise and sunset, on whether shadows are cast on the slope from surrounding topography (Oliver 1992; Sun et al. 2003; Zoumakis et al. 2006). The complicated time evolution of shadows and insolation on sloping surfaces in Arizona's Meteor Crater are shown as an example of this factor in **Fig. 5**. Matzinger et al. (2003) and Rotach and Zardi (2007) suggest that the daytime spatial variation of sensible heat fluxes over complex terrain can be reasonably well estimated by relating sensible heat fluxes to global insolation on slopes. This approach is promising, but it is clear from (7) that many other factors affect the sensible heat flux, including both radiative and surface energy budget variables.

During nighttime, solar radiative fluxes become zero, but additional factors lead to significant spatial variations in sensible heat flux on the sidewalls. Strong vertical variations in temperature are superimposed on the slopes once an inversion forms and grows in the valley, affecting outgoing longwave radiation. At the same time, incoming longwave fluxes vary along the slope due to their varying views of the sky and surrounding terrain, with significant amounts of back radiation received at low elevation sites from the surrounding terrain.

A review paper by Duguay (1993) summarized some of the interactions between the radiation field and topography, focusing on the challenge of modeling radiative fluxes in complex topography. Key questions were the parameterization of diffuse sky radiation and of the terrain-reflected shortwave radiation, and the difficulty of dealing with anisotropic radiation fields. Other investigators have addressed individual aspects of the radiative transfer problem. Olyphant (1986) investigated the influence of longwave radiation from surrounding topography on the energy balance of snowfields in the Colorado Front Range. Longwave loss is typically reduced by about 50% when compared to the ridge tops. Plüss and Ohmura (1997) addressed the influence of longwave counter-radiation from elevated snow-covered terrain in mountainous terrain in a modeling study. They stress the importance of the surface temperature of the sky-obstructing terrain, and also of the air temperature in between the point of interest and the surrounding terrain, especially for inclined surfaces. In snow-covered environments, neglecting the effects of the usually warmer air temperatures leads to an underestimation of the radiation emitted from the obstructed parts of the hemisphere. Height dependence of fluxes and of other influences such as seasonal dependencies, cloud radiative forcing, the Greenhouse Effect, etc. were investigated by Marty et al. (2002), Philipona et al. (2004) and Iziomon et al. (2001).

The effects of the smaller scale topography on the radiation field arising from variations in exposure, shading and sky view effects as well as surface properties like albedo were investigated by Whiteman et al. (1989a) and Matzinger et al. (2003) by measuring radiative fluxes on surfaces parallel to the underlying topography. Oliphant et al. (2003) addressed these terrain effects by combining simple radiometric measurements with modeling efforts. Whiteman et al. (1989a) reported instantaneous values and daily totals of radiation budget components for 5 sites in different physiographic regions of Colorado's semiarid, northwest-southeast-oriented Brush Creek Valley for a clear-sky day near the fall equinox, finding significant differences in the radiation budgets between sites. A higher daytime net radiation gain and a higher nighttime net radiation loss at a ridge top site were attributed to its unobstructed view of the sky. Oliphant et al. (2003) found slope aspect and slope angle to be the dominant features in the radiation budget of a complex terrain area in New Zealand, followed by elevation, albedo, shading, sky view factor and leaf area index. Matzinger et al. (2003), in a cross-section through Switzerland's Riviera Valley, found a decrease in downward longwave radiation and an increase of net radiation with height. Müller and Scherer (2005) recognized the importance of including topographic influences on the radiation balance in mesoscale weather forecast models. They introduced a subgrid scale parameterization of the topographic effects and

managed to improve 2-m temperature forecasts for areas where the interaction between topography and radiation was most apparent. These include areas dominated by wintertime shading, areas with increased daytime sun exposure, and deeper valleys where nighttime counter-radiation is important. Others have addressed more specific topographic effects and their impacts on slope boundary layer evolution. Colette et al. (2003) focused on the effect of terrain shading on the modeled morning break-up of the nocturnal stable boundary layer in an idealized valley, finding that shading can have a significant impact on the timing of inversion break-up.

Soil moisture and spatial variations of soil moisture also affect slope flows (Banta and Gannon 1995). Using a numerical model, they found that higher soil moisture values during daytime partition more energy into latent heat flux (Q_E in (7)), reducing sensible heat flux and decreasing upslope flow strength. The main effect of high soil moisture during nighttime, in contrast, is an increase in soil heat conductivity so that heat diffuses upward from a deeper layer of soil (Q_G in (7)) to replace the energy lost by longwave radiation at the surface.

2.3. Role of turbulence in slope flows

The bulk of the research on slope flows to date has been concerned with the mean characteristics of the slope flows, such as their depths, strengths, wind profiles, relationships to temperature structure, etc. The important role of turbulence in producing these characteristics has received much less attention. In contrast to flat terrain, where calm or very weak winds often accompany fair weather conditions, marked up- and downslope flows usually occur over slopes on fair weather days. Turbulent kinetic energy (TKE) in slope flows is always produced, as in neutrally stratified turbulent shear layers, by the coupling between vertical wind shear that develops in the mean slope flow profile and the momentum flux. However buoyancy contributes too, either to produce turbulent energy, when the sensible heat flux is upwards, or to suppress it, when the flux is downward. This turbulence is critical to the vertical mixing of heat and momentum that governs the height of the jet, the depth of the flow and the ultimate equilibrium temperature deficit (Cuxart et al. 2011).

Turbulence in upslope flows is generally considered to be a more tractable problem than turbulence in downslope flows. This comes from parallels with the study of turbulence over flat, homogeneous terrain, where understanding of turbulence has progressed much faster for convective boundary layers than for stable boundary layers. Towers on slopes are generally too short to fully encompass the rapidly growing upslope flow layer, however. Thus, unless additional observational tools can be developed for measuring turbulence over deeper layers above slopes, future improvements in understanding of upslope flows may come primarily from modeling studies.

The continuous turbulence production by shear in the wind profile in fully developed shallow downslope flows is expected to be a much more manageable problem than turbulence in the deeper stable boundary layers that form over both flat and complex terrain areas, where the turbulence is intermittent and discontinuous (Mahrt 1999; Van de Wiel et al. 2003). The shallow downslope boundary layers are more accessible to tower measurements, but appropriate measurement techniques and post-processing methods (e. g. filtering, wind component rotations, and alignment to an appropriate reference frame) are still problematical. Turbulence data are generally obtained from high-rate sampling of the three components of the wind. Additional sampling of scalar variables (temperature, humidity, CO₂ concentrations, etc.) on the same time scale can be used to correlate fluctuations of the wind components and scalars to determine fluxes. Representative measurements require that the upwind fetch be homogeneous with respect to sources and sinks of scalars and surface properties. Following the collection of wind data on the slope, the wind measurements are usually rotated to align the coordinate system to the mean wind, which is generally parallel to the underlying ground (at least, near the surface). Flaws in the typical double- or triple-rotation method used over flat terrain are encountered in sloping terrain (see Finnigan et al. 2003), so that the ‘planar-fit’ approach developed by Wilczak et al. (2001) is considered preferable. But an appropriate post-processing also requires carefully designed filtering and averaging procedures to extract turbulent quantities from the often non-stationary mean flows encountered over slopes (de Franceschi and Zardi 2003; Weigel et al. 2007; de Franceschi et al. 2009).

Few model simulations of turbulent quantities are yet available for downslope flows since most of the RANS numerical models to date have been developed for mesoscale simulations on much larger scales than the slope flows. The lack of vertical resolution of the slope flows in these models, and uncertainty in the

applicability of the turbulence parameterizations have limited their utility. Recent improvements in LES model formulations (also see Chapter 10), and corresponding increases in computer power, are now leading to continuously improved simulations as to grid resolution, numerical schemes and appropriateness of turbulence closures (Skylingstad 2003; Chow et al. 2006; Axelsen and Van Dop 2008, 2009; Serafin and Zardi 2010a).

2.4 Upslope flows

The radiative heating of the ground and the resulting upward turbulent sensible heat fluxes, typically occurring in connection with upslope flows, increase rapidly after sunrise, reaching magnitudes that are much higher than those associated with downslope flows. As a consequence of increasing heat flux, upslope flows cannot approach a steady state, but rather grow continuously with time in strength and depth. Upslope flows are confined to a layer over the heated slope in the morning by the highly stable air that formed above the slope overnight (the confining stability can be especially strong over valley sidewalls, compared to slopes on isolated mountainsides). Like the situation over flat ground, heating of the slopes causes an unstable or convective boundary layer to grow upward into the remnants of the nighttime stable layer. The daytime boundary layer over slopes, in contrast to over flat ground, is a convective-advective boundary layer, with bent-over plumes and convective elements moving up the slope. While the upslope flow grows in depth and strengthens with time after sunrise, the volume flux of the flow increases with upslope distance as air is entrained into the flow at its upper boundary. The growing depth of the convective-advective upslope flow layer eventually allows the convection to break through the stable layer. Following the breakup of the confining stable layer, one might expect the convective currents to simply rise vertically from the heated ground. In fact, the flow continues to rise up the slope. This is apparently caused by a horizontal pressure gradient associated with the inclined superadiabatic sub-layer that forms over the slope. The upslope flows are often disturbed, however, by convective mixing that brings down the generally stronger background winds from higher layers of the atmosphere.

Our understanding of upslope flows has suffered from the lack of observational tools for making continuous measurements of the mean and turbulent profiles through the full depth of the growing upslope flow layer. Towers are generally not tall enough to penetrate this layer and the non-stationarity and inhomogeneity of the flows has made observations particularly difficult. Some field observations (Kuwagata and Kondo 1989; Van Gorsel et al. 2003a; Reuten et al. 2005; Geerts et al. 2008; De Wekker 2008), laboratory simulations (Hunt et al. 2003; Princevac and Fernando 2007; Reuten et al. 2007; Reuten 2008) and model simulations (Kuwagata and Kondo 1989; Schumann 1990; Atkinson and Shahub 1994; Axelsen and van Dop 2008) have improved this situation. Two interesting observations on upslope flows came from a field experiment over an isolated slope northeast of Vancouver, BC, in 2001. The observed depression of a mixed layer at the base of the mountain slope is thought to have been caused by subsidence in the return branch of the upslope circulation (De Wekker 2008, Serafin and Zardi 2010a). On a different day, scanning Doppler lidar observations up the slope appeared to show a closed slope flow circulation *within* the inclined convective boundary layer (Reuten et al. 2005), although these findings are controversial.

Schumann (1990) simulated upslope flows over an infinite, uniform, heated, sloping surface for a range of slope angles and surface roughness. The simulations were revolutionary, providing new insight into the role of turbulence in upslope flows and the utility of LES modeling to improve understanding of geophysical phenomena on small length scales. Schumann's work, as a parametric study, was limited to a constant ambient stability (3 K km^{-1}) and sensible heating rate (about 100 W m^{-2}), with a quiescent atmosphere above the slope flow layer. The simulated steady-state profiles of upslope wind speed and excess temperature (with respect to the unperturbed thermal structure) for slopes of different inclination angle from 2° to 30° are shown in **Fig. 6**, where the axis variables are normalized by a scale height H of 58 m, a wind speed scale v_* of 0.58 m s^{-1} , and a temperature scale θ_* of 0.17 K. A dry adiabatic lapse rate curve is provided on the temperature profile plot for comparison with the simulated profiles. Several interesting features are seen in the simulations. The steady state was attained by a balance between the buoyancy term and surface friction in (2) and between the surface heating and upslope advection of heat against the mean temperature gradient in (4), just like in Prandtl's model. As expected, the temperature excess present at the ground decayed with height. Temperature profiles, except those over the steepest slopes, were characterized by a near-adiabatic temperature decrease with altitude, indicating good mixing in the turbulent flows. Strong local minima occurred in the velocity and temperature profiles at the upper edge of the mixed layer. Upslope flow depths and volume fluxes were greatest over low-angle slopes. Shallow and weak upslope flows occurred on steeper slopes. Wind maxima occurred within about 50 m of the surface over slopes of

all inclination angles. The turbulence kinetic energy profile in the upslope flow was generated by vertical shear, with high positive values of shear just above the ground but below the height of the jet maximum and high negative values of shear above the jet maximum. This resulted in a slope-normal transport of momentum both upward and downward from the jet level (see **Fig. 2**).

LES simulations such as this have the advantage of being able to produce profiles of all turbulence quantities above the slope and to determine all contributions to the turbulence kinetic energy budget. One caveat, however, is that subgrid scale TKE contributions are parameterized. The contributions of these terms near the surface, where eddies are small, have not been verified. It is important to note that detailed observations are, so far, unavailable to properly test LES simulations of the upslope boundary layer. The idealized nature of the LES simulations should also be emphasized. In real, three-dimensional topography, slopes are very inhomogeneous in terms of slope angle, roughness, vegetative cover, sensible heat flux, non-planarity, etc. and the flows are distinctly non-stationary. In contrast, the LES simulations were conducted on uniform slopes and the equations were integrated until steady-state solutions were reached. The simulations certainly have interesting implications for upslope flows on sidewalls with varying inclination angles. In these cases, along-slope convergences or divergences of mass in the upslope layer will cause detrainment and entrainment from the slope flow layer (see, also, Vergeiner and Dreiseitl 1987), with implications for the air mass over the valley center. There are ample opportunities to extend Schumann's (1990) initial work.

2.5. Downslope flows

Downslope flows on isolated mountainsides and on valley sidewalls have been studied extensively over the years. In this section we will summarize current knowledge about the mean and turbulence structure of downslope flows using observations and simulations, concentrating on research conducted since about 1990.

For downslope flows, the terms of importance in the governing equations, (2) – (4), have been evaluated mainly with hydraulic models (Manins and Sawford 1979b; Horst and Doran 1988; Papadopoulos et al. 1997; Haiden and Whiteman 2005). Steady-state flow on mid-latitude slopes is typically an ‘equilibrium flow’ balance between buoyancy and turbulent momentum flux divergence (i.e., friction), in agreement with the local equilibrium assumption made in Prandtl's (1942) analytical model. The surface stress is thought to contribute more friction than the entrainment of slower moving air from above the downslope layer. The balance can sometimes include a significant along-slope advective contribution in the momentum balance near the height of the wind maximum, where shear changes sign (Skylingstad 2003), in agreement with Horst and Doran's (1988) results. The slope-perpendicular momentum equation, since the RHS of (3) is near zero, is a balance between the two advection terms. The thermodynamic energy equation, (4), is a balance between the radiative and sensible heat flux divergences and temperature advection.

Horst and Doran (1988) found that the turbulence structure over slopes was consistent with local shear production of turbulence. Turbulence, which is generated primarily by vertical wind shear and destroyed by viscous dissipation, is critical for the vertical mixing of momentum and buoyancy in the mean flow. The jet-like wind profile associated with downslope flows produces a turbulence structure (**Fig. 2**) that is quite different from that over flat terrain. Vertical shear is positive below the jet, disappears at the height of the jet and is negative above the jet. This vertical distribution of wind shear produces TKE profiles with a maximum near the surface, and a local minimum at the height of the wind maximum. Above that height, TKE is highly dependent on the speed and direction of the ambient wind. Turbulence above the wind maximum is decoupled from the surface so that normal surface similarity theory is not expected to be applicable above the jet. Vertical velocity variance profiles depend on cooling rates and external wind speeds (Coulter and Martin 1996).

In the remainder of this section we will highlight the important influences of slope angle, ambient stability, external flows and other disturbances on downslope flows. We begin with slope angle.

2.5.1 Impact of slope angle on downslope flows

If a continuous source of cold air were introduced at the top of a slope (as in Burkholder et al. 2009), the downslope flow would be stronger on steeper slopes where the along-slope component of the gravity vector is maximized. But, downslope flows in valleys and on mountainsides are not generally fed by a source of

cold air at the top of the slope. Rather, cold air forms *in place* on the slope through a downward flux of sensible heat to the underlying radiatively cooled surface. The air moves down the slope only as long as it is negatively buoyant with respect to the ambient environment. The air in the flow is heated adiabatically at $9.8\text{ }^{\circ}\text{C km}^{-1}$ as it moves down the slope. To continue its descent it must be continuously cooled by a downward sensible heat flux to the cold underlying surface. The faster the flow, the lower the rate of cooling per unit mass of flow. On low angle slopes, the air travels a greater horizontal distance along a slope to descend the same vertical distance compared to a steeper slope. The air loses heat through downward sensible heat flux along its entire trajectory, which is longer on a shallow slope than on a steep slope.

Slope flows will not form on horizontal surfaces, where radiative loss to the sky and downward sensible heat flux occur but the along-surface component of the gravity vector is zero. At the other limit, a vertical surface will have a strong component of the gravity vector along the slope, but a vertical surface will not radiate well to the sky and, because of the small distance that the air would travel along the slope to lose a unit of altitude, the rate of cooling of the flow to the underlying surface would be small. The strongest downslope flows will thus develop on slopes of intermediate angle where there is a combination of good outgoing longwave radiative loss to the sky that drives a slope-normal sensible heat flux and a component of the gravity vector acting along the slope.

Observations (**Table 1**) on simple slopes show that downslope flows on low-angle slopes are deeper and stronger than those on steeper slopes. Slope flows are often strongest in the early evening when the ambient stability is weak. For slopes on valley sidewalls, this is the time before the overlying valley flows strengthen to produce a cross-slope shear that disturbs the slope flows. The temperature deficit layer over the slope (i.e., inversion depth) often has a depth corresponding to about 5% of the vertical drop from the top of the slope and the height of the wind maximum is usually within the temperature inversion layer, often at heights that are 30-60% of the inversion depth. The downslope flow itself usually extends much higher than the height of the wind maximum or the height of the inversion top because of the entrainment of ambient air by the downslope flow (Princevac et al. 2005). But, this height is much more variable than the inversion height and is very dependent on the speed and direction of the ambient flow above the slope flow layer. In general, the downslope flow extends to heights of several times the inversion depth.

The speed and depth of downslope flows (and, thus mass or volume flux) increase with downslope distance. This has been seen in experiments on Rattlesnake Mountain, Washington (Horst and Doran 1986), on a low angle slope in Utah's Salt Lake Valley (Haiden and Whiteman 2005; Whiteman and Zhong 2008), and on Greece's Mt. Hymettos (Amanatidis et al. 1992; Papadopoulos and Helmis 1999). An example illustrating this increase in depth and speed is shown in **Fig. 7**. Downslope flows accelerate with downslope distance while increasing their depth as additional mass is entrained into the flowing layer at its upper boundary. Some of the simple steady-state analytical slope flow models (see, e.g., those reviewed by Barry 2008) are in conflict with observations and with predictions from full physics models. Because the models are often run using the same sensible heat flux forcing on slopes of all angles, they have led to the mistaken concept that downslope flows on upper steeper slopes are stronger and deeper than flows on lower slopes, and will overrun the flows on lower slopes or will travel down the slope as frontal disturbances. While such frontal propagation episodes can occur in special circumstances (e.g., when the upper slopes go first into shadow while the lower slopes are still in sunlight), they appear to be atypical.

RANS and LES models are in agreement with field data, predicting weaker downslope flows (i.e. displaying both smaller maximum jet speed and smaller mass flux) on steeper slopes (Skylkingstad 2003; Zhong and Whiteman 2008; Axelsen and Van Dop 2009). The effect of stepwise changes in slope angle partway down a mountainside were investigated using both RANS and LES models by Smith and Skylkingstad (2005) for an 11.6° slope that changed suddenly to a 1.6° slope at a lower elevation. The slope flow depth increased rapidly over a distance of 500 m at the slope angle juncture and the height of the maximum velocity moved upward about 5-10 m. Below the juncture, a new equilibrium was established with a decreased rate of growth in slope flow depth and more rapid cooling of the near-surface temperatures. Near-surface downslope velocity decreased, producing a distinct detached and elevated jet structure. Potential energy generated at the top of the slope by continued cooling was transported downslope and converted into kinetic energy at the slope base.

2.5.2 Impact of ambient stability on downslope flows

The effect of ambient stability on downslope flows is now well known from both simulations on simple slopes and from field experiments. The downslope flow must adjust to any changes in ambient stability of the atmosphere adjacent to the slope. If the flow, for example, encounters a sudden increase in ambient stability, it must be cooled at a higher rate to be advected along the surface at the same speed. Downslope flow intensity is thus inversely proportional to ambient stability (Rao and Snodgrass 1981; King et al., 1987; Ye et al., 1990; Helmis and Papadopoulos 1996; Zhong and Whiteman 2008). The nighttime buildup in ambient stability within valleys reduces downslope flow speed and may even suppress downslope currents. In enclosed basins, downslope flows die in the late evening as ambient stability increases and the atmosphere becomes increasingly horizontally stratified and quiescent (Clements et al. 2003; Whiteman et al. 2004a, c; Steinacker et al. 2007).

2.5.3 Impact of background flow on downslope flows

Downslope flows, which are usually rather weak and shallow air currents, are quite sensitive to disturbance by background or ambient flows (Fitzjarrald 1984; Barr and Orgill 1989; Doran 1991) that may oppose or follow the downslope flows or may have a significant cross-slope component. Background flows can originate as valley flows, larger mesoscale circulations, synoptic flows, sea or lake breezes, seiches, gravity waves, wakes from flow over ridges, etc. The effects of these differing phenomena on downslope flows are difficult to separate using field data, but it is generally understood that background flows with strengths of only 2-3 m s⁻¹ can have far reaching effects on the structure of the downslope flows and even their existence.

Downslope flows on valley sidewalls are routinely subject to the development of overlying valley flows. These valley flows, which have jet-like vertical and horizontal profiles within the valley cross-section, produce horizontal shears above the slope flows that vary with elevation. Because these flows are oriented along the valley axis, while the slope flows are perpendicular to the valley axis, they produce a strong directional shear through the shallow slope flow layer. When the valley winds get strong enough, horizontal and vertical shears and the associated turbulence can greatly modify the downslope flows or remove them entirely from valley sidewalls (Doran et al. 1990).

As cross-slope winds increase, slope flows deepen and behave more like a weakly stratified sheared boundary layer (Skylingstad 2003). The cross-slope flow produces an extra source of mixing from the additional vertical shear, which weakens the vertical stratification. Because the velocity near the surface becomes lower there is less loss of momentum to surface drag. But, as cross-slope flow increases, the downslope jet becomes weaker and deeper and is eventually overpowered by the cross-slope-generated turbulence.

2.5.4 The effects of slope inhomogeneity on downslope flows

Vergeiner and Dreiseitl (1987) pointed out that real mountain slopes are much more complicated than those assumed in existing models. Since, as emphasized above, radiative and turbulent fluxes vary in time and space, upslope and downslope flows must vary continuously in space and time in response to small-scale slope inhomogeneities. This variation makes it difficult to find representative measurement locations on slopes (e.g., sites with uniform slope angles and surface cover) to compare with idealized models. Slopes on mountain sides vary not only in topography and surface cover, but they are also subject to time- and space-varying interactions with larger scale flows and to varying ambient stabilities.

Only a few observational and modeling studies have investigated the response of slope flows to slope inhomogeneities. As mentioned, several studies have investigated the effects of changes in slope angle. Others have looked into the effects on downslope flows of forests (e.g., Lee and Hu 2002; van Gorsel 2003); differentially cooled sloping surfaces (Shapiro and Fedorovich 2007; Burkholder et al. 2009) and sunset time variations on complex slopes (Papadopoulos and Helmis 1999). Haiden and Whiteman's (2005) investigation of downslope flows on a visually rather uniform slope at the foot of Utah's Oquirrh Mountains found imbalances in both the momentum and heat budget equations that were attributed to small scale convexities and concavities on the slope that channeled the downslope currents. Monti et al. (2002) observed multi-layered stability above a slope that appeared to come from elevated downslope currents. They suggested that slope flows can develop features similar to hydraulic flows, such as jump conditions or turbulent transitions.

2.5.5 Drainage flow oscillations

Oscillations in drainage (i.e., downslope and down-valley) flow strengths with periodicities between about 5 and 90 minutes have been frequently observed. They can be produced by a variety of different mechanisms, including interactions between valley flows and tributary flows (Porch et al. 1989), variation of cold air sources from upstream (Allwine et al. 1992), interactions with mountain waves (Stone and Hoard 1989; Poulos et al. 2000, 2007), modulation of slope and valley flows by interactions of synoptic and mesoscale flows with surrounding topography (Mahrt and Larsen 1982; Doran et al. 1990; De Wekker 2002), interactions between slope flows and sea breezes (Bastin and Drobinski 2005), meandering motions in stratified flows and, in the case of downslope flows, by internal waves impinging normal to the slope (Princevac et al. 2008) and by overshooting and oscillations caused by the resulting buoyancy disequilibrium (Fleagle 1950; Doran and Horst 1981; McNider 1982; Helmis and Papadopoulos 1996; van Gorsel et al. 2003b; Chemel et al. 2009; Viana et al. 2010). Additionally, cold air forming over plateaus or other elevated terrain source areas sometimes cascades down the slopes at intervals as *cold air avalanches* (Küttner 1949). Atmospheric analogs to the *seiches* that form in ocean and lake basins have also been observed in basin temperature inversions, where it is common to see smoke plumes from chimneys and open fires that exhibit weak oscillatory motions in which the plume is carried back and forth quasi-horizontally relative to its source. The back-and-forth sloshing, if produced by seiches, should have a characteristic frequency that is dependent on basin topography, atmospheric stability and wind speed. Seiche-like oscillations with a periodicity of about 15 minutes were recently documented on the floor of Arizona's Meteor Crater (Whiteman et al. 2008), and a spectral element model (Fritts et al. 2010) has produced seiches in idealized topography similar to the crater.

2.5.6 Glacier winds

Slope flows are generally diurnally varying flows, but over a snow surface where the surface energy budget is consistently negative the resulting downward sensible heat flux from the adjacent atmosphere produces a shallow cold air layer with a continuous downslope flow. Over cold, high albedo glaciers or snow surfaces, this downslope flow has been called a *glacier wind*. A special feature of downslope winds over snow surfaces is the constrained upper limit value of surface temperature, 0°C. In daytime during the melt season when ambient air temperatures undergo their normal diurnal variation, this upper limit of surface temperature results in a temperature inversion above the melting surface whose maximum strength occurs in mid- to late-afternoon in the ablation zone, and at night at higher elevations where radiative cooling of the surface is more important (Oerlemans 1998).

Glacier winds, which occur on a variety of scales, have received increased attention in the last 20 years. Oerlemans et al. (1999) found temperature inversions of about 20 m depth and 8°C strength over a large maritime ice cap in Iceland. Near-steady-state glacier winds were nearly always present, except for periods with traveling intense storms, suggesting that glacier winds are the key factor shaping the microclimate of glaciers, at least in summer. Maximum downslope wind speeds of 3-10 m s⁻¹ were found at heights from several to a few tens of meters above the surface, although the winds often extended to heights exceeding 100 m. The momentum balance that produces the glacier wind appears to be a balance between buoyancy force and friction, as expressed in the Prandtl (1942) and Oerlemans and Grisogono (2002) models. In contrast, for a small, mid-latitude glacier in the Alps the buoyancy force was balanced by both friction and the mesoscale pressure gradient that drives the valley wind above the downslope layer (Van den Broeke 1997a, b).

3. The valley wind system

Diurnal valley winds are thermally driven winds that blow along the axis of a valley, with up-valley flows during daytime and down-valley flows during nighttime. Valley winds are the lower branch of a closed circulation that arises when air in a valley is colder or warmer than air that is farther down-valley or over the adjacent plain at the same altitude. Unlike slope winds, valley winds are not primarily a function of the slope of the underlying valley floor. In fact, they have been observed even in valleys with horizontal floors (Egger 1990; Rampanelli et al. 2004). Instead, they depend on other geometrical factors, such as the shape and aspect of the valley cross-section and their along-valley variations, including tributaries (Steinacker 1984), as discussed below. The diurnal reversal of the flow requires a larger daily temperature range within the valley than over the adjacent plain (Nickus and Vergeiner 1984; Vergeiner and Dreiseitl 1987). Horizontal pressure gradients that develop as a function of height between air columns with different vertical temperature structures over the valley and the adjacent plain drive the valley wind (**Fig. 8**). These pressure gradients can be observed directly (Khodayar et al. 2008; Cogliati and Mazzeo 2005). Along the Inn Valley, for example, thermally induced pressure differences of up to 5 hPa over a distance of 100 km

have been observed (Vergeiner and Dreiseitl 1987). As a consequence of the changing pressure distribution in the vertical, the vertical profile of along valley winds undergoes a cyclic evolution during the day (Gross 1990). Valley winds evolve gradually over the daily cycle and produce weak to moderate wind speeds. Peak wind speeds over the valley center are frequently in the range from 3 to 10 m s⁻¹.

Ideally, the upper branch of the closed circulation consists of an elevated horizontal flow running in the opposite direction from the winds in the valley below. Because the upper branch is unconfined by topography and thus broader in horizontal extent, it is generally quite weak and can be obscured by stronger synoptic-scale flows. The existence of these return flows or compensation currents was debated at the early stage of the scientific investigation of valley winds (cf. Wagner 1938) but is today considered a well-documented feature (McGowan 2004; Zängl and Vogt 2006). **Fig. 9**, for example, compares modeled temperature profiles within a valley and over the adjacent plain to illustrate the reversing temperature gradients with height that drive the elevated return circulations (from Rampanelli et al. 2004). Investigations by Buettner and Thyer (1966) in valleys that radiate out from the isolated volcano of Mt. Rainier, Washington (USA), found that the upper branches of the valley circulations there could even be observed within the terrain-confined upper altitudes of the valleys. They coined the term *anti-winds* for these confined currents, but the deeper currents above the ridgetops are more frequently called return or compensating flows.

The evening reversal of the daytime up-valley wind begins in late afternoon or early evening when the daytime wind system begins to lose strength. The gradual loss of strength, taking place over several hours, is caused by a decrease in the along-valley pressure gradient as temperatures along the valley axis are equilibrated by advection and as the sensible heat flux that maintained the temperature gradient decreases. Once the sensible heat flux reverses on the sidewalls or in the shadowed parts of the valley, downslope flows begin, transferring the cooling experienced in a shallow layer above the slopes to the valley atmosphere through compensatory rising and cooling motions. Radiative processes and turbulent sensible heat flux divergences also play a role. As the valley atmosphere cools, the horizontal pressure gradient between the valley and adjacent plain reverses and a down-valley flow begins. The valley wind reversal lags that of the slope flows because the large mass of the valley atmosphere must be cooled before the pressure gradient can reverse (Vergeiner 1987). The reversal typically begins at the floor of the valley, where cooling is most intense, with the formation of a temperature inversion. As the cooling progresses upwards, the down-valley flow deepens and strengthens. Within the nighttime inversion, the coldest temperatures are at the valley floor, and temperatures increase with height. This results in relatively warmer temperatures on the valley sidewalls than on the valley floor, i.e. a *warm slope zone* on the valley sidewalls (Koch 1961).

The morning reversal of the down-valley wind, which occurs after sunrise, similarly requires a reversal of the along-valley pressure gradient as the valley atmosphere warms. The reversal occurs several hours after upslope flows are initiated when the heat transfer processes become effective in warming the entire valley atmosphere. Further details on the heat transfer mechanisms are provided in the next section that focuses on interactions between the slope and valley wind circulations.

The warmer temperatures during daytime and colder temperatures during nighttime in the valley atmosphere compared to the atmosphere over the adjacent plain (or farther down the valley) are mainly caused by two factors. First, under low background wind conditions the valley atmosphere is protected by the surrounding topography from mass and heat exchange with the atmosphere above the valley so that heating will be more effectively concentrated in the valley during daytime and cooling will be enhanced in the valley during nighttime. A second, more important, factor has been termed the "area-height relationship" or "topographic amplification factor", TAF. The concept (see Whiteman 1990 or 2000 for fuller discussions), is that the daily temperature range in the valley will be amplified by the smaller mass of air that is heated or cooled within the confined valley volume than within the larger volume of the same depth and surface area at its top over the adjacent plain. The higher mean temperature inside the valley during daytime causes a pressure gradient to develop between valley and plain that drives an up-valley wind. The lower mean temperature and higher pressure in the valley during nighttime drive a down-valley wind.

The mechanisms by which valley geometry might affect cooling and warming of the valley atmosphere have been explored by various authors. Wagner (1932) was the first to express the TAF concept. Steinacker (1984) carried the concept further, computing the distribution of drainage area as a function of height in the Inn Valley and comparing it to that over the adjacent plain in southern Germany. McKee and O'Neal (1989)

then suggested that along-valley pressure gradient differences produced by changes in terrain cross-section along a valley's axis could explain along-valley wind speed variations. While the intuitive TAF concept, which focuses on valley geometry, helps to conceptualize the important thermodynamics leading to up- and down-valley flows, the simple concept involves inherent assumptions that has made it difficult to apply in practice.

There are inherent difficulties in evaluating precisely both the valley volume, and the heat fluxes across its boundaries. As to the volume, its top boundary is difficult to define in practice. An intuitive choice would be to locate it at crest height, yet in real valleys the crest height varies with down-valley distance and differs between the opposing sidewalls. Further, it appears that the volume of the valley tributaries has to be taken into account (Steinacker 1984). As to the fluxes, Gauss's divergence theorem can be used with a volume integral of (7) to determine the rate of change of the volume-average potential temperature in the valley. This rate of change is driven by the surface integral of the advective, turbulent and radiative heat fluxes across the surfaces bounding the volume, including the valley floor, sidewalls and the top boundary. However the flux distributions along the volume boundaries are generally not well known (e. g. on the valley sidewall slopes: see Section 2.2). Yet boundary conditions allow some simplifications: for instance, advection through the ground surface vanishes, since wind speed vanishes there. However this is not the case on the top surface, where heat advection through slope flows on the sidewalls and compensating subsidence at the valley core will play a crucial role in the daytime heating of the valley atmosphere (Rampanelli et al. 2004; Weigel et al. 2007; Schmidli and Rotunno, 2010; Serafin and Zardi, 2010b, c). Because the top boundary is not a solid surface, heat gain or loss in the volume is not normally confined to the volume. This is especially the case during daytime, when convective boundary layers can grow above ridge height. Similarly, the down- and up-valley ends of the volume are open: once an along-valley flow begins, advection acts to reduce temperature differences between valley and plain, or between segments of a valley. Further, the TAF concept in its simplest form does not consider that the rate of heat gain or loss may vary with height in the valley or plains volumes, and assumes that rates of heat gain and loss are equal in the two volumes. In fact, the surface energy budgets and heat transfer processes may be quite different in the two volumes. Heat transfer processes in the valley volume, for example, involve heat transfer over the slopes associated with up- and downslope flows, compensatory rising and sinking motions over the valley center, and radiative transfer processes that include back-radiation from the sidewalls (cf. Haiden 1998). Further information on these and other factors that lead to variations in the thermally driven pressure gradient along a valley including the partitioning between sensible and latent heat fluxes in the surface energy budget and the confinement of heated or cooled air within a valley can be found in publications by Zängl et al. (2001), Rampanelli (2004), Zängl (2004), Zängl and Vogt (2006), Serafin (2006), Rucker et al. (2008), Schmidli and Rotunno (2010), and Serafin and Zardi (2010a, b, c).

In the early evening, down-valley flows often converge into sub-basins or build up cold-air pools or lakes behind terrain constrictions (cf. Bodine et al. 2009). In general, though, if the valley does not have major constrictions along its length or major changes in surface microclimates, the nighttime down-valley flows accelerate and increase in depth with down-valley distance, resulting in an along-valley mass or volume flux divergence. Through the law of mass conservation, the existence of along-valley divergence requires the import of potentially warmer air into the valley from aloft or from tributaries. Interestingly, recent field measurements and model simulations have also shown a divergence of along-valley mass flux in the daytime up-valley flows for the Inn Valley (Vergeiner 1983; Freytag 1988; Zängl 2004), the Kali Gandaki Valley (Egger et al. 2000; Zängl et al. 2001) and in the Wipp Valley (Rucker et al. 2008). This along-valley mass flux divergence is somewhat counterintuitive, since one might expect an up-valley flow in the main valley to dissipate with up-valley distance as the flows turn up the slopes and tributaries. Various mechanisms have been invoked to explain the mass flux divergence, including compensating subsidence over the main valley, transition to supercritical flow in the widening part of a valley (possibly favored by gravity waves produced by protruding ridges), and intra-valley change in the horizontal pressure gradient induced by differential heating rates.

In different valleys (**Fig. 10**), the vertical structure, strength and duration of up- and down-valley flows differ, depending on climatic and/or local factors (Ekhart 1948; Löffler-Mang et al. 1997). One cannot assume that valleys with strong up-valley flows will also have strong down-valley flows. In the Kali Gandaki valley of Nepal, the daytime up-valley winds are much stronger than the nocturnal down-valley winds (Egger et al. 2000, 2002). In California's San Joaquin Valley, the up-valley flows can persist all night (Zhong et al. 2004). In other cases, such as in Chile's Elqui Valley, nocturnal down-valley winds are not observed at all (Kalthoff et al. 2002), while down-valley winds may persist all day in snow-covered valleys (Whiteman 1990).

Down-valley winds are often enhanced where valleys issue onto the adjacent plains or into wider valleys. Drainage flows in the valley decrease in depth, accelerate, and fan out onto the plain at the valley exit, producing a *valley exit jet*. The valley exit jet at the mouth of Austria's Inn Valley reaches speeds of 13 m s^{-1} at heights only 200 m above ground (Pamperin and Stilke 1985; Zängl 2004). Valley exit jets have also been observed at the mouths of tributary canyons that issue from the Wasatch Mountains into the wide Salt Lake Valley (Banta et al. 1995, 2004; Fast and Darby 2004; Darby and Banta 2006; Darby et al. 2006) and at canyons that flow onto the plains south of Boulder, Colorado (Coulter and Gudiksen 1995; Doran 1996; Varvayanni et al. 1997). They have also been observed at the exit of valleys issuing onto the Snake River Plain in eastern Idaho (Stewart et al. 2002). Valley exit jets, which are often a source of non-polluted or relatively clean air, can have important air pollution consequences (Darby et al. 2006) and can bring nighttime relief from high temperatures at canyon exits. The outflows of valley exit jets can be modulated by larger-scale influences including the thermally driven flows beyond the valley exit (Darby and Banta 2006).

3.1 The effects of boundary layer processes and turbulence on valley flows

Only recently have field research programs investigated the impact of turbulence on valley winds (Rao and Schaub 1990; Poulos et al. 2002; Rotach et al. 2004; Rotach and Zardi 2007). Turbulence measurements have been made primarily from instrumented towers using eddy correlation techniques, although some airborne measurements were made in the Riviera Valley during the Mesoscale Alpine Programme (Weigel et al. 2006, 2007; Rotach and Zardi 2007). Many good methods and techniques have been developed for processing and analyzing turbulence measurements from towers (see, e.g., Kaimal and Finnigan 1994), but airborne turbulence measurements are more difficult to make and analyze. Wind velocity components are retrieved as a difference between absolute airplane motion with respect to a fixed frame of reference and airspeed as indicated by the aircraft (Crawford and Dobosy 1992). These two terms are at least an order of magnitude larger than the difference between them. Thus, high accuracy in the wind velocity components requires quite high accuracy in the original measurements. Airborne measurements are, nonetheless, the most promising tool for analysis of turbulence properties far from the surface in the middle of valley volumes (Rotach et al. 2004; Weigel et al. 2007).

The dynamics of diurnal valley winds results from the combination of slope flows on the sidewalls and boundary layer processes on and above the valley floor, including such factors as free convection, shear, and compensatory subsidence in the valley core atmosphere. As a consequence, turbulent processes associated with valley winds occur on different space scales (height above the slope, slope length, boundary layer depth over the valley floor, valley width) and time scales (hour, morning, afternoon, daytime, nighttime). As a consequence it is difficult to ascertain their individual roles and interactions. A high site-to-site variability must be considered in designing measurement strategies (Doran et al. 1989). Even the application of standard turbulence analysis procedures, such as eddy covariance, requires consideration of site-specific characteristics. (Kaimal and Finnigan 1994; de Franceschi and Zardi 2003; Hiller et al. 2008; de Franceschi et al. 2009).

Over a homogeneous plain under fair weather conditions with weak synoptic winds, shear will be minimized and convection will be the dominant process producing turbulence. Under the same synoptic conditions, thermally driven flows will develop in valleys, and the dominant process leading to turbulence will be shear production, as turbulence in valleys is rarely caused by convection alone (Weigel et al. 2007; de Franceschi et al. 2009).

Some observations suggest that the classical Monin-Obukhov surface layer scaling for velocity and temperature variances holds in the middle of a wide valley with a flat floor (Moraes et al. 2004; de Franceschi 2004; de Franceschi et al. 2009). However, at other locations (e.g. sloping sidewalls) scaling approaches that are valid for flat horizontally homogeneous terrain need to be extended and/or modified (Andretta et al. 2001, 2002; van Gorsel et al. 2003a; Grisogono et al. 2007; Catalano and Moeng 2010).

In Switzerland's Riviera Valley during daytime in summer, the vertical TKE distribution throughout the valley core atmosphere scales with the convective velocity scale

$$w_* = \left(\frac{g}{\theta_0} \overline{w' \theta'_s} z_i \right)^{1/3} \quad (8)$$

defined, as usual, with gravity acceleration g , a temperature reference value θ_s , the convective boundary layer (CBL) height z_i , and the surface temperature flux $\overline{w'\theta'_s}$, provided the latter is determined at the slope rather than at the valley center (Weigel and Rotach 2004; Weigel 2005; Weigel et al. 2006, 2007; Rotach et al. 2008). Despite highly convective conditions, it is mainly shear (as opposed to buoyancy) that is responsible for TKE production. However the maximum of shear production occurs not at the valley surface, but rather at higher levels above the valley. This suggests that wind shear is mainly produced by the interaction of the up-valley wind with the background winds aloft, rather than by surface friction. As a consequence shear can be related to the wind strength in the core of the valley wind and investigators have found that the scaling velocity determined from the surface heat flux on the slope is closely related to the valley wind strength.

Surface fluxes of momentum, heat and water vapor are strongly affected by topography and land surface cover (the reader will find various examples of such variability in Whiteman et al. 1989b; Grimmond et al. 1996; Wotawa and Kromp-Kolb 2000; Grossi and Falappi 2003; Antonacci and Tubino 2005; Bertoldi et al. 2006; Kalthoff et al. 2006; Serafin 2006; Martínez et al. 2010). In particular, vegetation can strongly affect turbulence production and surface layer structure, e.g. by imposing displacement heights and roughness lengths (cf. de Franceschi et al. 2009), and affecting fluxes and budgets of momentum, energy and mass. Additional complications arise when boundary layer processes occur in urban areas located in mountain valleys (Kuttler et al. 1996, Piringer and Baumann 1999; Savijärvi and Liya 2001; Kolev et al. 2007; Giovannini et al. 2010; Fernando 2010). Transport and mixing of pollutants in complex terrain have been addressed by many authors (see, e.g., Salerno 1992; Prévôt et al. 1993, 2000; Wong and Hage 1995; Prabha and Mursch-Radlgruber 1999; Grell et al. 2000; Doran et al. 2002; Gohm et al. 2009; De Wekker et al. 2009; de Franceschi and Zardi 2009; Aryal et al. 2009; Kitada et al. 2003; Regmi et al. 2003; Lehner and Gohm 2010; Panday 2006; Panday and Prinn 2009; Panday et al. 2009; Szintai et al. 2010). These processes are also addressed in **Chapter 5**.

3.2. The effects of other winds on valley flows

Valley wind systems are often modified, or even overpowered, by larger-scale thermally driven flows or by dynamically driven flows above a valley produced by mesoscale or synoptic-scale processes. Dynamically driven winds, including those in valleys, are discussed in **Chapter 3**, so we give here only a short summary.

Background flows above mountainous terrain are driven by large-scale pressure gradients that are superimposed on the along-valley pressure gradients produced locally by intra-valley temperature differences. When the valley atmosphere has a high static stability, the background flows will often be *channeled* along the valley axis (Whiteman and Doran 1993). These flows, are not, however, thermally driven flows. They occur under more active synoptic conditions and do not reverse twice per day at the normal morning and evening transition times. They are also generally stronger than the diurnal valley flows and, since they are imposed from aloft, do not necessarily exhibit the typical jet-like vertical profile usually seen with valley flows. Nonetheless their interaction with the valley atmosphere may be significantly affected by changes in the surface heat flux during the diurnal cycle (see e. g. Jiang and Doyle 2008).

The direction of the flow in a valley (either up- or down-valley) may be driven by the pressure gradient aloft, rather than by locally generated temperature differences along the length of the valley. As valleys are often curved or bent, the along-valley component of the synoptic-scale pressure gradient may differ from one segment of the valley to another. Accordingly, changes in wind speed and direction will occur along the axis of a bent valley, depending on factors such as valley orientation, width and depth (Kossmann and Sturman 2003). This phenomenon in which winds within the valley are driven by pressure differences between the two ends of the valley is called *pressure-driven channeling*. The flow direction is from the high pressure end toward the low pressure end of the valley. This type of channeling is in contrast to *forced channeling* in which momentum from the winds aloft is carried down into the valley, producing winds along the valley axis whose direction is determined by the component along the valley axis of the wind velocity aloft. Forced channeling is often seen near mountain passes. In addition to these major types of channeling, smaller scale airflow separations, eddies, and dynamic instabilities can be produced by background flow/terrain interactions that will affect thermally driven flows within a valley (Orgill et al. 1992).

When static stability is low, downward momentum transport, associated with convection, can bring winds aloft into a valley with wind directions not necessarily aligned along the valley axis. These cross-valley

flows are more likely to be present in the upper altitudes of a valley, and are unlikely to be confused with thermally driven diurnal valley winds. Flows over valley ridges can have smaller-scale dynamic effects on valley winds. In addition to the channeling processes mentioned above, other effects on the structure and evolution of diurnal wind circulations within a valley come from large-scale background flows (see, e.g., Barr and Orgill 1989; Doran 1991; Orgill et al. 1992; Mursch-Radlgruber 1995; Zängl 2008; and Schmidli et al. 2009a). During daytime, ridge-level winds may significantly modify the subsidence over the valley center and produce asymmetries in the cross-valley circulation. A weak ridgetop wind may flush out the upper part of the valley and modify the valley circulation, whereas a stronger one may intrude into the valley and even reach the valley bottom. During nighttime, upper winds can penetrate into the valley and “erode” the existing ground based inversion. However, valley drainage, once established, is rather resistant to erosion from above, because of atmospheric stability, especially in valleys having large drainage areas. As an example, Orgill et al (1992) investigated the mesoscale external factors affecting nocturnal drainage winds in four different valleys in western Colorado during the ASCOT project. They found that in such valleys wind erosion can reduce drainage flows to less than half of the valley depth, the principal contributing factors to wind erosion processes being an along-valley wind component above the valley that opposes the drainage, a weak stability in the valley, and winds aloft with speeds exceeding a threshold around 5 m s^{-1} and accelerating at rates greater than 0.0004 m s^{-2} (Orgill et al. 1992). In the Rosalian mountain range in eastern Austria, Mursch-Radlgruber (1995) found that an opposing ambient flow decreased the down-valley flow depth in the shallow valleys studied, but did not reduce the jet speed maximum. In contrast, an ambient flow in the same direction as the drainage flow suppressed the drainage flow and led to stagnation or pooling on one night. This effect was explained by observing that the ambient wind produced a pressure low in the upper valley in the lee of the Rosalian range, thus counteracting the normally existing hydrostatic pressure gradient responsible for classical drainage flow.

The contrast in temperature between air over a water surface and air over the adjacent land typically drives diurnal sea/lake breezes that can interact with valley winds, significantly modifying both phenomena. The sea/lake breeze and the up-valley wind in a nearby valley may merge in a connected wind field called the Extended Sea Breeze (Kondo 1990) or Extended Lake Breeze (McGowan et al. 1995), producing long-range moisture transport (Sturman and McGowan 1995). This transport may provide significant moisture through dew deposition to arid valleys, as seen at the Elqui Valley in the Andes (Khodayar et al. 2008). Small bodies of water on valley floors do not develop appreciable lake breezes, although they can significantly affect surface energy budgets, valley wind strength and extent, and moisture distribution (Sturman et al. 2003a, b). Relatively large lakes on valley floors can develop lake breezes that interact with slope and valley wind systems, with internal boundary layers forming at the lake-land boundary (McGowan and Sturman 1996; Zardi et al. 1999; de Franceschi et al. 2002). Bergström and Juuso (2006) used a numerical simulation to compare up-valley winds occurring with and without a water body at the bottom of the valley, finding that the lower lake surface temperatures lead to higher daily average wind speeds.

3.3. Topographic effects on valley flows

3.3.1 Tributary valleys

In valleys with tributaries, upstream flows divide at each confluence of a side valley with the main valley, and downstream flows merge into a single down-valley wind. Bifurcating flows and merging flows have not been extensively researched, but one would expect that the topography in the vicinity of the merging valleys and wind system characteristics in the main and tributary valleys would be determining factors for the structure of the valley wind system. Because of the many different forms of topography and the range of wind system characteristics, it is not clear if investigation of a specific instance would provide information general enough to be applicable to other valleys. However detailed studies of the structure and dynamics of flow mergings or bifurcations at single situations are crucial to provide a better understanding of local pollutant concentrations, as shown by Banta et al. (1997), Fiedler et al. (2000) and Zängl and Vogt (2006). The requirement of mass flux balance may result in a closed circulation in which return flows produce enhanced subsidence or rising motions over the valley juncture, affecting temperature and wind structures there (Freytag 1988; Zängl 2004).

The bulk effect on nighttime along-valley mass flux in a main valley by inflow from a tributary box canyon was investigated in the Atmospheric Studies in Complex Terrain (ASCOT) program in the 1980s (Coulter et al. 1989, 1991; Porch et al. 1991). The tributary provided more mass flux to the main canyon than would have come from a simple valley sidewall. Simulations of ideal valley-tributary systems by O’Steen (2000) supported this conclusion. They also showed that the increase in down-valley mass flux in the main valley

begins well before the tributary is encountered, suggesting that the mechanism by which a tributary provides additional mass flow to the main valley is more complicated than suggested by the intuitive notion of a simple side-stream contribution at the confluence with a concomitant increase in valley flux downstream of the tributary. In some cases the flow down the main valley actually decreases in a layer corresponding to the outflow height of the tributary flow. This leads to a negative correlation of flow down the main valley and flow out of the tributary. Cold air flowing out of the tributary is apparently blocked by cold air flow coming down the main valley. Cold air thus tends to accumulate in the tributary and then enter the main valley through surges. Alternatively, the tributary contribution may glide over the main valley's core flow. Conservation of momentum requires that the increased mass of cold air from the tributary slows the main valley flow, allowing additional flow to exit the tributary. The latter may assume the form of a regularly pulsating outflow, and modulate low-frequency oscillations in the main valley wind, as shown by Porph et al. (1991).

Drainage flow from tributaries depends not only on cooling rates, but also on ambient winds. Unexpectedly, an external wind blowing in opposition to the drainage wind can strengthen the drainage wind. The mechanism is not fully understood: perhaps circulation cells introduce mass from the ambient wind into the tributary system (Coulter et al. 1989). In any case the orientation of the tributaries to the main valley appears to be a controlling factor in the interactions between tributary and valley flows, and periodic flow out of the tributaries can modulate oscillations in the main valley drainage flow (Coulter et al. 1991)

3.3.2 Canyons

Canyons, valleys having relatively high depth-to-width ratios and steep sidewalls, are subject to the same up- and down-valley flow regimes as valleys. A canyon that is a segment of a longer valley may have one of two effects on drainage flows. If the canyon is narrow or tortuous, it may restrict the valley flow. During nighttime this may cause a cold-air pool or cold air lake to develop above the canyon constriction (Whiteman 2000). If, on the other hand, the canyon is not too narrow, the air may accelerate through the constricted canyon to conserve the total momentum of the downvalley flow. The flow and temperature structure in a canyon are affected by several physical processes. Deep narrow canyons have weak downslope flows on the steep slopes (see section 2.5.1) because of a reduced longwave radiation loss caused by the restricted view of the sky and by enhanced radiative interactions between the sidewalls that tend to drive the canyon atmosphere toward isothermality. Turbulence generated at the ridgeline by terrain interactions with above-canyon flows, or turbulence generated in valley flows by terrain elements, tend to mix the canyon atmosphere (Start et al. 1975). Simulations of nocturnal drainage flows in small rugged canyons (Lee et al. 1995) have shown that coupling with upper winds may produce multi-vortex structures that are very sensitive to the radiation budget. Canyons sometimes act as conduits between segments of a valley having quite different climates (e.g., the Columbia Gorge, a canyon between Oregon and Washington, USA). Strong temperature contrasts between the segments can accelerate the normal canyon flows (e.g., Sharp and Mass 2004).

Arizona's Grand Canyon of the Colorado River, one of only a few deep canyons that have been investigated, maintains only weak stability during both day and night in winter (Whiteman et al. 1999c). This may be due to terrain-enhanced interactions between above-canyon flows and air within the canyon or to overturning of the canyon atmosphere by cold air generated on snow-covered mesas to the north and south of the canyon. Temperature jumps form at the top of the canyon when warm air advection occurs across the canyon rim. Because stability in the canyon is near-neutral, wintertime valley flows are weak and the flow along the canyon is driven by pressure gradients that are superimposed on the canyon by traveling synoptic-scale weather disturbances, with flow directed from the high pressure to the low pressure end of the canyon. Nonetheless, weak diurnal valley flows are sometimes present at the north end of the canyon in the vicinity of the Little Colorado River (Banta et al. 1999).

3.4 Modeling of the valley flows

The state of the art on modeling of thermally driven flows was reviewed by Egger (1990). Contributions to the understanding of diurnal valley flows have come from a range of modeling approaches including conceptual, laboratory tank, Navier-Stokes, analytical and large-eddy simulation models. By means of a simplified mixed layer model over idealized topography, Kimura and Kuwagata (1995) showed how the sensible and latent heat that accumulate in an atmospheric column are dependent on the scale of the topography. Whiteman and McKee (1982) used a simple thermodynamic model to explain the basic mechanisms governing the morning breakup of nocturnal inversions in valleys. Zoumakis and Efstathiou

(2006a, b) extended this approach to obtain a criterion for estimating the time required for the complete breakup and development of a CBL. Conceptual and analytical models relating the energy budget and valley geometry to the rate of atmospheric cooling in a valley were developed by McKee and O'Neal (1989). Vergeiner (1987) used an analytical model to study basic relationships between the strength and response time of a valley flow as a function of topographic characteristics such as valley length, width, or depth. A hydraulic model reproducing the development of diurnal up-valley wind, based on concepts of mixed layer schemes, was proposed by Zardi (2000).

Similarly to what has been discussed above for slope winds, a more complete understanding of the atmospheric processes leading to diurnal valley flows has been provided by numerical models. In the last two decades the achievements in this field have benefitted from the increasing availability of suitable computers and from the impressive progress in the development of numerical weather prediction models. Further information on numerical modeling is provided in **Chapters 9, 10 and 11**.

Diurnal mesoscale circulations such as slope and valleys flows are not resolved by the coarse grids in general circulation and climate models, and must accordingly be parameterized as turbulent motions. However, only smaller-scale turbulence and convection are presently represented in boundary-layer parameterizations, based on similarity arguments and data from flat terrain experiments. Even though vertical heat fluxes induced by the diurnal slope and valley flows are as large as or even larger than turbulent fluxes produced by smaller-scale turbulence and convection, they are not yet considered in these parameterizations (Noppel and Fiedler 2002; Rotach and Zardi 2007).

Simulations of idealized valleys, with simplified initial and boundary conditions, have led to a deeper insight into individual mechanisms affecting the dynamics of diurnal valley winds. These simulations are particularly valuable in identifying the relative roles of processes that are difficult to isolate in more realistic topography and weather situations. While many idealized simulations have already been mentioned in this chapter, space is unavailable here to provide a detailed account of all of them. Representative articles include those of Enger et al. (1993); Atkinson (1995); Anquetin et al. (1998); Li and Atkinson (1999); O'Steen (2000); Rampanelli et al. (2004); Bergström and Juuso (2006); Bitencourt and Acevedo (2008); Schmidli et al. (2010); Schmidli and Rotunno (2010); and Serafin and Zardi (2010a, b, c).

The complexity of real mountain valleys provides a stimulating challenge for numerical simulations. The spatial resolution of present models is not yet fine enough to reproduce all the small-scale features of valley winds. High resolution digital elevation databases have to be significantly smoothed before they are used for model runs, and information on land cover, land usage, and soil moisture is often approximate or incomplete. Nevertheless, many simulations of real cases have proven useful, as the reader may appreciate by inspecting the reference papers by Leone and Lee 1989; Gross 1990; Koračin and Enger 1994; Fast 1995, 2003; Ramanathan and Srinivasan 1998; Colette et al. 2003; Zhong and Fast 2003; De Wekker et al. 2005; Chow et al. 2006; Lee et al. 2006; Weigel et al. 2006; and Bischoff-Gauß et al. 2006, 2008. Model outputs must be carefully compared with available observations to make sure that the simulations capture the relevant mechanisms. Understanding of the model outputs benefits from good visualization tools and from physical insight and conceptual models. Additional confidence is gained when comprehensive field observations are available for comparison. Thus, simulations are usually done in conjunction with large observational programs.

3.5. Exceptions and anomalies

The occurrence of anomalous valley winds, i. e. developing in apparent contradiction to established concepts and theories, has stimulated broad debates and deeper analyses since earlier investigations in the field. Wagner's (1938) seminal paper, for example, mentioned two Alpine wind systems that were known to contradict valley wind theory. The Maloja wind in Switzerland's Upper Engadine Valley northeast of the Maloja Pass and the *Ora del Garda* in the Adige (in German, Etsch) Valley near Trento, Italy, are both known to blow down-valley during daytime.

The Maloja wind was investigated in a modeling study by Gross (1984, 1985), who also focused on the development of a narrow, elongated cloud (the *Maloja Schlange*, English: Maloja snake) that sometimes forms in conjunction with the wind and stretches northeastward from the pass. The anomalous Maloja wind is an up-valley wind from the Bergell Valley to the southwest of the pass that intrudes into the Upper Engadine Valley as a down-valley wind. The explanation for the anomalous wind is the peculiar

topography in the Maloja Pass region, where the Bergell ridgelines extend beyond the pass into the Upper Engadine Valley.

The outflow of the *Ora del Garda* in the Adige Valley during the early afternoon appears as an “abnormal flow development” (Wagner 1938) over a whole segment of the valley including the city of Trento. There, the wind near the surface flows down-valley for the whole afternoon, rather than blowing up-valley as expected. The down-valley flow is caused by the spillover into the Adige Valley of relatively cold air through an elevated saddle from the upper Valle dei Laghi, which joins the Adige Valley just up-valley from Trento (**Figure 11**). In the late morning a lake breeze develops at Lake Garda at the southern inlet of the Valle dei Laghi. The cold lake air is carried up-valley and over the elevated saddle. The airflow blowing down from this saddle onto the Adige valley floor in the early afternoon on fair weather days brings potentially cooler air, which then flows underneath the up-valley wind blowing at that time in the Adige Valley. The flow splits into an up-valley ground-level flow north of the junction and a down-valley flow south of the junction. Earlier researchers, relying only on surface observations, could not explain the phenomenon. Subsequent field campaigns (reported in Wagner 1938) and recent ones (de Franceschi et al. 2002) identified the vertical structure of the valley atmosphere and demonstrated that the flows are compatible with known dynamics.

In recent years, other cases of anomalous winds have been observed and explained. In most cases the aberrant winds are produced by a large source of cold or warm air at one end of the valley or the other. For example, nighttime down-valley winds often fail to reverse during daytime in winter when the valleys are covered with snow (Emeis et al. 2007; Schicker and Seibert 2009). Austria's Inn Valley (Whiteman 1990) and Germany's Loisach Valley (Whiteman 2000) are examples. Similarly, valleys with large sources of cold air at their lower end (e.g., an ocean or a long lake) can have up-valley winds that fail to reverse at night. The strong and continuous cold air advection can cause the valley atmosphere to remain stably stratified during daytime with only weak development of a shallow convective boundary layer at the valley floor. Examples of valleys exhibiting this behavior include Chile's Elqui Valley (Kalthoff et al. 2002; Khodayar et al. 2008), which ends at the Pacific Ocean, and California's San Joaquin Valley (Zhong et al. 2004; Bianco et al. 2011). Up-valley flows in the San Joaquin Valley are also promoted by a large source of warm air in a desert area at its upper end.

Anomalous nighttime up-valley and daytime down-valley winds occur at several sites along the Colorado River upstream of the Grand Canyon (Whiteman et al. 1999a). The valley floor in this area is a series of basins connected by narrow canyons. The anomalous winds represent flows that converge at the lower ends of the basins during nighttime and diverge out at the upper ends of the basins during daytime. Another anomaly can be observed in the Marble Canyon area north of the Grand Canyon where nighttime winds flow up-valley. This has been attributed to the presence of a major geological formation that tilts downward in the up-valley direction (Whiteman et al. 1999a).

4. Phases of and interactions between the slope and valley winds

The evolution of the coupled slope and valley systems during a typical day progresses through four distinct phases, described below.

4.1. Daytime phase

This phase typically begins in mid to late morning, after the nighttime valley temperature inversion has been removed by daytime heating. The air in the valley is warmer than over the adjacent plain, producing a lower pressure in the valley than over the plain, and the resulting horizontal pressure gradient causes air to flow up the valley axis (**Figure 8**, upper panel).

Once the nocturnal temperature inversion is destroyed, convection from the heated valley surfaces extends above the valley ridges. Vertical mixing associated with the convection couples the flow in the valley to the background or synoptic-scale flows aloft. The pressure gradients producing these flows are superimposed on the local, thermally produced pressure gradient within the valley. Winds within the valley can be affected by this coupling, although the background flows are generally channeled along the valley axis. It is typical, in fact, that wind speeds, both in a valley and over a plain, increase in the afternoon due to the coupling with the usually stronger winds aloft (Whiteman 2000).

Maintenance of the daytime up-valley flow requires that temperatures in the valley cross-section be greater than at the same level over the adjacent plain (or at the same altitude farther down the valley). The TAF contributes to additional heating in the valley, as solar radiation coming across the top of the valley at ridgetop level, once converted to sensible heat flux at the valley floor and sidewalls, overheats the air in the valley relative to the adjacent plain because of the smaller volume in the valley. Radiative processes are also more effective within the valley than over the surrounding plain because the valley air mass is partially enclosed by radiating surfaces. In addition, advective heat transfer to the valley atmosphere is more effective than the convective heat transfer to the same elevation over the lower-altitude plain, again due to the smaller volume of air to be heated. The extra heating in the valley invigorates the convection from the valley after the inversion is destroyed, but this effect decreases as the mixed layer grows deeper above the ridges.

4.2. Evening transition phase

The surface energy budget reverses above valley surfaces when outgoing longwave radiation first exceeds incoming shortwave radiation. This usually occurs initially in late afternoon in areas of the valley that are shadowed by terrain. With this energy budget reversal, the ground begins to cool and a downward turbulent sensible heat flux begins to remove heat from a layer of air above the surface. A shallow layer of cooled air thus forms over the sidewalls and floor of the valley. Over the slopes, the air in this layer becomes negatively buoyant compared to the air adjacent to the slope, and begins to move down the slope. The downslope flows converge onto the valley floor or, after a temperature inversion forms on the valley floor, into the elevated portion of the inversion. Rising motions over the valley center that compensate for downslope flows on the sidewalls produce upward cold air advection that cools the entire valley cross-section (Whiteman 2000; Fast and Darby 2004; Brazel et al. 2005). Other processes play a role, including radiative transfer and the continuing cold air advection associated with the daytime up-valley flow. Up-valley winds continue to blow for several hours after the energy budget reversal because of inertial effects and because it takes some time for the cooling over the valley slopes to be transferred to the entire valley volume through compensatory rising motions and other processes. The temporary post-sunset continuance of the up-valley flow generates shear that increases turbulent sensible heat flux in the surface layer (Kuwapata and Kimura 1995, 1997; de Franceschi et al. 2002, 2009; de Franceschi 2004). Once the air in the valley cross-section becomes colder than the air over the adjacent plain, the pressure gradient reverses and the winds reverse from up-valley to down-valley. The reversal occurs first in the ground-based stable layer (temperature inversion) that forms on the valley floor. The stable layer containing down-valley winds grows rapidly in depth in the early evening, causing the down-valley winds to increase in strength and depth. The rate of growth of the inversion gradually decreases as it fills the valley (Whiteman 1986) and the cooling rate decreases exponentially for the remainder of the night. The bulk of the total nighttime cooling occurs in the first few hours following sunset (De Wekker and Whiteman 2006). The residual air layer, previously flowing up-valley, is then lifted above the growing stable layer. This up-valley flow gradually decreases in strength until it is overcome by background flows above the valley, which are often channeled along the valley axis.

During the evening transition period the downslope flows that defined the beginning of the period gradually decay as a strong stable layer builds up within the valley and as down-valley flows in the stable layer expand to fill the valley volume. The downslope flows on the valley sidewalls within the growing stable layer respond to the increasing ambient stability by decreasing their strength. They continue on the upper sidewalls of the valley above the growing stable layer, but leave the sidewall and converge into the main valley volume once encountering the growing stable layer (cf. Catalano and Cenedese 2010).

During the period of weakening up-valley flow and reversal to down-valley flow, strong radiative cooling along the uneven valley floor and slopes results in the formation of shallow cold air layers, that preferentially fill low spots on the valley floor and extend up the sidewalls. These near-surface stable layers decouple the surface from the flow aloft. During this period of light and variable winds the surface-based temperature inversion often strengthens (Fast and Darby 2004). The formation of the shallow cold air layer on the floor and sidewalls tends to decouple the valley winds (whether up- or down-valley) from the friction of the earth's surface. Sometimes, an acceleration in valley wind caused by this decoupling increases the shear across the shallow layers and briefly mixes them out, producing transient evening temperature rises at the valley floor or on the slopes (Whiteman et al. 2009). Oscillations may be generated in the valley and slope winds if the cold air layer repeatedly reforms and decays.

4.3. Nighttime phase

The beginning of the nighttime phase is hard to define because it is tied to the gradual buildup of a stable layer containing down-valley winds rather than to a discrete event. Typically, in clear undisturbed conditions the nighttime phase starts sometime during the period from several hours after sunset until about midnight.

The main characteristic of the nighttime phase is the predominance of down-valley flows throughout the valley volume. The maintenance of the down-valley wind requires that the atmospheric cross-section continues to cool relative to the adjacent plain. Because the downslope flows become weaker and shallower during the latter part of the evening transition phase and are more and more affected by (i.e., turned into the direction of) the down-valley flows (Whiteman and Zhong 2008) the importance of compensatory rising motions over the valley center to this cooling is reduced. Instead, horizontal and vertical shears at the valley surfaces produced by the increasing strength of the down-valley flow throughout the cross-section become increasingly responsible for turbulent transport of heat toward the radiatively cooling surfaces and the continued cooling of the valley cross-section.

The pressure gradient that drives the valley flow is at a maximum at the valley floor. The vertical wind profile, however, takes a jet-like shape with the wind maximum displaced 10s to 100s of meters above the floor. The wind speed is reduced at the surface by friction (Khodayar et al. 2008), and the winds above the jet gradually give way to the gradient flow above (Zhong et al. 2004). Wind profiles on a horizontal valley cross-section also show a jet-like shape with the peak wind over the valley center where the frictional influence of the sidewalls is minimized. The nighttime down-valley wind current is thus sometimes called a *down-valley jet* (DVJ), and vertical and horizontal cross-sections through the current in a deep valley can be described in terms of Prandtl's well-known mathematical expression and a parabolic profile, respectively (Clements et al. 1989; Coulter and Gudiksen 1995; Fast and Darby 2004). Because the peak winds generally occur over the valley center, measurements taken at one location on a valley cross-section may be not representative of the overall wind structure (King 1989). The establishment of the DVJ is sometimes associated with abrupt warming at low levels as a result of downward mixing and vertical transport of warm air from the inversion layer above (Pinto et al. 2006). Time-periodic phenomena, such as pulses in the strength of the DVJ (possibly contributing to vertical transport by creating localized areas of low-level convergence) as well as gravity waves and Kelvin–Helmholtz waves, which facilitate vertical mixing near the surface and atop the DVJ, are commonly observed. These are reflected in the spectra of velocity and temperature fluctuations (Stone and Hoard 1989). Typical periods of these oscillations are around 20 min (Porch et al. 1991).

Nocturnal drainage flow along the valley floor displays very irregular behavior, its structure being strongly determined by the local orography (Trachte et al. 2010). Experimental evidence confirms the intuitive idea that drainage winds “slide” along the ground and strongly adhere to its shape (Clements et al. 1989; Eckman 1998; Fiedler et al. 2000; Haiden and Whiteman 2005). The down-valley flow sloshes toward the outside of valley bends due to inertial forces (Sakiyama 1990).

4.4. Morning transition phase

The morning transition begins shortly after sunrise, when incoming solar radiation exceeds longwave radiation loss and the surface energy budget reverses on the sidewalls. The end of the morning transition is marked by the break-up of the ground-based inversion that fills the valley at night. Inversions break up occurs in a fundamentally different way in valleys (Whiteman 2000) than over plains (Stull 1988). Whereas the plains atmosphere is heated primarily by the upward growth of an unstable or convective boundary layer, heating of the valley atmosphere results not only from the (limited) growth of an unstable boundary layer (cf. Weigel et al. 2007), but also from subsiding motions in the valley core that compensate for upslope flows on the sidewalls.

After sunrise, as the slopes and valley floor are illuminated by the sun, the surface energy budget reverses, and heat is transferred upward from the surface to an initially shallow but progressively growing layer of air above the heated surfaces. The layer of warming air over the sidewalls is on an inclined surface. Air at any point within this layer is warmer than the air outside the layer at the same height, resulting in an upslope flow. Differences in insolation on slopes – due to slope exposure, shadows, ground cover, etc. – cause the incipient upslope flows to be somewhat intermittent and inhomogeneous. Convection above the heated slopes and valley floor entrains air from the elevated remnant of the nocturnal inversion (“stable core”) into the upslope flow, which carries it to the valley ridgelines and vents it into the free atmosphere. During this

process, some horizontal transport of mass and heat can contribute to the heating of the valley atmosphere, especially when mid-level stable layers are encountered, or when topography projects into the valley atmosphere. The transport of heated air up the sidewalls is compensated by sinking of the stable core over the valley center. Because the stable core is statically stable, subsidence causes downward advection of potentially warmer air, heating the atmosphere over the valley center, and eventually causing the valley atmosphere to become warmer than the air over the plain. The resulting horizontal pressure difference between the valley atmosphere and the atmosphere over the adjacent plain initiates an up-valley flow.

The break-up of nocturnal inversions in valleys was investigated in western Colorado valleys by Whiteman (1982), resulting in a conceptual model and a simple thermodynamic model (Whiteman and McKee 1982), and by Brehm and Freytag (1982) in the Alps. Break-up requires that a valley be warmed from its initial inversion temperature profile to a neutral profile having the potential temperature of the inversion top at sunrise. The two main processes accomplishing the breakup are the warming associated with convective boundary layer growth upward from the heated ground and the warming caused by subsidence that compensates for mass removal from the valley atmosphere by upslope flows. The warming can be amplified by valley geometry as explained by the TAF principle. The time required to destroy the Colorado inversions depended on inversion strength at sunrise and the rate of input of sensible heat from the valley surfaces after sunrise, which varies with season and snow cover. The Colorado valley inversions typically broke up within 3 to 5 hours after sunrise. Bader and McKee (1983), in a numerical model study, found that a third mechanism, horizontal heat transfer from the sidewalls, could also heat the valley atmosphere and contribute to inversion breakup. This process is particularly effective in the short period of time between sunrise and the time when upslope flows extend continuously up the sidewalls. Upslope flows may detach from the slopes and intrude horizontally into the valley atmosphere at elevations where sub-layers of high stability occur within the stable core (Harnisch et al. 2009). Eckman (1998) and Rampanelli et al. (2004) performed simulations in idealized valleys to investigate along-valley aspects of the inversion breakup. They found that if the plain and the valley floor are perfectly horizontal, effects of valley-plain contrasts concentrate in a region close to the mouth of the valley and weaken with distance up the valley. Accordingly, the valley winds develop only in a limited region upstream and downstream of the mouth of the valley. However, when the valley floor is even weakly inclined, buoyancy effects can drive valley winds farther up the valley (Rampanelli et al. 2004). By modifying Whiteman and McKee's thermodynamic model of valley inversion breakup, Zoumakis and Efstathiou (2006a, b) focused on the relative partitioning of energy into convective boundary layer growth and subsidence warming, but without considering horizontal heat transfer. The occurrence of warm or cold air advection over the valley during the inversion breakup period can change the heating requirement (Whiteman 1982; Whiteman and McKee 1982). Warm air advection increases the time required to destroy the inversion, while cold air advection has the opposite effect. Further, cold air advection within the valley atmosphere increases the heating requirement, and thus the time required to break the inversion.

The warming effect of compensatory sinking motions decreases in wider valleys (Serafin and Zardi 2010b) and simulations show that compensatory sinking plays only a small role in inversion breakup if the valley's width to depth ratio exceeds about 24 (Bader and McKee 1985). Inversions take longer to break up in wintertime and in deep valleys (Whiteman 1982; Kelly 1988; Colette et al. 2003). The asymmetric distribution of surface sensible heat flux between the opposing sidewalls of a valley may result in a nonuniform inversion breakup (Urfer-Henneberger 1970; Kelly 1988; Ramanathan and Srinivasan 1998; Anquetin et al. 1998; Matzinger et al. 2003; Whiteman et al. 2004b). Gravity waves and horizontal mixing within the stable layer effectively redistribute warm air and reduce temperature differences due to differential sidewall heating (Bader and McKee 1983). Cross-valley flows may develop and be superimposed on the valley circulations when sensible heat fluxes differ greatly on the opposing sidewalls of a valley (Gleeson 1951; Bader and Whiteman 1989; Atkinson 1995).

Especially in narrow valleys, the stable core inhibits the growth of a convective boundary layer above the valley floor and sidewalls and delays the development of deep convection (Furger et al. 2000; Bischoff-Gauß et al. 2006; Chemel and Chollet 2006). Indeed, convective boundary layers over a valley floor are typically not as deep as over an adjacent plain (Dosio et al. 2001; de Franceschi et al. 2003; Rampanelli and Zardi 2004; Rampanelli et al. 2004; Weigel and Rotach 2004; Bergström and Juuso 2006; Chemel and Chollet 2006; Weigel et al. 2006; Bischoff-Gauß et al. 2008). Convective eddies in the relatively shallow convective boundary layer over the valley floor efficiently mix and horizontally homogenize the convective boundary layer. It thus exhibits weak cross- and along-valley variability over the valley floor (Zängl et al. 2001; De Wekker et al. 2005; Chemel and Chollet 2006) unless strong terrain heterogeneities exist (Ramanathan and Srinivasan 1998).

Switzerland's Riviera Valley (Weigel and Rotach 2004; De Wekker et al. 2005; Weigel et al. 2006) exhibits some hitherto unknown meteorological characteristics that are produced by a bend in the valley. During the morning transition period inertia causes the up-valley flow that enters the valley from the Magadino plain to drift toward the outside of a bend at the lower end of the valley and develop a cross-valley wind component. This produces a cross-valley tilt of the inversion layer and anomalous downslope flows on the sunlit western sidewall that transport warm air downward toward the valley floor, stabilizing the valley atmosphere. Cold-air advection in the up-valley flow, subsidence of warm air from the free atmosphere aloft (compensating for up-slope flows), and curvature-induced secondary circulations in the southern half of the valley produce a tendency for the valley atmosphere to remain rather stable all day, although a shallow convective boundary layer does grow slowly upward from the valley floor during daytime. The valley circulation thus has a prolonged morning transition phase, rather than a daytime phase. Other investigators (Cox 2005; Bergström and Juuso 2006; Bischoff-Gauß et al. 2006) have also reported valleys that maintain persistent stable layers during daytime up-valley flows. A common characteristic of several such valleys is a large source of cold air at the valley mouth, such as a long lake or an ocean. During daytime, a stable stratification and negative sensible heat fluxes can be maintained over lake and ocean surfaces while the nearby land surfaces maintain strong positive fluxes (McGowan and Sturman 1996; Bischoff-Gauß et al. 2006). These cases provide examples of another mechanism by which cold air can be advected continuously up the valley, reducing temperatures, maintaining stability and suppressing CBL growth.

5. The mountain-plain wind system

The daytime heating and nighttime cooling contrast between the mountain atmosphere over the outer slopes of the mountain massif and the free atmosphere over the surrounding plain produces the horizontal pressure differences that drive this wind system. The mountain-plain wind system brings low level air into the mountain massif during daytime (the plain-to-mountain wind), with a weak return circulation aloft. During nighttime, the circulation reverses, bringing air out of the mountain massif at lower levels (the mountain-to-plain wind), with a weak return circulation aloft. The daytime circulations are naturally somewhat deeper and more energetic than the nighttime circulations because of the larger daytime heat fluxes and the correspondingly deeper daytime boundary layer. The reversal of this large-scale wind system is somewhat delayed relative to the slope and valley wind systems because of its larger mass.

The mountain-plain circulation is associated with a diurnal pressure oscillation between the mountainous region and the adjacent plains (for the Alps, cf. Frei and Davies 1993; for the Rocky Mountains, cf. Li and Smith 2010). For the largest mountain, this oscillation can be detected in one or more modes of the atmospheric tides observed at global scale (Dai and Wang 2000).

According to Ekhardt (1948), the mountain-plain wind system occupies a separate outer layer from the valley and slope wind systems (see **Figure 1**). An alternative way of thinking of the mountain-plain wind would be to consider it as encompassing both the slope and valley wind systems, as all three wind systems interact to transport mass to and from a mountain massif from its surroundings.

Mountain-plain circulations play a key role in moisture transport and initiation of moist convection (see also **Chapters 6** and **7**) as well as in long-range transport of air pollutants and their precursors (see also **Chapter 5**). Convergence of the daytime flows over the mountains produces afternoon clouds and air mass thunderstorms, and the divergent nighttime sinking motions produce late afternoon and evening clearing. Pollutants associated with population centers on the plains adjacent to mountains are carried toward the mountains during daytime, where they are transported vertically to higher altitudes (Henne et al. 2005).

Due to the large spatial extent of mountain-plain circulations, their basic features can be monitored by conventional networks of surface and upper air observing stations (Kalthoff et al. 2002; Lugauer and Winkler 2005; Henne et al. 2005, 2008; Taylor et al. 2005; Steinacker et al. 2006; Bica et al. 2007; Li et al. 2009). Mountain-plain flows are generally weak, usually below 2 m s^{-1} , with much lower speeds in the broader and often deeper return flows aloft, and can easily be overpowered by prevailing large scale flows. The mountain-plain circulation is diurnal, with its evolution occurring in phases (Bossert and Cotton 1994a, b) and may be influenced by large-scale conditions (Lugauer and Winkler 2005). The characteristic weather associated with the plain-to-mountain circulation depends on the moisture levels in the surroundings. Where dry air masses are present, such as in the Colorado Plateau (Bossert et al. 1989; Bossert and Cotton 1994a, b), the circulations are marked by strong winds, low cloudiness, and isolated thunderstorms. Where

the mountains are surrounded by oceans or other sources of low-level moisture, as in Western Sumatra (Sasaki et al. 2004; Wu et al. 2009) or the Alps (Ekhardt 1948; Weissmann et al. 2005), the daytime rising motions transport moisture to higher levels of the atmosphere and produce widespread clouds and precipitation. In some cases mountain-plain circulations also interact with sea breezes (Taylor et al. 2005; Hughes et al. 2007).

Persistent temperature differences between the mountain atmosphere and the surroundings occur seasonally in some mountain ranges. Seasonal thermal contrasts are the primary driver of *monsoonal circulation*, that bring cold air out the mountain massif during winter and into the mountain massif during summer. These large-scale seasonal circulations are a type of mountain-plain circulation, often with diurnal oscillations of wind strength superimposed on them. The initiation of the summer monsoon caused by the heating of the mountain atmosphere in spring is responsible for the initiation, for example, of the Himalayan Monsoon (Barros and Lang 2003) and the variously named North American, Southwest, Mexican or Arizona Monsoon that affects the southwestern United States (Higgins et al. 2006).

The remainder of this section will discuss mountain-plain circulations that develop around the east-west oriented Alps and around the north-south oriented Rocky Mountains of North America. The mountain-plain system develops regardless of the orientation of a mountain range. The mountain-plain circulations that develop between plains and *elevated basins or plateaus* are discussed in section 2.6.

5.1. Mountain-plain winds in the Alps

The theory of diurnally reversing mountain wind circulations published by Prof. A. Wagner (1932, 1938) included a postulated "equalizing flow" between the plains and mountains. The evidence for these flows was collected by Wagner and his students, most notably E. Ekhardt and A. Burger. Burger and Ekhardt (1937) analyzed summer wind data obtained by the optical tracking of pilot balloons released twice-daily from 20 stations located in and around the Alps to find that a daytime circulation brought air into the Alps from the surrounding plains, with a weak compensation current ("Ausgleichströmung"), or return circulation, aloft. The thermal origin of this phenomenon and the associated horizontal pressure differences that drive the mountain-plain circulation were investigated further by Ekhardt (1948). In recent years new analysis tools such as the Vienna Enhanced Resolution Analysis (VERA; Steinacker et al. 2006; Bica et al. 2007) have been used with the dense network of surface stations in the Alps to provide additional information on the thermal forcing of mountain-plain circulations.

New information on the Alpine mountain-plain circulation has come from a research program called Vertikaler Austausch und Orographie (VERTIKATOR, or Vertical Exchange and Orography), which supported a major field experiment in July 2002 on the north side of the Alps in the Bavarian foreland (Lugauer et al. 2003). On summer days radiative heating of the Alps produces a horizontal transport of air from the foreland into the Alps, and a vertical transport from the boundary layer into the free troposphere above the mountains. The daily vertical transport of air and moisture over the Alps by the mountain-plain circulation has been termed "Alpine pumping" (Lugauer et al. 2003). Climatological investigations, using the extensive network of surface stations in the Alpine foreland, have provided additional information on the spatial and temporal extent of the circulation (Lugauer and Winkler 2005; Winkler et al. 2006). The circulation is strongest on days when background upper-air flows are weak and when daily incoming solar radiation exceeds about 20 MJ m^{-2} . Because incoming radiation is strongest in summer, the flows are most common and best developed between April and September. The diurnally reversing mountain-plain circulation extends approximately 100 km north of the Alps to the Danube River. The low-level flow coming into the Alps during daytime, with speeds generally less than 2 m s^{-1} , extends gradually farther into the plains during daytime and extends vertically to reach about 1-2 km depths at the edge of the Alps by mid-afternoon. Rising motions over the Alps produce cloudiness and precipitation, while the descending return branch of the circulation suppresses convective cloud formation north of the Alps. An intensive VERTIKATOR field study on 12 July 2002 used an airborne Doppler lidar, a wind-temperature radar, dropsondes, and rawinsondes to gain additional information on the daytime circulation (Weissmann et al. 2005). Vertical velocities in the rising branch of the circulation were on the order of 0.05 to 0.10 m s^{-1} . Despite its large scale, the plain-to-mountain circulation responded readily to local geographical and dynamic features. High-resolution simulations with numerical models were able to reproduce the general flow structure and, when combined with vertical motion data from the lidar, were able to estimate the daytime mass fluxes into the Alps (Weissmann et al. 2005).

5.2. Mountain-plain winds in the Rocky Mountains

A robust mountain-plain circulation, forced by the diurnal cycle of solar heating and longwave cooling, is a key feature of flows around the Rocky Mountains (Reiter and Tang 1984). The circulation is strongest on clear days and nights, when background synoptic-scale flows are weak. These conditions occur most frequently in summer and fall. The diurnal geopotential height differences between the Rocky Mountains and the surrounding plains, and the resulting near-surface diurnal inflows and outflows, cause moisture convergence and divergence (Reiter and Tang 1984). The daytime convergence over the mountain crests produces afternoon thunderstorms and affects precipitation patterns. The nighttime divergence causes sinking motions over the mountains that tend to reduce cloudiness and precipitation. The inflow and outflow cycle can be detected in wind observations at mountaintop locations, with inflows and outflows at speeds of several meters per second (Bossert et al. 1989). Transition periods tend to be long. The transition from the daytime inflow to nighttime outflow occurs from 1900 to 0200 MST, the outflow to inflow transition takes place from 0600 to 1100 MST. The transition from inflow to outflow is much faster on highly convective days when evaporation of precipitation cools the heated boundary layer over the mountains.

Harmonic analysis of summer wind data from the network of radar wind profilers in the central United States shows that diurnal circulations extend up to 1200 km eastward from the Rocky Mountains over the gently sloping Great Plains to the Mississippi River (Whiteman and Bian 1998). The strongest mountain-plain flows occur in the lowest kilometer of the atmosphere where speeds, as averaged over the 100-m range gates of the radars, reach up to 3.5 m s^{-1} just east of the mountains. The return flow aloft is distributed through a layer extending above the highest mountains ($\sim 4000 \text{ m}$) at speeds of a few tenths of a meter per second. The mountain-plain circulation decays with distance from the mountains.

Much of the research on the mountain-plain circulation has focused on the extensive plains to the east of the Rocky Mountains, where observational networks are fairly dense, but the wind system also is present on the western slopes of the Rockies and on the periphery of the mountain massif (Reiter and Tang 1984).

6. Diurnal wind systems in basins and over plateaus

Basins and plateaus, common landforms in many parts of the world, influence atmospheric motions on a variety of scales, from tens of meters to thousands of kilometers. Basins are hollows or depressions in the earth's surface, wholly or partly surrounded by higher land. An example of a basin that is only partly surrounded by mountains is the Los Angeles basin (Lu and Turco 1995), which is open to the Pacific Ocean on its western side. Closed basins with level unbroken ridgetops are rarely encountered. Plateaus are elevated, comparatively level expanses of land. Large plateaus include the Tibetan Plateau and the Bolivian Altiplano. A plateau partially or completely surrounded by mountains can also be referred to as an elevated basin.

Diurnal wind systems in basins and over plateaus are driven by horizontal pressure gradients that develop between the atmosphere within or over the topography and the free atmosphere of its surroundings. Basins and plateaus experience diurnal slope and mountain-plain wind systems but, if there is no well-defined channel, they lack a valley wind system. The large-scale mountain-plain wind system that carries air between an elevated basin and the surrounding plains is called a *basin-plain wind*. The daytime branch is the plain-to-basin wind and the nighttime branch is the basin-to-plain wind (Kimura and Kuwagata 1993). Similarly, the mountain-plain wind system over a plateau is called a *plateau-plain wind*. The daytime branch is the plain-to-plateau wind and the nighttime branch is the plateau-to-plain wind (Mannouji 1982).

6.1. Diurnal wind systems in basins

Meteorological experiments have been conducted in basins all around the world, including the Aizu (Kondo et al. 1989) and Ina Basins (Kimura and Kuwagata 1993) and a small frost hollow (Iijima and Shinoda 2000) in Japan, the McKenzie Lake basin (Kossmann et al. 2002; Zawar-Reza et al. 2004; Zawar-Reza and Sturman 2006a, b) in New Zealand, the Grünloch (Pospichal 2004; Whiteman et al. 2004a, b, c; Steinacker et al. 2007) and Danube Valley (Zängl 2005) basins in Austria, other small Alpine basins or *dolines* (Vertacnik et al. 2007), the Duero Basin in Spain (Cuxart 2008); a basin on the island of Majorca (Cuxart et al. 2007; Martínez 2011), in the Columbia (Whiteman et al. 2001; Zhong et al. 2001) and Colorado Plateaus basins (Whiteman et al. 1999b) of the western United States, and in Colorado's Sinbad Basin (Whiteman et al. 1996; Fast et al. 1996), Utah's Peter Sinks basin (Clements et al. 2003), and Arizona's Meteor Crater

(Savage et al. 2008; Whiteman et al. 2008; Yao and Zhong 2009; Fritts et al. 2010; Lehner et al. 2010; Whiteman et al. 2010; Haiden et al. 2011).

Slope winds are a feature of basin meteorology, just as they are for valley and plateau meteorology. Basins, however, if surrounded by mountains, have no equivalent to the valley wind. The absence of this wind system is responsible for the unusually cold nighttime minimum temperatures often experienced in basins. The low nighttime temperature minima (see examples in **Table 2**) can be explained by contrasting the situation in a closed basin to that in a valley. Air in a valley at night, once it becomes colder than air at the same level over the plains, begins to flow down the valley axis and is replaced by air that sinks into the valley from above. The air that sinks into the valley is statically stable and also warms adiabatically as it sinks, so that it is warmer than the air it is replacing. The down-valley flow thus causes a continuous import of warm air into a valley from aloft, reducing the potential for cold nighttime minima. Basins, in contrast, trap air in place and cool it continuously throughout the night. Extremes of minimum temperature are attained by radiative cooling on clear, dry, winter nights following synoptic incursions of cold air masses into a region. Cooling is increased on long winter nights and can be especially strong if a fresh cover of new snow insulates the basin air from ground heat fluxes. When winds aloft are weak, buoyancy forces tend to cause isentropes to become horizontal within the inversion in a confined basin. Thus, temperature measurements on the sidewalls become good proxies for free air temperatures over the basin center, allowing temperature 'soundings' to be made from surface-based instruments (Whiteman et al. 2004a).

Nocturnal cooling is often confined within a basin during the night, although in shallow basins the cooling may extend above the ridgeline and produce basin-to-plain outflows over the lower passes (Pospichal et al. 2003). Because TAF causes additional cooling in basins compared to the surrounding plains, a temperature jump may develop at night above the basin between the air cooled within the basin and the still-warm free atmosphere above (see e.g. Clements et al. 2003).

6.1.1 The diurnal cycle in basins

In fair weather conditions, undisturbed by clouds or background flows, the diurnal temperature structure in basins evolves similarly from day to day. During daytime, the basin atmosphere becomes well mixed, with a neutral temperature profile. In late afternoon, as shadows are cast on the sidewalls, the net longwave loss exceeds the net solar input, and the local energy budget reverses, with downward turbulent sensible heat flux removing heat from a shallow air layer above the slopes. As the shadows progress, the energy budget reverses over more and more of the surface area of the basin and downslope flows begin as cold air layers form over the slopes.

A common misperception, which arises by making an analogy between air and water, is that the nighttime cooling of the basin air mass is produced solely by the convergence of downslope flows onto the basin floor and the cooling induced by compensatory rising motions over the basin center. If this were the case, a series of soundings of the basin atmosphere would show the continuous rising of the top of a temperature inversion as the cold pool became deeper and deeper. In fact, as a layer of cold air builds up on the floor of a basin, the downslope flows no longer have the temperature deficit to reach all the way to the basin floor, and they converge near the top of the growing inversion layer. Observations show that much of the cooling in a basin takes place continuously throughout the basin's full depth, and this cooling continues throughout the night, even after the downslope flows slow and die as the ambient stability builds up within the basin. The radiative and sensible heat flux divergences that produce the cooling responsible for inversion buildup over flat plains, where no downslope flows are involved, also play a major role in basins. De Wekker and Whiteman (2006) have compared the cooling rates of valley, plain and basin atmospheres and have found that basin atmospheres cool more rapidly than those over plains or valleys. This is, no doubt, due to the TAF, the sheltering of the basin from background winds by surrounding terrain (Vosper and Brown 2008), the divergence of heat from the confined volume, and the exclusion of diurnal valley flows (which advect warm air into valleys from above and thus reduce their cooling rates). The mechanisms by which the basin atmosphere cools have been discussed by Magono et al. (1982), Maki et al. (1986), Maki and Harimaya (1988), Neff and King (1989), Kondo and Okusa (1990), and Vrhovec (1991). The cooling rates of basin (and valley) atmospheres usually decrease during the night, but the relative roles of turbulent and radiative flux divergences and advection are still unresolved. Cooling rates in basins and valleys can be reduced by cloudiness or when heat is released at the ground with the formation of dew or frost (Whiteman et al. 2007).

Nighttime temperature inversions in basins break up after sunrise (Triantafyllou et al. 1995; Whiteman et al. 2004b) following the same patterns that have been observed in valleys. The warming of the basin

atmosphere and the ultimate destruction of the nocturnal inversion is accomplished by convective currents from the heated floor and sidewalls, the transport of mass from the basin by advection in upslope flows over the sidewalls, and warming due to subsiding motions over the basin center that compensate for mass carried up the sidewalls. Subsiding motions are weaker in wider basins. Cross-basin asymmetries in the warming and in the convective boundary layer and wind structure can occur because of shadows cast into the basin by the surrounding terrain and by spatial variations in the receipt of solar radiation on sloping surfaces of different aspect (Hoch and Whiteman 2010). Cross-basin differences in insolation produce cross-valley temperature and pressure differences that produce cross-basin flows toward the warmer sidewall (Lehner et al. 2010). Inversions in small basins in Austria and the Western US, despite their great strength, break up somewhat earlier than inversions in western U.S. valleys (Whiteman et al. 2004b).

The daytime cycle of warming often extends high above a basin, because of strong daytime sensible heat fluxes and convection. The horizontal pressure gradients between the air over the basin and the air over the surrounding plain produce a plain-to-basin pressure gradient during daytime. In large basins the inflows are delayed by upslope circulation cells from inside and outside the basin that become anchored to the ridgeline surrounding the basin. This mechanism is explained further in the plateaus section below. A modeling study by De Wekker et al. (1998) shows that flows into an idealized basin (one with consistent ridge height) come over the basin ridgetop when horizontal pressure differences are present above the ridgeline, but the pressure gradient between air confined inside the basin and air outside the basin at the same height plays no role in initiating or maintaining the plain-basin flow unless there are gaps in the ridgeline.

Temperature inversions in basins often develop quite regularly on undisturbed nights, but there are a variety of perturbations that can occur in their development under disturbed conditions. A typical time series of temperature measurements at different heights on the sidewalls of the 150-m deep Gruenloch Basin are shown in **Fig. 12** for a period of four consecutive winter days following new snow on 30 November. The night of 1-2 December was a typical undisturbed night with clear skies and weak background winds. On disturbed nights, temperature inversions in this basin exhibit a variety of disturbances to the normal evolution of temperature structure, as shown in **Fig. 13**. These schematic illustrations of selected cold-pool disturbances were observed using the same sensors as for **Fig. 12**, but on disturbed nights in the 9-month period from October 2001 to early June 2002. Inversion structure is sensitive to cloudiness, to background flows (especially Föhn or strong winds above the basin), turbulent erosion at the top of the cold pool (Petkovšek 1992; Rakovec et al. 2002; Zhong et al. 2003), to cold-air intrusions coming over the basin ridgeline (Whiteman et al. 2010; Haiden et al. 2010) and to variations in the surface energy budget. A numerical modeling study by Zängl (2003) determined the effects of upstream blocking, drainage flows and geostrophic pressure gradient on cold-air pool persistence for a basin similar in shape to the Gruenloch Basin.

6.1.2 Persistent wintertime inversions in basins

Persistent or multi-day temperature inversions or cold-air pools have generally adverse effects on valley and basin populations (Smith et al. 1997). Temperatures remain cold during such events, suppressing the normal diurnal temperature range. The strong stability in the inversion causes air pollution and moisture to build up from sources within the pool. Poor air quality may persist for days (cf. Cuxart and Jiménez 2011). Fog may form and lift to produce stratus. Light rain, snow or drizzle may be produced if clouds persist or become thicker, or if they are seeded by higher clouds. Rain or drizzle may freeze when reaching the cold ground. Low cloud bases, visibility restrictions in fog, rain, snow or drizzle, and icy runway conditions may close airports and cause transportation problems.

Multi-day temperature inversions are primarily a wintertime phenomenon. They are produced when incoming energy during daytime is insufficient to remove cold air that has settled into the basin or valley. The cold air may form initially through the usual nocturnal inversion formation processes or may be left in low-lying terrain following the passage of a cold front. Inversions, whether at the incipient or fully formed stages, can be strengthened by differential advection when relatively warm air is advected over the basin or can be weakened when cold air is advected over the basin (Whiteman et al. 1999b). The shorter days of winter, lower sun angles, and the presence of snow cover are usually responsible for the changes in the surface energy budget at the basin floor that reduce the daytime turbulent sensible heat flux and convection below that required to break the inversion. Additionally, fog or stratus clouds that form in the cold-air pool may reduce insolation and sensible heat flux at the cold pool base.

Both the onset and cessation times of persistent cold-air pools are difficult to forecast. Forecast “busts” lead to especially large errors in maximum and minimum temperature forecasts. Forecasting the cessation of cold-air pools is particularly problematic because the many different processes that can affect breakup occur on different scales. Local processes such as evaporation or melting at the basin surface or changes in cloud cover within the pool have an effect, as do synoptic-scale warm or cold advection above the pool, turbulent erosion at the top of the cold pool, or drag or pressure forces that may be strong enough to push the cold pool to one side of a basin, to cause seiches within the pool, or to produce vertical oscillations at the top of the cold-air pool. Forecasts of cold pool breakup usually are based on the forecast passage of troughs or low-pressure weather systems (cf. Reeves and Stensrud 2009). These passages are accompanied by advection of colder air above the pool, destabilizing the cold-air pool, and by stronger winds that may assist in breakup. Cold air remnants are likely to persist at the lowest altitudes of a valley or basin even when the cold pool is thought to be fully removed. Studies of cold-air pools in the Colorado Plateaus Basin show that the final breakup, including any remnants at the lowest elevations, usually occurs in the afternoon with assistance from a final burst of convection (Whiteman et al. 1999b).

While most of the research on persistent cold-air pools to date has been on non-cloudy pools, cloudy cold-air pools sometimes form as moisture builds up within the inversion layer due to evaporation from the underlying ground. These pools have a weaker, near-moist-adiabatic stability. This is apparently caused by the sinking of cold air produced at cloud top by longwave radiation loss and the resultant overturning and vertical mixing between the cloud top and the ground. Because of the weaker stability, air pollutants generated inside cloudy cold-air pools will be better mixed in the vertical than for non-cloudy pools.

6.2. Diurnal wind systems over plateaus

Diurnal wind systems over plateaus have received much less research attention than diurnal wind systems in valleys and basins. Nonetheless, simulations of idealized plateaus have appeared (Egger 1987; De Wekker et al. 1998; Zängl and Chico 2006) and field studies have been conducted on the Mexican Plateau (Bossert 1997; Doran et al. 1998; Fast and Zhong 1998; Doran and Zhong 2000; Whiteman et al. 2000), especially in connection with air pollution problems (de Foy et al. 2008), in a valley feeding the Himalayan Plateau (Egger et al. 2000, 2002; Zängl et al. 2001) and on the Altiplano of Bolivia (Zängl and Egger 2005; Egger et al. 2005; Reuder and Egger 2006).

Plateaus provide elevated surfaces on which nighttime cooling and daytime heating can take place. During nighttime, air is cooled above the plateau. When the plateau is a tabletop, much of the cold air that forms (especially if the tabletop is narrow or has a small area) drains off the plateau sides, leaving only a shallow and relatively weak inversion on the plateau. If the plateau is surrounded by mountains the cooling can be confined in the elevated basin and produce stronger and deeper inversions than over plateaus with no surrounding mountains. During daytime, a convective boundary layer grows above the elevated heating surface. The daytime destruction of the nocturnal inversions often involves interactions with flows aloft (Banta and Cotton 1981; Banta 1984), which are generally stronger at higher elevations. If there is a weak nocturnal inversion on the plateau, the convection is able to grow quickly upwards through the inversion and can often reach quite high levels of the atmosphere. The warm air above a plateau can be advected off the plateau into the surrounding atmosphere if background winds are present. For example, the easterly advection of warm air from the South Park plateau in the central Rocky Mountains of Colorado can sometimes be detected east of the plateau where it affects the development of afternoon thunderstorms over the adjacent plains (Arritt et al. 1992).

An interesting latency occurs in the development of the daytime wind over plateau regions. There is often a very late break-in of plain-to-plateau or plain-to-basin winds that occurs in the late afternoon or early evening rather than in the late morning when the temperature difference between the air over the plateau and its surroundings starts to build up, as illustrated in a conceptual model in **Fig. 14** based on observations and modeling of the Mexican Plateau (Whiteman et al. 2000). During daytime, convection builds up a deep boundary layer above an elevated plateau that is warmer than the air surrounding the plateau. Upslope flows form on the outer periphery of the plateau and on the plateau itself, with return circulations aloft. The circulation cells converge at the plateau rim or edge, and the convergence anchors the circulation cells there during daytime (Bossert and Cotton 1994a, b). The normal tendency of the atmosphere to produce circulations to equilibrate temperature differences that develop between the air over the plateau and its surroundings is therefore restrained. Cold air can intrude onto the plateau, however, through passes and gaps at the plateau edge and through valleys that cut into the plateau (Egger 1987; Doran and Zhong 2000; Egger et al. 2000, 2002; Zängl et al. 2001; Zängl and Egger 2005; Egger et al. 2005). Because the

circulations are anchored to the plateau edge, a baroclinic zone forms during daytime around the periphery of the plateau, where the temperature gradient becomes strong. As the sun starts to set, the slope flows weaken, the circulation cell boundaries are no longer anchored to the plateau edge, and a strong flow of cold air comes across the baroclinic zone onto the plateau. This sudden break-in of cold air onto the plateau from all sides often occurs in early evening, and its progression across the plateau depends on plateau width. Model simulations show that gravity waves are an important mechanism that allows the warm air in the convective column above the plateau to equilibrate with the surrounding air during the nighttime (Whiteman et al. 2000; Zängl and Chico 2006).

As an example, the afternoon or early evening break-in of flows from outside a plateau or elevated basin is depicted in the conceptual model of **Fig. 15** for the South, Middle and North Park basins of Colorado, as based on observations and numerical modeling by Bossert and Cotton (1994a, b)

7. Forecasting

The many practical applications of knowledge concerning diurnal mountain winds were enumerated in the introduction to this chapter. Because diurnal mountain winds affect so many aspects of human life and the environment, there is a need to make accurate forecasts of diurnal mountain winds.

Forecasting of diurnal mountain winds is, in some respects, relatively simple. Climatological investigations have told us much about the regular development and characteristics of diurnal mountain winds. They form regularly and reliably under high-pressure synoptic conditions when skies are clear and background winds are weak. The underlying topography provides the channels for these flows. Airflows are down the terrain (slopes, valleys and mountains) during nighttime and up the terrain during daytime, with lags that correspond to the mass of the wind system and the corresponding rate of heat transfer required to reverse it. The larger the temperature contrasts that form inside the terrain or between the terrain and the surrounding plain, the stronger the flows. Stronger temperature contrasts and stronger flows occur when the diurnal cycle of sensible heat flux is strongest, in the summer half-year. Increasing cloudiness and interactions with strong flows aloft decrease the temperature and pressure contrasts that drive the wind systems. A decreased amplitude of the sensible heat flux or failure of the sensible heat flux to change sign diurnally decreases the intensity of the diurnal wind systems or eliminates the diurnal reversal that is their chief characteristic. The decreased amplitude could be caused by rain, high soil moisture, increasing cloudiness, or an increased albedo due to snow. Changes in climate along a valley can affect the amplitude of temperature contrast along a valley's axis, affecting wind system strength. The diurnal wind system is often present, but weaker and less regular in its time of reversal, on cloudy and windy days.

The more difficult aspect of forecasting comes with the need to predict wind system strength and characteristics for specific locations and at specific times. Present-day operational weather models are presently able to provide accurate simulations of general synoptic weather conditions and are now reaching the horizontal resolution (1-2 km) necessary to resolve large valleys such as the Inn, Rhine and Rhone Valleys of the Alps. These models, however, need further improvements to provide accurate forecasts for individual valleys. Horizontal and vertical grid and terrain resolutions should be improved, as well as boundary layer and surface property parameterizations. We know that some valleys in a region have stronger wind systems than others and that wind systems in some valleys are more susceptible to interference from external conditions. The increasingly high resolution attained by numerical research models is expected to provide more and more precise indications of the relative strengths of wind systems in different valleys under synoptic conditions, or even of different segments of an individual valley. Such simulations, however, will need to be evaluated with field data, to verify that the models are performing adequately. Some simpler models, such as the German Weather Service's proprietary KLAM_21 drainage flow model (Sievers 2005) have proven useful in simulations on a range of scales from an individual vineyard to a domain of several 10s of kilometers. A simpler approach (McKee and O'Neal 1989) using topographic maps investigates the along-valley variation of TAF (i.e., terrain cross-sections) and may have some utility, although the results to date have been mixed.

A number of pattern recognition approaches have been used to determine connections between synoptic-scale patterns and observed features of local winds in multi-valley target areas where wind and supporting data are available (Guardans and Palomino 1995; Weber and Kaufmann 1995; Kaufmann and Weber 1996, 1998; Kastendeuch and Kaufmann 1997; Weber and Kaufmann 1998; Kaufmann and Whiteman 1999; Kastendeuch et al. 2000; Ludwig et al. 2004). In the Basel, Switzerland area, for example, smaller valleys in the mountain complex have a high frequency of drainage flows, while larger valleys more often

experience interactions with synoptic-scale winds that produce channeled flows. Up-valley flows are generally stronger in this valley complex than down-valley flows, and the frequency of days with thermally driven flows varies little with season (Weber and Kaufmann 1998). Although the theoretical number of possible wind patterns is very large in a complicated terrain area, complex topography tends to constrain the observed fields to a small number of typical patterns. Recurrent wind patterns can also be determined by means of conditional sampling (Zaremba and Carroll 1999). Such information should prove useful for forecasting.

To overcome the inherent complexity and highly resource-demanding dynamical modeling, an alternative approach is offered by the increasing performance and flexibility of Geographic Information Systems (GIS). The latter can easily represent small-scale local features strongly affecting diurnal flows such as topography, land cover, surface budgets, etc. Supported by statistical analysis of long term observations, and with an input of ambient conditions from either station networks or large-scale numerical models, they can provide a first guess of wind and temperature fields at local scale, as well as a basis for the estimate of related quantities such as surface fluxes of heat, water vapor and passive scalars (Carrega 1995; Fast 1995; Ciolli et al. 2004; Deng and Stull 2005, 2007; Bertoldi et al. 2006; Schicker and Seibert 2009).

When forecasts are needed for a mountainous region, both real time and climatological data from weather stations can be analyzed to get a basic understanding of the strength and timing of the diurnal wind systems. Where quantitative data are available, general conceptual models of the phenomena can be used along with advice from individuals with local experience. Major federal projects, such as fighting a wildland fire, can sometimes justify the on-site assignment of a weather observer/forecaster, who can assist with interpretation and provide useful daily feedback on forecast accuracy.

8. Past progress, future objectives

Significant progress has been made in the understanding of diurnal mountain winds since the last AMS monograph on mountain meteorology was published (Blumen 1990). Field experiments, both large international efforts and single investigator projects, have been conducted taking advantage of new instrumentation and data platforms. Modeling of diurnal mountain winds has improved as advances have been made in hardware and software and as more detailed field data have become available.

Over the past two decades, field studies and modeling of diurnal mountain winds have worked in tandem. This collaboration should continue: field studies provide the data required to evaluate and refine models, and modeling work is invaluable in conceptualizing the processes observed in the field. Improvements can be expected in both areas. The introduction of higher horizontal and vertical grid and terrain resolution, better numerical approaches, more adequate boundary layer parameterizations, better modeling of turbulent processes and better handling of non-uniform surface cover and irregular terrain into models will bring significant advances to our understanding of mountain and valley atmospheres. The use of remote sensing instruments capable of scanning larger target volumes (e.g., De Wekker and Mayor 2009) is expected to produce more comprehensive and highly resolved observational data sets, which will allow the proper evaluation of increasingly sophisticated models.

In recent years, international cooperation has become a hallmark of research of diurnal mountain winds. Yearly international conferences alternating between the AMS Mountain Meteorology Conference and the International Conference on Alpine Meteorology, periodic short courses and large, international research programs will continue to strengthen international ties.

Future research into diurnal mountain winds will benefit not only from broad cooperation within the global mountain meteorology community but also from interdisciplinary cooperation. Researchers in related fields – including mathematics, numerical analysis, physics, fluid mechanics, turbulence dynamics, chemistry, and hydrology – will contribute to a clearer understanding of the mountain and valley atmosphere.

In the coming decades, an effort must be made to make research findings available to the applications community. Weather forecasters, environmental and civil engineers, land use planners, agricultural experts and wildland fire managers, among others, would benefit from the knowledge gained and the tools developed by basic research.

To date, research on diurnal mountain winds has mostly focused on individual phases of the wind systems and individual processes, including the morning transition, the evening transition, slope winds, surface

energy budgets and so on. This research will continue to be valuable. A number of interesting questions invite further investigation.

- With respect to slope flows, additional research is needed on upslope flows, on turbulent and radiative processes, on the external influences of ambient stability and ambient flows, and on the effects on slope flows of inhomogeneities of surface properties and heat budget components along a slope. Models should be developed to apply to realistic slopes and should be tested against new, higher resolution data sets. Large eddy simulation models should be applied to gain knowledge of mean and turbulent processes in slope flows.
- Understanding of valley flows would benefit from a comprehensive investigation of heat transport processes within the valley atmosphere, of the factors affecting inversion development and characteristics, and of the interactions between flows from multiple valleys.
- Research programs on mountain-plain circulations occurring in the major mountain ranges in the world could build on the VERTIKATOR results from Europe, with many scientific and practical benefits. For instance, concerning the Rocky Mountains, such a program could improve understanding of the role of the mountain-plain circulations on the transport of moisture and pollutants to the Rocky Mountains in diurnal and monsoonal wind systems. These circulations are closely connected to the Great Plains Low-Level Jet and the North American Monsoon, and play a role in the timing and movement of thunderstorm and mesoscale convective systems over the Great Plains.
- Research is needed on persistent wintertime cold-air pools to address increasing air pollution problems being experienced in urban basins and to improve the forecasting of their buildup and breakup. Because wintertime cold-air pools are experienced in many countries, an international research program on this topic would be warranted.

Additionally, and perhaps more importantly, there is a clear need to take a comprehensive look at thermally driven circulations in complex terrain, the interactions of the component parts, the interactions of these winds with winds aloft and the role of turbulence in wind characteristics. The initiatives investigating these processes should be multi-national, interdisciplinary and include weather forecasters and applications scientists.

Finally, there is a need for a textbook on diurnal mountain winds for graduate students, young researchers, weather forecasters and other professionals that summarizes the state of the science by offering a comprehensive and systematic treatment of all the aspects of the science including an historical perspective, a geographical overview, a review of investigative observational and modeling techniques, and a focus on applications.

Acknowledgments

We thank the monograph editors for the opportunity to contribute to this monograph and the associated 2008 Mountain Weather Workshop. Special thanks go to authors and organizations which provided figures for this chapter. The University of Trento and Prof. Dino Zardi are thanked for providing the financial support and warm hospitality for Dr. Whiteman's two-month visit to the University of Trento in 2008 to begin the collaborative work on this chapter. Moreover D. Zardi is grateful to the University of Trento for granting him a sabbatical leave during the academic year 2009/2010. We greatly appreciate the editorial assistance of Johanna Whiteman, the initial reviews of portions of this chapter by Thomas Haiden, Thomas W. Horst, Stephan De Wekker, Tina Katopodes Chow, and Stefano Serafin and the valuable comments provided by anonymous reviewers. Dr. Whiteman wishes to acknowledge partial funding support from National Science Foundation grants ATM-0837870 and ATM-0444205 and from the National Oceanic and Atmospheric Administration's National Weather Service CSTAR grant NA07NWS4680003.

REFERENCES

- Aigner, S., 1952: Die Temperaturminima im Gstettnerboden bei Lunz am See, Niederösterreich [The minimum temperatures in the Gstettner basin near Lunz, Lower Austria]. *Wetter und Leben, Sonderheft*, 34-37.
- Allwine, K. J., B. K. Lamb, and R. Eskridge, 1992: Wintertime dispersion in a mountainous basin at Roanoke, Virginia: Tracer study. *J. Appl. Meteor.*, **31**, 1295-1311.
- Amanatidis, G. T., K. H. Papadopoulos, J. G. Bartzis, and C. G. Helmis, 1992: Evidence of katabatic flows deduced from a 84 m meteorological tower in Athens, Greece. *Bound.-Layer Meteor.*, **58**, 117-132.
- André, J. C., and L. Mahrt, 1982: The nocturnal surface inversion and influence of clear-air radiative cooling. *J. Atmos. Sci.*, **39**, 864-878.
- Andretta M., A. Weiss, N. Kljun, and M. W. Rotach, 2001: Near-surface turbulent momentum flux in an Alpine valley: Observational results. *MAP newsletter*, **15**, 122-125.
- Andretta, M., A. H. Weigel, and M. W. Rotach, 2002: Eddy correlation flux measurements in an Alpine valley under different mesoscale circulations. *Preprints 10th AMS Conf. Mountain Meteor.*, 17-21 June 2002, Park City, UT, 109-111.
- Anquetin, S., C. Guilbaud, and J.-P. Chollet, 1998: The formation and destruction of inversion layers within a deep valley. *J. Appl. Meteor.*, **37**, 1547-1560.
- Antonacci, A., and M. Tubino, 2005: An estimate of day-time turbulent diffusivity over complex terrain from standard weather data. *Theor. Appl. Climatol.*, **80**, 205-212.
- Arritt, R. W., J. M. Wilczak, and G. S. Young, 1992: Observations and numerical modeling of an elevated mixed layer. *Mon. Wea. Rev.*, **120**, 2869-2880.
- Aryal, R. K., B.-K. Leeb, R. Karki, A. Gurung, B. Baral, and S.-H. Byeonb, 2009: Dynamics of PM_{2.5} concentrations in Kathmandu Valley, Nepal. *J. Haz. Mat.*, **168**, 732-738.
- Atkinson, B. W., 1981: *Meso-scale Atmospheric Circulations*. Academic Press, 495 pp.
- Atkinson, B. W., 1995: Orographic and stability effects on valley-side drainage flows. *Bound.-Layer Meteor.*, **75**, 403-428.
- Atkinson, B. W., and A. N. Shahub, 1994: Orographic and stability effects on day-time, valley-side slope flows. *Bound.-Layer Meteor.*, **68**, 275-300.
- Axelsen, S. L., and H. van Dop, 2008: Large-eddy simulation and observations of slope flow. *Acta Geophysica*, **57**, 803-836.
- Axelsen, S. L., and H. van Dop, 2009: Large-eddy simulation of katabatic flow over an infinite slope. *Acta Geophysica*, **57**, 837-856.
- Bader, D. C., and T. B. McKee, 1983: Dynamical model simulation of the morning boundary layer development in deep mountain valleys. *J. Climate Appl. Meteor.*, **22**, 341-351.
- Bader, D. C., and T. B. McKee, 1985: Effects of shear, stability and valley characteristics on the destruction of temperature inversions. *J. Climate Appl. Meteor.*, **24**, 822-832.
- Bader, D. C., and C. D. Whiteman, 1989: Numerical simulation of cross-valley plume dispersion during the morning transition period. *J. Appl. Meteor.*, **28**, 652-664.
- Baines, P. G., 2001: Mixing in flows down gentle slopes into stratified environments. *J. Fluid Mech.*, **443**, 237-270.
- Baines, P. G., 2005: Mixing regimes for the flow of dense fluid down slopes into stratified environments. *J. Fluid Mech.*, **538**, 245-267.
- Banta, R. M., 1984: Daytime boundary-layer evolution over mountainous terrain. Part I: Observations of the dry circulations. *Mon. Wea. Rev.*, **112**, 340-356.
- Banta, R., and W. R. Cotton, 1981: An analysis of the structure of local wind systems in a broad mountain basin. *J. Appl. Meteor.*, **20**, 1255-1266.
- Banta, R. M., and P. T. Gannon, 1995: Influence of soil moisture on simulations of katabatic flow. *Theor. Appl. Climatol.*, **52**, 85-94.
- Banta, R. M., L. D. Olivier, W. D. Neff, D. H. Levinson, and D. Ruffieux, 1995: Influence of canyon-induced flows on flow and dispersion over adjacent plains. *Theor. Appl. Climatol.*, **52**, 27-42.
- Banta, R. M., and Coauthors, 1997: Nocturnal cleansing flows in a tributary valley. *Atmos. Environ.*, **31**, 2147-2162.
- Banta, R. M., L. S. Darby, P. Kaufmann, D. H. Levinson, and C.-J. Zhu, 1999: Wind-flow patterns in the Grand Canyon as revealed by Doppler lidar. *J. Appl. Meteor.*, **38**, 1069-1083.
- Banta, R. M., L. S. Darby, J. D. Fast, J. Pinto, C. D. Whiteman, W. J. Shaw, and B. D. Orr, 2004: Nocturnal low-level jet in a mountain basin complex. I: Evolution and effects on local flows. *J. Appl. Meteor.*, **43**, 1348-1365.
- Barr, S., and M. M. Orgill, 1989: Influence of external meteorology on nocturnal valley drainage winds. *J. Appl. Meteor.*, **28**, 497-517.

- Barros, A. P., and T. J. Lang, 2003: Monitoring the monsoon in the Himalayas: Observations in Central Nepal, June 2001. *Mon. Wea. Rev.*, **131**, 1408-1427.
- Barry, R. G., 2008: *Mountain Weather And Climate, 3rd Edition*. Cambridge University Press, 506pp.
- Bastin, S., and P. Drobinski, 2005: Temperature and wind velocity oscillations along a gentle slope during sea-breeze events. *Bound.-Layer Meteor.*, **114**, 573-594.
- Bergström, H., and N. Juuso, 2006: A study of valley winds using the MIUU mesoscale model. *Wind Energy*, **9**, 109-129.
- Bertoldi, G., R. Rigon, and T. M. Over, 2006: Impact of watershed geomorphic characteristics on the energy and water budgets. *J. Hydrometeor.*, **7**, 389-403.
- Bhatt, B. C., and K. Nakamura, 2006: A climatological-dynamical analysis associated with precipitation around the southern part of the Himalayas. *J. Geophys. Res.*, **111**, D02115, doi:10.1029/2005JD006197.
- Bianco, L., I. V. Djalalova, C. W. King, and J. M. Wilczak, 2011: Diurnal evolution and annual variability of boundary-layer height and its correlation to other meteorological variables in California's Central Valley. *Bound.-Layer Meteor.* **140**, 491-511.
- Bica, B., and Coauthors, 2007: Thermally and dynamically induced pressure features over complex terrain from high-resolution analyses. *J. Appl. Meteor. Climatol.*, **46**, 50-65.
- Bischoff-Gauß, I., N. Kalthoff, and M. Fiebig-Wittmaack, 2006: The influence of a storage lake in the Arid Elqui valley in Chile on local climate. *Theor. Appl. Climatol.*, **85**, 227-241.
- Bischoff-Gauß, I., N. Kalthoff, S. Khodayar, M. Fiebig-Wittmaack, and S. Montecinos, 2008: Model simulations of the boundary-layer evolution over an arid Andes valley. *Bound.-Layer Meteor.*, **128**, 357-379.
- Bitencourt, D. P., and O. C. Acevedo, 2008: Modelling the interaction between a river surface and the atmosphere at the bottom of a valley. *Bound.-Layer Meteor.*, **129**, 309-321.
- Blumen, W. (Ed.), 1990: Atmospheric Processes over Complex Terrain. *Meteor. Monogr.*, **23** (no. 45), Amer. Meteor. Soc., Boston, Massachusetts.
- Bodine, D., P. M. Klein, S. C. Arms, and A. Shapiro, 2009: Variability of surface air temperature over gently sloped terrain. *J. Appl. Meteor. Climatol.*, **48**, 1117-1141.
- Bossert, J. E., 1997: An investigation of flow regimes affecting the Mexico City region. *J. Appl. Meteor.*, **36**, 119-140.
- Bossert, J. E., and W. R. Cotton, 1994a: Regional-scale flows in mountainous terrain. Part I: A numerical and observational comparison. *Mon. Wea. Rev.*, **122**, 1449-1471.
- Bossert, J. E., and W. R. Cotton, 1994b: Regional-scale flows in mountainous terrain. Part II: Simplified numerical experiments. *Mon. Wea. Rev.*, **122**, 1472-1489.
- Bossert, J. E., J. D. Sheaffer, and E. R. Reiter, 1989: Aspects of regional-scale flows in mountainous terrain. *J. Appl. Meteorol.*, **28**, 590-601.
- Brazel, A.J., H. J. S. Fernando, J. C. R. Hunt, N. Selover, B. C. Hedquist, and E. Pardyjak, 2005: Evening transition observations in Phoenix, Arizona. *J. Applied Meteor.*, **44**, 99-112.
- Brehm, M. 1986: Experimentelle und numerische Untersuchungen der Hangwindschicht und ihrer Rolle bei der Erwärmung von Tälern. [Experimental and numerical investigations of the slope wind layer and its role in the warming of valleys]. *Wiss. Mitt. Nr. 54*, dissertation, Universität München - Meteorologisches Institut, München, FRG.
- Brehm, M., and C. Freytag, 1982: Erosion of the night-time thermal circulation in an Alpine valley. *Arch. Meteor. Geophys. Bioclimatol., Ser. B*, **31**, 331-352.
- Buettner, K. J. K., and N. Thyer, 1966: Valley winds in the Mount Rainier area. *Arch. Meteor. Geophys. Bioclimatol., Ser. B*, **14**, 125-147.
- Burger, A., and E. Ekhardt, 1937: Über die tägliche Zirkulation der Atmosphäre im Bereiche der Alpen [The daily atmospheric circulation in the Alpine region]. *Gerl. Beitr.*, **49**, 341-367.
- Burkholder, B. A., A. Shapiro and E. Fedorovich, 2009: Katabatic flow induced by a cross-slope band of surface cooling. *Acta Geophysica*, **57**, 923-949.
- Carrega, P., 1995: A method for the reconstruction of mountain air temperatures with cartographic applications. *Theor. Appl. Climatol.*, **52**, 69-84.
- Catalano, F., and A. Cenedese, 2010: High-resolution numerical modeling of thermally driven slope winds in a valley with strong capping. *J. Appl. Meteor. Climatol.*, **49**, 1859-1880.
- Catalano, F., and C.-H. Moeng, 2010: Large-eddy simulation of the daytime boundary layer in an idealized valley using the Weather Research and Forecasting numerical model. *Bound.-Layer Meteor.*, **137**, 49-75.
- Chemel, C., and J. P. Chollet, 2006: Observations of the daytime boundary layer in deep Alpine valleys. *Bound.-Layer Meteor.*, **119**, 239-262.
- Chemel, C., C. Staquet, and Y. Largeron, 2009: Generation of internal gravity waves by a katabatic wind in an idealized alpine valley. *Meteor. Atmos Phys.*, **103**, 187-194.

- Chen, Y., A. Hall, and K. N. Liou, 2006: Application of 3D solar radiative transfer to mountains. *J. Geophys. Res.*, **111**, D21111, doi:10.1029/2006JD007163.
- Chow, F. K., A. P. Weigel, R. L. Street, M. W. Rotach, and M. Xue. 2006. High-resolution large-eddy simulations of flow in a steep Alpine valley. Part I: Methodology, verification, and sensitivity experiments. *J. Appl. Meteor. Climatol.*, **45**, 63-86.
- Ciolfi, M., M. de Franceschi, R. Rea, A. Vitti, D. Zardi, and P. Zatelli, 2004: Development and application of 2D and 3D GRASS modules for simulation of thermally driven slope winds. *Transactions in GIS*, **8**, 191-209.
- Clements, W. E., J. A. Archuleta, and D. E. Hoard, 1989: Mean structure of the nocturnal drainage flow in a deep valley. *J. Appl. Meteor.*, **28**, 457-462.
- Clements, C. B., C. D. Whiteman, and J. D. Horel, 2003: Cold-air-pool structure and evolution in a mountain basin: Peter Sinks, Utah. *J. Appl. Meteor.*, **42**, 752-768.
- Cogliati, M. G., and N. A. Mazzeo, 2005: Air flow analysis in the upper Rio Negro Valley (Argentina). *Atmos. Res.*, **80**, 263-279.
- Colette, A., F. K. Chow, and R. L. Street, 2003: A numerical study of inversion-layer breakup and the effects of topographic shading in idealized valleys. *J. Appl. Meteor.*, **42**, 1255-1272.
- Coulter, R. L., and P. Gudiksen, 1995: The dependence of canyon winds on surface cooling and external forcing in Colorado's Front Range. *J. Appl. Meteor.*, **34**, 1419-1429.
- Coulter, R. L., and T. J. Martin, 1996: Effects of stability on the profiles of vertical velocity and its variance in katabatic flow. *Bound.-Layer Meteor.*, **81**, 23-33.
- Coulter, R. L., M. Orgill, and W. Porch, 1989: Tributary fluxes into Brush Creek Valley. *J. Appl. Meteor.*, **28**, 555- 568.
- Coulter, R. L., T. J. Martin, and W. M. Porch, 1991: A comparison of nocturnal drainage flow in three tributaries. *J. Appl. Meteor.*, **30**, 157-169.
- Cox, J. A. W., 2005: The sensitivity of thermally driven mountain flows to land-cover change. Dissertation, Univ. Utah, Meteorology Department. 109pp.
- Crawford, T. L., and R. J. Dobosy, 1992: A sensitive fast-response probe to measure turbulence and heat flux from any airplane. *Bound.-Layer Meteor.*, **59**, 257-278.
- Cuxart, J., 2008: Nocturnal basin low-level jets: An integrated study. *Acta Geophysica*, **56**, 100-113.
- Cuxart, J., and M. A. Jiménez, 2011: Deep radiation fog in a wide closed valley: Study by numerical modeling and remote sensing. *Pure Appl. Geophys.* In press. DOI: 10.1007/s00024-011-0365-4.
- Cuxart, J., M. A. Jiménez, and D. Martínez, 2007: Nocturnal meso-beta basin and katabatic flows on a midlatitude island. *Mon. Wea. Rev.*, **135**, 918-932.
- Cuxart, J., J. Cunillera, M. A. Jiménez, D. Martínez, F. Molinos, and J. L. Palau, 2011: Study of mesobeta basin flows by remote sensing. *Bound.-Layer Meteor.* In press. DOI: 10.1007/s10546-011-9655-8.
- Dai, A., and J. Wang, 1999: Diurnal and semidiurnal tides in global surface pressure fields. *J. Atmos. Sci.*, **56**, 3874-3891
- Darby, L. S., and R. M. Banta, 2006: The modulation of canyon flows by larger-scale influences. *Ext. Abstr., 12th Conf. Mountain Meteor.*, Santa Fe, NM. Amer. Meteor. Soc., Boston, MA.
- Darby, L. S., K. J. Allwine, and R. M. Banta, 2006: Nocturnal low-level jet in a mountain basin complex. Part II: Transport and diffusion of tracer under stable conditions. *J. Appl. Meteor. Climatol.*, **45**, 740-753.
- Defant, F., 1949: Zur Theorie der Hangwinde, nebst Bemerkungen zur Theorie der Berg- und Talwinde. [A theory of slope winds, along with remarks on the theory of mountain winds and valley winds]. *Arch. Meteor. Geophys. Bioclimatol., Ser. A*, **1**, 421-450 (Theoretical and Applied Climatology). [English translation: Whiteman, C.D., and E. Dreiseitl, 1984: Alpine meteorology: Translations of classic contributions by A. Wagner, E. Ekhardt and F. Defant. PNL-5141 / ASCOT-84-3. Pacific Northwest Laboratory, Richland, Washington, 121 pp].
- Defant, F., 1951: Local Winds. In: *Compendium of Meteorology*, T. M. Malone (Ed.), Boston, Amer. Meteor. Soc., 655-672.
- de Foy, B., and Coauthors, 2008: Basin-scale wind transport during the MILAGRO field campaign and comparison to climatology using cluster analysis. *Atmos. Chem. Phys.*, **8**, 1209-1224.
- de Franceschi, M., 2004: Investigation of atmospheric boundary layer dynamics in Alpine valleys. Ph.D. thesis in Environmental Engineering, University of Trento, Italy, 136pp. <http://www.ing.unitn.it/dica/eng/monographs/index.php>.
- de Franceschi, M., and D. Zardi, 2003: Evaluation of cut-off frequency and correction of filter-induced phase lag and attenuation in eddy covariance analysis of turbulence data. *Bound.-Layer Meteor.*, **108**, 289-303.
- de Franceschi, M., and D. Zardi, 2009: Study of wintertime high pollution episodes during the Brenner-South ALPNAP measurement campaign. *Meteor. Atmos. Phys.*, **103**, 237-250.

- de Franceschi, M., G. Rampanelli, and D. Zardi, 2002: Further investigations of the "Ora del Garda" valley wind. *10th Conf. Mount. Meteor. and MAP Meeting*, 13-21 June 2002, Park City, UT, American Meteorological Society, Boston, MA. Available at <http://ams.confex.com/ams/pdfpapers/39949.pdf>.
- de Franceschi, M., G. Rampanelli, D. Sguerso, D. Zardi, and P. Zatelli, 2003: Development of a measurement platform on a light airplane and analysis of airborne measurements in the atmospheric boundary layer. *Ann. Geophys.*, **46**, 269-283.
- de Franceschi, M., D. Zardi, M. Tagliazucca, and F. Tampieri, 2009: Analysis of second order moments in the surface layer turbulence in an Alpine valley. *Quart. J. Roy. Meteor. Soc.*, **135**, 1750-1765.
- De Wekker, S. F. J., 2002: Structure and morphology of the convective boundary layer in mountainous terrain. Dissertation, University of British Columbia, Department of Earth and Ocean Sciences, Vancouver, Canada, 191pp.
- De Wekker, S. F. J., 2008: Observational and numerical evidence of depressed convective boundary layer heights near a mountain base. *J. Appl. Meteor.*, **47**, 1017-1026.
- De Wekker, S. F. J., and S. D. Mayor, 2009: Observations of atmospheric structure and dynamics in the Owens Valley of California with a ground-based, eye-safe, scanning aerosol lidar. *J. Appl. Meteor. Climatol.*, **48**, 1483-1499.
- De Wekker, S. F. J., and C. D. Whiteman, 2006: On the time scale of nocturnal boundary layer cooling in valleys and basins and over plains. *J. Appl. Meteor.*, **45**, 813-820.
- De Wekker, S. F. J., S. Zhong, J. D. Fast, and C. D. Whiteman, 1998: A numerical study of the thermally driven plain-to-basin wind over idealized basin topographies. *J. Appl. Meteor.*, **37**, 606-622.
- De Wekker, S. F. J., D. G. Steyn, J. D. Fast, M. W. Rotach, and S. Zhong, 2005: The performance of RAMS in representing the convective boundary layer structure in a very steep valley. *Environ. Fluid Mech.*, **5**, 35-62.
- De Wekker S. F. J., A. Ameen, G. Song, B. B. Stephens, A. G. Hallar and I. B. McCubbin, 2009: A preliminary investigation of boundary layer effects on daytime atmospheric CO₂ concentrations at a mountaintop location in the Rocky Mountains *Acta Geophysica*, **57**, 904-922.
- Denby, B., 1999: Second-order modelling of turbulence in katabatic flows. *Bound.-Layer Meteor.*, **92**, 67-100.
- Deng, X., and R. Stull, 2005: A mesoscale analysis method for surface potential temperature in mountainous and coastal terrain. *Mon. Wea. Rev.*, **133**, 389-408.
- Deng, X., and R. Stull, 2007: Assimilating surface weather observations from complex terrain into a high-resolution numerical weather prediction model. *Mon. Wea. Rev.*, **135**, 1037-1054.
- Dixit, P. N., and D. Chen, 2011: Effect of topography on farm-scale spatial variation in extreme temperatures in the Southern Mallee of Victoria, Australia. *Theor. Appl. Climatol.*, **103**, 533-542.
- Doran, J. C., 1991: The effect of ambient winds on valley drainage flows. *Bound.-Layer Meteor.*, **55**, 177-189.
- Doran, J. C., 1996: The influence of canyon winds on flow fields near Colorado's Front Range. *J. Appl. Meteor.*, **35**, 587-600.
- Doran, J. C., and T. W. Horst, 1981: Velocity and temperature oscillations in drainage winds. *J. Appl. Meteor.*, **20**, 361-364.
- Doran, J. C., and S. Zhong, 2000: Thermally driven gap winds into the Mexico City basin. *J. Appl. Meteor.*, **39**, 1330-1340.
- Doran, J. C., M. L. Wesley, R. T. McMillen, and W. D. Neff, 1989: Measurements of turbulent heat and momentum fluxes in a mountain valley. *J. Appl. Meteor.*, **28**, 438-444.
- Doran, J. C., T. W. Horst, and C. D. Whiteman, 1990: The development and structure of nocturnal slope winds in a simple valley. *Bound.-Layer Meteor.*, **52**, 41-68.
- Doran, J. C., and Coauthors, 1998: The IMADA-AVER boundary-layer experiment in the Mexico City area. *Bull. Amer. Meteor. Soc.*, **79**, 2497-2508.
- Doran, J. C., J. D. Fast, and J. Horel, 2002: The VTMX 2000 campaign. *Bull. Amer. Meteor. Soc.*, **83**, 537-551.
- Dorning, M., Whiteman, C. D., B. Bica, S. Eisenbach, B. Pospichal, and R. Steinacker, 2011: Meteorological events affecting cold-air pools in a small basin. *J. Appl. Meteor. Climatol.* Accepted.
- Dosio, A., S. Emeis, G. Graziani, W. Junkermann, and A. Levy, 2001: Assessing the meteorological conditions of a deep Italian Alpine valley system by means of a measuring campaign and simulations with two models during a summer smog episode. *Atmos. Environ.*, **35**, 5441-5454.
- Duguay, C. R., 1993: Radiation modeling in mountainous terrain: Review and status. *Mount. Res. Dev.*, **13**, 339-357.
- Eckman, R. M., 1998: Observations and numerical simulations of winds in a broad forested valley. *J. Appl. Meteor.*, **37**, 206-219.
- Egger, J., 1987: Valley winds and the diurnal circulation over plateaus. *Mon. Wea. Rev.*, **115**, 2177-2186.

- Egger, J., 1990: Thermally forced flows: Theory. In W. Blumen (Ed.), *Atmospheric Processes over Complex Terrain*. Amer. Meteor. Soc., Boston, 43-57.
- Egger, J., S. Bajrachaya, U. Egger, R. Heinrich, J. Reuder, P. Shayka, H. Wendt, and V. Wirth, 2000: Diurnal winds in the Himalayan Kali Gandaki Valley. Part I: Observations. *Mon. Wea. Rev.*, **128**, 1106-1122.
- Egger, J., and Coauthors, 2002: Diurnal winds in the Himalayan Kali Gandaki valley. Part III: Remotely piloted aircraft soundings. *Mon. Wea. Rev.*, **130**, 2042-2058.
- Egger, J., and Coauthors, 2005: Diurnal circulation of the Bolivian Altiplano. Part I: Observations. *Mon. Wea. Rev.*, **133**, 911-924.
- Ekhart, E., 1944: Beiträge zur alpinen Meteorologie. [Contributions to Alpine Meteorology]. *Meteor. Z.*, **61**, 217-231. [English translation: Whiteman, C.D., and E. Dreiseitl, 1984: *Alpine Meteorology: Translations of Classic Contributions by A. Wagner, E. Ekhart and F. Defant*. PNL-5141 / ASCOT-84-3. Pacific Northwest Laboratory, Richland, Washington, 121 pp].
- Ekhart, E., 1948: De la structure thermique de l'atmosphère dans la montagne [On the thermal structure of the mountain atmosphere]. *La Meteorologie*, **4**, 3-26. [English translation: Whiteman, C.D., and E. Dreiseitl: 1984. *Alpine Meteorology: Translations of Classic Contributions by A. Wagner, E. Ekhart and F. Defant*. PNL-5141 / ASCOT-84-3. Pacific Northwest Laboratory, Richland, Washington, 121 pp].
- Emeis, S., C. Jahn, C. Münkler, C. Münsterer, and K. Schäfer, 2007: Multiple atmospheric layering and mixing-layer height in the Inn valley observed by remote sensing. *Meteor. Z.*, **16**, 415-424.
- Enger, L., D. Koračin, and X. Yang, 1993: A numerical study of boundary-layer dynamics in a mountain valley. Part I: Model validation and sensitivity experiment. *Bound.-Layer Meteor.*, **66**, 357-394.
- Fast, J. D., 1995: Mesoscale modeling and four-dimensional data assimilation in areas of highly complex terrain. *J. Appl. Meteor.*, **34**, 2762-2782.
- Fast, J. D., 2003: Forecasts of valley circulations using the terrain-following and step-mountain vertical coordinates in the Meso-Eta model. *Wea. Forecasting*, **18**, 1192-1206.
- Fast, J. D., and S. Zhong, 1998: Meteorological factors associated with inhomogeneous ozone concentrations within the Mexico City basin. *J. Geophys. Res.*, **103** (D15), 18,927-18,946.
- Fast, J. D., and L. S. Darby, 2004: An evaluation of mesoscale model predictions of down-valley and canyon flows and their consequences using Doppler lidar measurements during VTMX 2000. *J. Appl. Meteor.*, **43**, 420-436.
- Fast, J., S. Zhong, and C. D. Whiteman, 1996: Boundary layer evolution within a canyonland basin. Part II. Numerical simulations of nocturnal flows and heat budgets. *J. Appl. Meteor.*, **35**, 2162-2178.
- Fernando, H. J. S., 2010: Fluid dynamics of urban atmospheres in complex terrain. *Ann. Rev. Fluid Mech.* **42**, 365-89.
- Fiedler, F., I. Bischoff-Gauß, N. Kalthoff, and G. Adrian, 2000: Modeling of the transport and diffusion of a tracer in the Freiburg-Schauinsland area. *J. Geophys. Res.*, **105**, D1, 1599-1610.
- Finnigan, J. J., R. Clement, Y. Malhi, R. Leuning, and H. A. Cleugh, 2003: A re-evaluation of long-term flux measurement techniques. Part I. Averaging and coordinate rotation. *Bound.-Layer Meteor.*, **107**, 1-48.
- Fitzjarrald, D. R., 1984: Katabatic winds in opposing flow. *J. Atmos. Sci.*, **41**, 1143-1158.
- Fleagle, R. G., 1950: A theory of air drainage. *J. Meteor.*, **7**, 227-232.
- Frei, C., and H. C. Davies, 1993: Anomaly in the Alpine diurnal pressure signal: Observations and theory. *Quart. J. Roy. Meteor. Soc.*, **119**, 1269-1289.
- Freytag, C., 1988: Atmosphärische Grenzschicht in einem Gebirgstal bei Berg- und Talwind. [Atmospheric boundary layer in a mountain valley during mountain and valley winds]. *Wiss. Mitteil. Nr. 60*, Münchener Universitätsschriften, Fakultät für Physik, Universität München - Meteorologisches Institut, 197 pp.
- Fritts, D. C., D. Goldstein, and T. Lund, 2010: High-resolution numerical studies of stable boundary layer flows in a closed basin: Evolution of steady and oscillatory flows in an axisymmetric Arizona Meteor Crater. *J. Geophys. Res.*, **115**, D18109, doi:10.1029/2009JD013359.
- Furger, M., and Coauthors, 2000: The VOTALP Mesolcina Valley campaign 1996 - Concept, background and some highlights. *Atmos. Environ.*, **34**, 1395-1412.
- Garratt, J. R., and R. A. Brost, 1981: Radiative cooling effects within and above the nocturnal boundary layer. *J. Atmos. Sci.*, **38**, 2730-2746.
- Geerts, B., Q. Miao, and J. C. Demko, 2008: Pressure perturbations and upslope flow over a heated, isolated mountain. *Mon. Wea. Rev.*, **136**, 4272-4288.
- Geiger, R., R. H. Aron, and P. Todhunter, 2009: *The Climate Near the Ground, 7th Edition*. Roman and Littlefield Publishers, Maryland, 523pp.

- Giovannini, L., D. Zardi, and M. de Franceschi, 2011: Analysis of the urban thermal fingerprint of the city of Trento in the Alps. *J. Appl. Meteor. Climatol.*, **50**, 1145-1162.
- Gleeson, T. A., 1951: On the theory of cross-valley winds arising from differential heating of the slopes. *J. Meteor.*, **8**, 398-405.
- Gohm, A., F. Harnisch, J. Vergeiner, F. Obleitner, R. Schnitzhofer, A. Hansel, A. Fix, B. Neininger, S. Emeis, and K. Schäfer, 2009: Air pollution transport in an Alpine valley: Results from airborne and ground-based observations. *Bound.-Layer Meteor.*, **131**, 441-463.
- Grell, G. A., S. Emeis, W. R. Stockwell, T. Schoenemey, R. Forkel, J. Michalakes, R. Knoche, and W. Seidl, 2000: Application of a multiscale, coupled MM5/chemistry model to the complex terrain of the VOTALP valley campaign. *Atmos. Environ.*, **34**, 1435-1453.
- Grimmond, C. S. B., C. Souch, and M. D. Hubble, 1996: Influence of tree cover on summertime surface energy balance fluxes, San Gabriel Valley, Los Angeles. *Climate Research*, **6**, 45-57.
- Grisogono, B., 2003: Post-onset behaviour of the pure katabatic flow. *Bound.-Layer Meteor.*, **107**, 157-175.
- Grisogono, B., and J. Oerlemans, 2001a: A theory for the estimation of surface fluxes in simple katabatic flow. *Quart. J. Roy. Meteor. Soc.*, **127**, 2125-2139.
- Grisogono, B., and J. Oerlemans, 2001b: Katabatic flow: Analytic solution for gradually varying eddy diffusivities. *J. Atmos. Sci.*, **58**, 3349-3354.
- Grisogono, B., L. Kraljevič, and A. Jeričević, 2007: The low-level katabatic jet height versus Monin-Obukhov height. *Quart. J. Roy. Meteor. Soc.*, **133**, 2133-2136.
- Gross, G., 1984: Eine Erklärung des Phänomens Maloja-Schlange Mittels Numerischer Simulation. [An Explanation of the Maloja Snake (Cloud) Phenomenon by Means of a Numerical Simulation]. Dissertation, Technischen Hochschule Darmstadt, Darmstadt, FRG.
- Gross, G., 1985: An explanation of the Maloja-serpent by numerical simulation, *Beitr. Phys. Atmos.*, **58**, 441-457.
- Gross, G., 1990: On the wind field in the Loisach Valley—Numerical simulation and comparison with the LOWEX III data. *Meteor. Atmos. Phys.*, **42**, 231-247.
- Grossi, G., and L. Falappi, 2003: Comparison of energy fluxes at the land surface-atmosphere interface in an Alpine valley as simulated with different models. *Hydrology and Earth System Sciences*, **7**, 920-936.
- Guardans, R., and I. Palomino, 1995: Description of wind field dynamic patterns in a valley and their relation to mesoscale and synoptic-scale situations. *J. Appl. Meteor.*, **34**, 49-67.
- Gustavsson, T., M. Karlsson, J. Bogren, and S. Lindqvist, 1998: Development of temperature patterns during clear nights. *J. Appl. Meteor.*, **37**, 559-571.
- Ha, K.-J., and L. Mahrt, 2003: Radiative and turbulent fluxes in the nocturnal boundary layer. *Tellus*, **55A**, 317-327.
- Haiden, T., 1998: Analytical aspects of mixed-layer growth in complex terrain. Preprints, *Eighth Conf. Mountain Meteorology*, Amer. Meteor. Soc., Flagstaff, Arizona, 368-372.
- Haiden, T., 2003: On the pressure field in the slope wind layer. *J. Atmos. Sci.*, **60**, 1632-1635.
- Haiden, T., and C. D. Whiteman, 2005: Katabatic flow mechanisms on a low-angle slope. *J. Appl. Meteor.*, **44**, 113-126.
- Haiden, T., C. D. Whiteman, S. W. Hoch, and M. Lehner, 2011: A mass-flux model of nocturnal cold air intrusions into a closed basin. *J. Appl. Meteor. Climatol.*, **50**, 933-943.
- Harnisch, F., A. Gohm, A. Fix, R. Schnitzhofer, A. Hansel, and B. Neininger, 2009: Spatial distribution of aerosols in the Inn Valley atmosphere during wintertime. *Meteor. Atmos. Phys.*, **103**, 215-228.
- Hauge, G., and L. R. Hole, 2003: Implementation of slope irradiance in Mesoscale Model version 5 and its effect on temperature and wind fields during the breakup of a temperature inversion. *J. Geophys. Res.*, **108**, D2, 4058, doi:10.1029/2002JD002575.
- Hawkes, H. B., 1947: Mountain and valley winds with special reference to the diurnal mountain winds of the Great Salt Lake region. Dissertation, Ohio State University, 312 pp.
- Helmis, C. G., and K. H. Papadopoulos, 1996: Some aspects of the variation with time of katabatic flows over a simple slope. *Quart. J. Roy. Meteor. Soc.*, **122**, 595-610.
- Henne, S., M. Furger, and A. S. H. Prévôt, 2005: Climatology of mountain venting-induced elevated moisture layers in the lee of the Alps. *J. Appl. Meteor.*, **44**, 620-633.
- Henne, S., W. Junkermann, J. M. Kariuki, J. Aseyo, and J. Klausen, 2008: The establishment of the Mt. Kenya GAW station: Installation and meteorological characterization. *J. Appl. Meteor. Climatol.*, **47**, 2946-2962.
- Higgins, W., and Coauthors, 2006: The NAME 2004 field campaign and modeling strategy. *Bull. Amer. Meteor. Soc.*, **87**, 79-94.
- Hiller, R., M. Zeeman, and W. Eugster, 2008: Eddy-covariance flux measurements in the complex terrain of an Alpine valley in Switzerland. *Bound.-Layer Meteor.*, **127**, 449-467.

- Hoch, S. W., and C. D. Whiteman, 2010: Topographic effects on the surface radiation balance in and around Arizona's Meteor Crater. *J. Appl. Meteor. Climat.*, **49**, 1894-1905.
- Hoch, S. W., C. D. Whiteman, and B. Mayer, 2011: A systematic study of longwave radiative heating and cooling within valleys and basins using a three-dimensional radiative transfer model. *J. Appl. Meteor. Climatol.* In press.
- Holton, J. R., 1966: The diurnal boundary layer wind oscillation above sloping terrain. *Tellus*, **19**, 199-205.
- Horst, T. W., and J. C. Doran, 1986: Nocturnal drainage flow on simple slopes. *Bound.-Layer Meteor.*, **34**, 263-286.
- Horst, T. W., and J. C. Doran, 1988: The turbulence structure of nocturnal slope flows. *J. Atmos. Sci.*, **45**, 605-616.
- Hughes, M., A. Hall, and G. Fovell, 2007: Dynamical controls on the diurnal cycle of temperature in complex topography. *Clim. Dyn.*, **29**, 277-292.
- Hunt, J. C. R., H. J. S. Fernando, and M. Princevac, 2003: Unsteady thermally driven flows on gentle slopes. *J. Atmos. Sci.*, **60**, 2169-2182.
- Iijima, Y., and M. Shinoda, 2000: Seasonal changes in the cold-air pool formation in a subalpine hollow, central Japan. *Int. J. Climatol.*, **20**, 1471-1483.
- Iziomon, M. G., H. Mayer, W. Wicke, and A. Matzarakis, 2001: Radiation balance over low-lying and mountainous areas in southwest Germany. *Theor. Appl. Climatol.*, **68**, 219-231.
- Jiang, Q., and J. D. Doyle, 2008: Diurnal variation of downslope winds in Owens Valley during the Sierra Rotor experiment. *Mon. Wea. Rev.*, **136**, 3760-3780.
- Kaimal, J. C., and J. J. Finnigan, 1994: Atmospheric boundary-layer flows: Their structure and measurement. Oxford University Press, New York, 289 pp.
- Kalthoff, N., and Coauthors, 2002: Mesoscale wind regimes in Chile at 30° S. *J. Appl. Meteor.*, **41**, 953-970.
- Kalthoff, N., M. Fiebig-Wittmaack, C. Meißner, M. Kohler, M. Uriarte, I. Bischoff-Gauß, and E. Gonzales, 2006: The energy balance, evapo-transpiration and nocturnal dew deposition of an arid valley in the Andes. *J. Arid Environments*, **65**, 420-443.
- Kalthoff, N., and Coauthors, 2009: The impact of convergence zones on the initiation of deep convection: A case study from COPS. *Atmos. Res.*, **93**, 680 – 694.
- Kastendeuch, P. P., and P. Kaufmann, 1997: Classification of summer wind fields over complex terrain. *Int. J. Climatol.*, **17**, 521-534.
- Kastendeuch, P. P., P. Lacarrere, G. Najjar, J. Noilhan, F. Gassmann, and P. Paul, 2000: Mesoscale simulations of thermodynamic fluxes over complex terrain. *Int. J. Climatol.*, **20**, 1249-1264.
- Kaufmann, P., and R. O. Weber, 1996: Classification of mesoscale wind fields in the MISTRAL field experiment. *J. Appl. Meteor.*, **35**, 1963-1979.
- Kaufmann, P., and R. O. Weber, 1998: Directional correlation coefficient for channeled flow and application to wind data over complex terrain. *J. Atmos. Oceanic. Technol.*, **15**, 89-97.
- Kaufmann, P., and C. D. Whiteman, 1999: Cluster-analysis classification of wintertime wind patterns in the Grand Canyon region. *J. Appl. Meteor.*, **38**, 1131-1147.
- Kavčič, I., and B. Grisogono, 2007: Katabatic flow with Coriolis effect and gradually varying eddy diffusivity. *Bound.-Layer Meteor.*, **125**, 377-387.
- Kelly, R. D., 1988: Asymmetric removal of temperature inversions in a high mountain valley. *J. Appl. Meteor.*, **27**, 664-673.
- Khodayar, S., N. Kalthoff, M. Fiebig-Wittmaack, and M. Kohler, 2008: Evolution of the atmospheric boundary-layer structure of an arid Andes valley. *Meteor. Atmos. Phys.*, **99**, 181-198.
- Kimura, F., and T. Kuwagata, 1993: Thermally induced wind passing from plain to basin over a mountain range. *J. Appl. Meteor.*, **32**, 1538-1547.
- Kimura, F., and T. Kuwagata, 1995: Horizontal heat fluxes over complex terrain computed using a simple mixed-layer model and a numerical model. *J. Appl. Meteor.*, **34**, 549-558.
- King, C. W., 1989: Representativeness of single vertical wind profiles for determining volume fluxes in valleys. *J. Appl. Meteor.*, **28**, 463-466.
- King, J. A., F. H. Shair, and D. D. Reible, 1987: The influence of atmospheric stability on pollutant transport by slope winds. *Atmos. Environ.*, **21**, 53-59.
- Kitada, T., and R. P. Regmi, 2003: Dynamics of air pollution transport in late wintertime over Kathmandu Valley, Nepal: As revealed with numerical simulation. *J. Appl. Meteor.*, **42**, 1770-1798.
- Koch, H. G., 1961: Die warme Hangzone. Neue Anschauungen zur nächtlichen Kaltluftschichtung in Tälern und an Hängen. [The warm slope zone. New views of the nocturnal cold air layer in valleys and on slopes]. *Z. Meteor.*, **15**, 151-171.

- Kolev, N., I. Grigorov, I. Kolev, P. C. S. Devara, P. E. Raj, and K. K. Dan, 2007: Lidar and sun photometer observations of atmospheric boundary-layer characteristics over an urban area in a mountain valley. *Bound.-Layer Meteor.*, **124**, 99–115.
- Kondo, H., 1990: A numerical experiment on the interaction between sea breeze and valley wind to generate the so-called "extended sea breeze." *J. Meteor. Soc. Japan*, **68**, 435-446.
- Kondo, J., and N. Okusa, 1990: A simple numerical prediction model of nocturnal cooling in a basin with various topographic parameters. *J. Appl. Meteor.*, **29**, 604-619.
- Kondo, J., T. Kuwagata, and S. Haginoya, 1989: Heat budget analysis of nocturnal cooling and daytime heating in a basin. *J. Atmos. Sci.*, **19**, 2917-2933.
- Koračin, D., and L. Enger, 1994: A numerical study of boundary-layer dynamics in a mountain valley. Part 2: Observed and simulated characteristics of atmospheric stability and local flows. *Bound.-Layer Meteor.*, **69**, 249–283.
- Kossmann, M., and A. P. Sturman, 2003: Pressure-driven channeling effects in bent valleys. *J. Appl. Meteor.*, **42**, 151-158.
- Kossmann, M., A. P. Sturman, P. Zawar-Reza, H. A. McGowan, A. J. Oliphant, I. F. Owens, and R. A. Spronken-Smith, 2002: Analysis of the wind field and heat budget in an alpine lake basin during summertime fair weather conditions. *Meteor. Atmos. Phys.*, **81**, 27-52.
- Küttner, J., 1949: Periodische Luftlawinen. [Periodic air avalanches]. *Meteor. Rundsch.*, **2**, 183-184.
- Kuttler, W., A.-B. Barlag, and F. Roßmann, 1996: Study of the thermal structure of a town in a narrow valley. *Atmos. Environ.*, **30**, 365–378.
- Kuwagata, T., and J. Kondo, 1989: Observation and modeling of thermally induced upslope flow. *Bound.-Layer Meteor.*, **49**, 265-293.
- Kuwagata, T., and F. Kimura, 1995: Daytime boundary layer evolution in a deep valley. Part I: Observations in the Ina Valley. *J. Appl. Meteor.*, **34**, 1082-1091.
- Kuwagata, T., and F. Kimura, 1997: Daytime boundary layer evolution in a deep valley. Part II: Numerical simulation of the cross-valley circulation. *J. Appl. Meteor.*, **36**, 883-895.
- Lee, I. Y., R. L. Coulter, H. M. Park, and J.-H. Oh, 1995: Numerical simulation of nocturnal drainage flow properties in a rugged canyon. *Bound.-Layer Meteor.*, **72**, 305-321.
- Lee, S.-M., W. Giori, M. Princevac, and H. J. S. Fernando, 2006: Implementation of a stable PBL turbulence parameterization for the mesoscale model MM5: Nocturnal flow in complex terrain. *Bound.-Layer Meteor.*, **119**, 109-134.
- Lee, X., and X. Hu, 2002: Forest-air fluxes of carbon, water and energy over non-flat terrain. *Bound.-Layer Meteor.*, **103**, 277-301.
- Lehner, M., and A. Gohm, 2010: Idealised simulations of daytime pollution transport in a steep valley and its sensitivity to thermal stratification and surface albedo. *Bound.-Layer Meteor.*, **134**, 327–351.
- Lehner, M., C. D. Whiteman, and S. W. Hoch, 2010: Diurnal cycle of thermally driven cross-basin winds in Arizona's Meteor Crater. *J. Appl. Meteor. Climatol.*, **50**, 729-744.
- Leone, J. M., Jr., and R. L. Lee, 1989: Numerical simulation of drainage flow in Brush Creek, Colorado. *J. Appl. Meteor.*, **28**, 530-542.
- Li, J.-G., and B. W. Atkinson, 1999: Transition regimes in valley airflows. *Bound.-Layer Meteor.*, **91**, 385-411.
- Li, Y., and R. B. Smith, 2010: The detection and significance of diurnal pressure and potential vorticity anomalies east of the Rockies. *J. Atmos. Sci.*, **67**, 2734–2751.
- Li, Y., R. B. Smith, and V. Grubišić, 2009: Using surface pressure variations to categorize the diurnal valley circulations: Experiments in Owens Valley. *Mon. Wea. Rev.*, **137**, 1753-1769.
- Lindkvist, L., and S. Lindqvist, 1997: Spatial and temporal variability of nocturnal summer frost in elevated complex terrain. *Agric. Forest Meteor.*, **87**, 139-153.
- Lindkvist, L., T. Gustavsson, and J. Bogren, 2000: A frost assessment method for mountainous areas. *Agric. Forest Meteor.*, **102**, 51-67.
- Liu, X., A. Bai, and C. Liu, 2009: Diurnal variations of summertime precipitation over the Tibetan Plateau in relation to orographically-induced regional circulations. *Environ. Res. Lett.*, **4**, 045203. doi:10.1088/1748-9326/4/4/045203.
- Löffler-Mang, M., M. Kossmann, R. Vöggtlin, and F. Fiedler, 1997: Valley wind systems and their influences on nocturnal ozone concentrations. *Beitr. Phys. Atmosph.*, **70**, 1-14.
- Lu, R., and R. P. Turco, 1995: Air pollutant transport in a coastal environment – II. Three-dimensional simulations over Los Angeles basin. *Atmos. Environ.*, **29**, 1499-1518.
- Ludwig, F. L., J. Horel, and C. D. Whiteman, 2004: Using EOF analysis to identify important surface wind patterns in mountain valleys. *J. Appl. Meteor.*, **43**, 969-983.
- Lugauer, M., and P. Winkler, 2005: Thermal circulation in South Bavaria - climatology and synoptic aspects. *Meteor. Z.*, **14**, 15-30.

- Lugauer, M., and Coauthors, 2003: An overview of the VERTIKATOR project and results of Alpine pumping. *Extended Abstracts, Vol. A, International Conf. on Alpine Meteor. and MAP-Meeting 2003*, May 19-23, 2003, Brig, Switzerland. Publications of MeteoSwiss, No. 66, 129-132.
- Luhar, A. K., and S. K. Rao, 1993: Random-walk model studies of the transport and diffusion of pollutants in katabatic flows. *Bound.-Layer Meteor.*, **66**, 395-412.
- Magono, C., C. Nakamura, and Y. Yoshida, 1982: Nocturnal cooling of the Moshiri Basin, Hokkaido in midwinter. *J. Meteor. Soc. Japan*, **60**, 1106-1116.
- Mahrt, L., 1982: Momentum balance of gravity flows. *J. Atmos. Sci.*, **39**, 2701-2711.
- Mahrt, L., 1999: Stratified atmospheric boundary layers. *Bound.-Layer Meteor.*, **90**, 375-396.
- Mahrt, L., 2006: Variation of surface air temperature in complex terrain. *J. Appl. Meteor. Climatol.*, **45**, 1481-1493.
- Mahrt, L. J., and S. Larsen, 1982: Small scale drainage flow. *Tellus*, **34**, 579-587.
- Mahrt, L., D. Vickers, R. Nakamura, M. R. Soler, J. Sun, S. Burns, and D. H. Lenschow, 2001: Shallow drainage flows. *Bound.-Layer Meteor.*, **101**, 243-260.
- Maki, M., and T. Harimaya, 1988: The effect of advection and accumulation of downslope cold air on nocturnal cooling in basins. *J. Meteor. Soc. Japan*, **66**, 581-597.
- Maki, M., T. Harimaya, and K. Kikuchi, 1986: Heat budget studies on nocturnal cooling in a basin. *J. Meteor. Soc. Japan*, **64**, 727-740.
- Manins, P. C., 1992: Vertical fluxes in katabatic flows. *Bound.-Layer Meteor.*, **60**, 169-178.
- Manins, P. C., and B. L. Sawford, 1979a: Katabatic winds: A field case study. *Quart. J. Roy. Meteor. Soc.*, **105**, 1011-1025.
- Manins, P. C., and B. L. Sawford, 1979b: A model of katabatic winds. *J. Atmos. Sci.*, **36**, 619-630.
- Mannouji, N., 1982: A numerical experiment on the mountain and valley winds. *J. Meteorol. Soc. Jap.*, **60**, 1085-1105.
- Martínez, D., 2011: Topographically induced flows and nocturnal cooling in the atmospheric boundary layer. Doctoral dissertation. Department of Physics, University of the Balearic Islands.
- Martínez, D., and J. Cuxart, 2009: Assessment of the hydraulic slope flow approach using a mesoscale model. *Acta Geophys.*, **57**, 882-903.
- Martínez, D., J. Cuxart, and J. Cunillera, 2008: Conditioned climatology for stably stratified nights in the Lleida area. *Tethys*, **5**, 13-24.
- Martínez, D., M. A. Jiménez, J. Cuxart, and L. Mahrt, 2010: Heterogeneous nocturnal cooling in a large basin under very stable conditions. *Bound.-Layer Meteor.*, **137**, 97-113.
- Marty, C., R. Philipona, C. Fröhlich, and A. Ohmura, 2002: Altitude dependence of surface radiation fluxes and cloud forcing in the alps: results from the alpine surface radiation budget network. *Theor. Appl. Climatol.*, **72**, 137-155.
- Matzinger, N., M. Andretta, E. van Gorsel, R. Vogt, A. Ohmura, and M. W. Rotach, 2003: Surface radiation budget of an Alpine valley. *Quart. J. Roy. Meteor. Soc.*, **129**, 877-895.
- Mayer, B., 2009: Radiative transfer in the cloudy atmosphere. *Eur. Phys. J. Conf.*, **1**, 75-99.
- Mayer, B., and A. Kylling, 2005: Technical note: The libRadtran software package for radiative transfer calculations – Description and examples of use. *Atmos. Chem. Phys.*, **5**, 1855-1877.
- Mayer, B., S. W. Hoch, and C. D. Whiteman, 2010: Validating the MYSTIC three-dimensional radiative transfer model with observations from the complex topography of Arizona's Meteor Crater. *Atmos. Chem. Phys. Discuss.*, **10**, 13373-13405.
- McGowan, H. A., 2004: Observations of anti-winds in a deep Alpine valley, Lake Tekapo, New Zealand. *Arctic, Antarctic, and Alpine Res.*, **36**, 495-501.
- McGowan, H. A., and A. P. Sturman, 1996: Interacting multi-scale wind systems within an alpine basin, Lake Tekapo. *New Zealand Meteor. Atmos. Phys.*, **58**, 165-177.
- McGowan, H. A., I. F. Owens, and A. P. Sturman, 1995: Thermal and dynamic characteristics of alpine lake breezes, Lake Tekapo, New Zealand. *Bound.-Layer Meteor.*, **76**, 3-24.
- McKee, T. B., and R. D. O'Neal, 1989: The role of valley geometry and energy budget in the formation of nocturnal valley winds. *J. Appl. Meteor.*, **28**, 445-456.
- McNider, R. T., 1982: A note on velocity fluctuations in drainage flows. *J. Atmos. Sci.*, **39**, 1658-1660.
- Monti, P., H. J. S. Fernando, M. Princevac, W. C. Chan, T. A. Kowalewski, and E. R. Pardyjak, 2002: Observations of flow and turbulence in the nocturnal boundary layer over a slope. *J. Atmos. Sci.*, **59**, 2513-2534.
- Moraes, O. L. L., O. C. Acevedo, R. Da Silva, R. Magnago, and A. C. Siqueira, 2004: Nocturnal surface-layer characteristics at the bottom of a valley. *Bound.-Layer Meteor.*, **112**, 159-177.
- Müller, M. D., and D. Scherer, 2005: A grid- and subgrid-scale radiation parameterization of topographic effects for mesoscale weather forecast models. *Mon. Wea. Rev.*, **133**, 1431-1442.
- Mursch-Radlgruber, E., 1995: Observations of flow structure in a small forested valley system. *Theor.*

- Appl. Climatol.*, **52**, 3-17.
- Neff, W. D., and C. W. King, 1989: The accumulation and pooling of drainage flows in a large basin. *J. Appl. Meteor.*, **28**, 518-529.
- Nickus, U., and I. Vergeiner, 1984: The thermal structure of the Inn Valley atmosphere. *Arch. Meteor. Geophys. Bioclimatol., Ser. A*, **33**, 199-215.
- Noppel, H., and F. Fiedler, 2002: Mesoscale heat transport over complex terrain by slope winds – A conceptual model and numerical simulations. *Bound.-Layer Meteor.*, **104**, 73-97.
- O'Steen, L. B., 2000: Numerical simulation of nocturnal drainage flows in idealized valley-tributary systems. *J. Appl. Meteor.*, **39**, 1845-1860.
- Oerlemans, J., 1998: The atmospheric boundary layer over melting glaciers. Chapter 6 in: *Clear and Cloudy Boundary Layers* (Eds: A. A. M. Holtslag and P. G. Duynkerke), Royal Netherlands Academy of Arts and Sciences, 129–153.
- Oerlemans, J., and B. Grisogono, 2002: Glacier winds and parameterisation of the related surface heat fluxes. *Tellus A*, **54**, 440-452.
- Oerlemans, J., H. Björnsson, M. Kuhn, F. Obleitner, F. Pálsson, C. J. P. P. Smeets, H. F. Vugts, and J. De Wolde, 1999: Glacio-meteorological investigations on Vatnajökull, Iceland, summer 1996: An overview. *Bound.-Layer Meteor.*, **92**, 3-26.
- Oliphant, A. J., R. A. Spronken-Smith, A. P. Sturman, and I. F. Owens, 2003: Spatial variability of surface radiation fluxes in mountainous terrain. *J. Appl. Meteor.*, **42**, 113-128.
- Oliver, H. R., 1992: Studies of the energy budget of sloping terrain. *Int. J. Climatol.*, **12**, 55-68.
- Olyphant, G. A., 1986: Longwave radiation in mountainous areas and its influence on the energy balance of alpine snowfields. *Water Resources Res.*, **22**, 62-66.
- Oncley, S. P., and Coauthors, 2007: The Energy Balance Experiment EBEX-2000. Part I: Overview and energy balance. *Bound.-Layer Meteor.*, **123**, 1-28.
- Orgill, M. M., J. D. Kincheloe, and R. A. Sutherland, 1992: Influences on nocturnal valley drainage winds in Western Colorado valleys. *J. Appl. Meteor.*, **31**, 121-141.
- Pamperin, H., and G. Stilke, 1985: Nächtliche Grenzschicht und LLJ im Alpenvorland nahe dem Inntalausgang. [Nocturnal boundary layer and low level jet near the Inn Valley exit]. *Meteor. Rundsch.*, **38**, 145-156.
- Panday, A. K., 2006: The diurnal cycle of air pollution in the Kathmandu Valley, Nepal. Dissertation No. 37361. Massachusetts Institute of Technology. [<http://hdl.handle.net/1721.1/37361>]
- Panday, A. K., and R. G. Prinn, 2009: Diurnal cycle of air pollution in the Kathmandu Valley, Nepal: Observations. *J. Geophys. Res.*, **114**, D09305, doi:10.1029/2008JD009777.
- Panday, A. K., R. G. Prinn, and C. Schär, 2009: Diurnal cycle of air pollution in the Kathmandu Valley, Nepal: 2. Modeling results. *J. Geophys. Res.*, **114**, D21308, doi:10.1029/2008JD009808.
- Papadopoulos, K. H., and C. G. Helmis, 1999: Evening and morning transition of katabatic flows. *Bound.-Layer Meteor.*, **92**, 195-227.
- Papadopoulos, K. H., C. G. Helmis, A. T. Soilemes, J. Kalogiros, P. G. Papageorgas, and D. N. Asimakopoulos, 1997: The structure of katabatic flows down a simple slope. *Quart. J. Roy. Meteor. Soc.*, **123**, 1581-1601.
- Parish, T. R., and L. D. Oolman, 2010: On the role of sloping terrain in the forcing of the Great Plains low-level jet. *J. Atmos. Sci.*, **67**, 2690–2699.
- Petkovšek, Z., 1992: Turbulent dissipation of cold air lake in a basin. *Meteor. Atmos. Phys.*, **47**, 237-245.
- Philipona, R., B. Dürr, and C. Marty, 2004: Greenhouse effect and altitude gradients over the Alps - by surface longwave radiation measurements and model calculated LOR. *Theor. Appl. Climatol.*, **77**, 1-7.
- Pielke, R. A., J. H. Rodriguez, J. L. Eastman, R. L. Walko, and R. A. Stocker, 1993: Influence of albedo variability in complex terrain on mesoscale systems. *J. Climate*, **6**, 1798-1806.
- Pinto, J. O., D. B. Parsons, W. O. J. Brown, S. Cohn, N. Chamberlain, and B. Morley, 2006: Coevolution of down-valley flow and the nocturnal boundary layer in complex terrain. *J. Appl. Meteor. Climatol.*, **45**, 1429-1449.
- Piringer, M., and K. Baumann, 1999: Modifications of a valley wind system by an urban area - Experimental results. *Meteor. Atmos. Phys.*, **71**, 117-125.
- Plüss, C., and A. Ohmura, 1997: Longwave radiation on snow-covered mountainous surfaces. *J. Appl. Meteor.*, **36**, 818-824.
- Porch, W. M., R. B. Fritz, R. L. Coulter, and P. H. Gudiksen, 1989: Tributary, valley and sidewall air flow interactions in a deep valley. *J. Appl. Meteor.*, **28**, 578-589.
- Porch, W. M., W. E. Clements, and R. L. Coulter, 1991: Nighttime valley waves. *J. Appl. Meteor.*, **30**, 145-156.
- Pope, D., and C. Brough, 1996: Utah's Weather and Climate. Publishers Press, 245pp.

- Pospichal, B., 2004: Struktur und Auflösung von Temperaturinversionen in Dolinen am Beispiel Grünloch [Structure and breakup of temperature inversions in Dolines, with an example from the Grünloch]. Diplomarbeit, Instit. Meteor. u. Geophysik, Univ. Wien, 69pp.
- Pospichal, B., S. Eisenbach, C. D. Whiteman, R. Steinacker, and M. Dorninger, 2003: Observations of the cold air outflow from a basin cold pool through a low pass. *Ext. Abstr., Vol. A, Intl Conf. Alpine Meteor. and the MAP-Meeting 2003*, Brig, Switzerland, 19-23 May 2003, 153-156. Available as MeteoSwiss Publication 66, MeteoSwiss, Zurich, Switzerland.
- Poulos, G. S., and S. Zhong, 2008: The observational history of small-scale katabatic winds in mid-latitudes. *Geography Compass*, **2**, 1-24.
- Poulos, G. S., J. E. Bossert, T. B. McKee, and R. A. Pielke, 2000: The interaction of katabatic flow and mountain waves. Part I: Observations and idealized simulations. *J. Atmos. Sci.*, **57**, 1919-1936.
- Poulos, G. S., and Coauthors, 2002: CASES-99: A comprehensive investigation of the stable nocturnal boundary layer. *Bull. Amer. Meteor. Soc.*, **83**, 555-581.
- Poulos, G. S., J. E. Bossert, T. B. McKee, and R. A. Pielke, Sr., 2007: The interaction of katabatic flow and mountain waves. Part II: Case study analysis and conceptual model. *J. Atmos. Sci.*, **64**, 1857-1879.
- Prabha, T. V., and E. Mursch-Radlgruber, 1999: Modeling of diffusion in a wide Alpine valley. *Theor. Appl. Climatol.* **64**, 93-103.
- Prandtl, L., 1942: *Strömungslehre* [Flow Studies]. Vieweg und Sohn, Braunschweig, 382 pp.
- Prévôt, A. S. H., J. Staehelin, H. Richner, and T. Griesser, 1993: A thermally driven wind system influencing concentrations of ozone precursors and photo-oxidants at a receptor site in the Alpine foothills. *Meteor. Z., N.F.*, **2**, 167-177.
- Prévôt, A. S. H., J. Dommen, M. Bäumle, and M. Furger, 2000: Diurnal variations of volatile organic compounds and local circulation systems in an Alpine valley. *Atmos. Environ.*, **34**, 1413-1423.
- Princevac, M., and H. J. S. Fernando, 2007: A criterion for the generation of turbulent anabatic flows. *Phys. Fluids*, **19**, 105102, doi:10.1063/1.2775932.
- Princevac, M., and H. J. S. Fernando, 2008: Morning breakup of cold pools in complex terrain. *J. Fluid Mech.*, **616**, 99-109.
- Princevac, M., H. J. S. Fernando, and C. D. Whiteman, 2005: Turbulent entrainment into natural gravity-driven flows. *J. Fluid Mech.*, **533**, 259-268.
- Princevac, M., J. C. R. Hunt, and H. J. S. Fernando, 2008: Quasi-steady katabatic winds on slopes in wide valleys: Hydraulic theory and observations. *J. Atmos. Sci.*, **65**, 627-643.
- Räisänen, P., 1996: The effect of vertical resolution on clear-sky radiation calculations: tests with two schemes. *Tellus*, **48A**, 403-423.
- Rakovec, J., J. Merše, S. Jernej, and B. Paradiž, 2002: Turbulent dissipation of the cold-air pool in a basin: Comparison of observed and simulated development. *Meteor. Atmos. Phys.*, **79**, 195-213.
- Ramanathan, N., and K. Srinivasan, 1998: Simulation of airflow in Kashmir valley for a summer day. *J. Appl. Meteor.*, **37**, 497-508.
- Rampanelli, G., 2004: Diurnal thermally-induced flows in Alpine valleys. Ph.D. thesis in Environmental Engineering, University of Trento, Italy.
- Rampanelli, G., and D. Zardi, 2004: A method to determine the capping inversion of the convective boundary layer. *J. Appl. Meteor.*, **43**, 925-933.
- Rampanelli, G., D. Zardi, and R. Rotunno, 2004: Mechanisms of up-valley winds. *J. Atmos. Sci.*, **61**, 3097-3111.
- Rao, S. K., and M. A. Schaub, 1990: Observed variations of σ_c and σ_b in the nocturnal drainage flow in a deep valley. *Bound.-Layer Meteor.*, **51**, 31-48.
- Rao, K. S., and H. F. Snodgrass, 1981: A nonstationary nocturnal drainage flow model. *Bound.-Layer Meteor.*, **20**, 309-320.
- Reeves, H. D., and D. J. Stensrud, 2009: Synoptic-scale flow and valley cold pool evolution in the Western United States. *Wea. Forecasting*, **24**, 1625-1643.
- Regmi, R. P., T. Kitada, and G. Kurata, 2003: Numerical simulation of late wintertime local flows in Kathmandu Valley, Nepal: Implication for air pollution transport. *J. Appl. Meteor.*, **42**, 389-403.
- Reiter, E. R., and M. Tang, 1984: Plateau effects on diurnal circulation patterns. *Mon. Wea. Rev.*, **112**, 638-651.
- Reuder, J., and J. Egger, 2006: Diurnal circulation of the South American Altiplano: Observations in a valley and at a pass. *Tellus A*, **58**, 254-262.
- Reuten, C., 2008: *Upslope flow systems: Scaling, structure, and kinematics in tank and atmosphere*. VDM Verlag Dr. Mueller e.K., Saarbrücken, Germany, 200pp.
- Reuten, C., D. G. Steyn, K. B. Strawbridge, and P. Bovis, 2005: Observations of the relation between upslope flows and the convective boundary layer in steep terrain. *Bound.-Layer Meteor.*, **116**, 37-61.

- Reuten, C., D. G. Steyn, and S. E. Allen, 2007: Water tank studies of atmospheric boundary layer structure and air pollution transport in upslope flow systems. *J. Geophys. Res.*, **112**, D11114, doi:10.1029/2006JD008045.
- Rotach, M. W., and D. Zardi, 2007: On the boundary layer structure over complex terrain: Key findings from MAP. *Quart. J. Roy. Meteor. Soc.*, **133**, 937-948.
- Rotach M. W., and Coauthors, 2004: Turbulence structure and exchange processes in an Alpine valley: The Riviera project. *Bull. Amer. Meteor. Soc.*, **85**, 1367-1385.
- Rotach, M. W., M. Andretta, P. Calanca, A. P. Weigel, and A. Weiss, 2008: Turbulence characteristics and exchange mechanisms in highly complex terrain. *Acta Geophysicae*, **56**, 194-219.
- Rucker, M., R. M. Banta, and D. G. Steyn, 2008: Along-valley structure of daytime thermally driven flows in the Wipp Valley. *J. Appl. Meteor. Climatol.*, **47**, 733-751.
- Sakiyama, S. K., 1990: Drainage flow characteristics and inversion breakup in two Alberta mountain valleys. *J. Appl. Meteor.*, **29**, 1015-1030.
- Salerno, R., 1992: Analysis of flow and pollutant dispersion by tracer experiments in south Alpine valleys. *Theor. Appl. Climatol.* **45**, 19-35.
- Sasaki, T., and Coauthors, 2004: Vertical moisture transport above the mixed layer around the mountains in western Sumatra. *Geophys. Res. Lett.*, **31**, L08106, doi:10.1029/2004GL019730.
- Savage, L. C., III, S. Zhong, W. Yao, W. J. O. Brown, T. W. Horst, and C. D. Whiteman, 2008: An observational and numerical study of a regional-scale downslope flow in northern Arizona. *J. Geophys. Res.*, **113**, D14114, doi:10.1029/2007JD009623.
- Savijärvi H., and J. Liya, 2001: Local winds in a valley city. *Bound.-Layer Meteor.*, **100**, 301-319.
- Schicker, I., and P. Seibert, 2009. Simulation of the meteorological conditions during a winter smog episode in the Inn Valley. *Meteor. Atmos. Phys.*, **103**, 203-214.
- Schmidli, J., and R. Rotunno, 2010: Mechanisms of along-valley winds and heat exchange over mountainous terrain. *J. Atmos. Sci.*, **67**, 3033-3047.
- Schmidli, J., G. S. Poulos, M. H. Daniels, and F. K. Chow, 2009a: External Influences on nocturnal thermally driven flows in a deep valley. *J. Appl. Meteor. Climatol.*, **48**, 3–23.
- Schmidli, J., B. Billings, F. K. Chow, J. Doyle, V. Grubišić, T. Holt, Q. Jiang, K. A. Lundquist, P. Sheridan, S. Vosper, S. F. J. de Wekker, C. D. Whiteman, A. A. Wyszogrodzki, and G. Zängl, 2010: Intercomparison of mesoscale model simulations of the daytime valley wind system. *Mon. Wea. Rev.*, **139**, 1389-1409.
- Schumann, U., 1990: Large-eddy simulation of the up-slope boundary layer. *Quart. J. Roy. Meteor. Soc.*, **116**, 637-670.
- Serafin, S., 2006: Boundary-layer processes and thermally driven flows over complex terrain. Ph.D. thesis in Environmental Engineering, Univ. of Trento, Italy, 200pp. <http://www.ing.unitn.it/dica/eng/monographs/index.php>.
- Serafin, S., and D. Zardi, 2010a: Structure of the atmospheric boundary layer in the vicinity of a developing upslope flow system: A numerical model study. *J Atmos. Sci.*, **67**, 1171-1185.
- Serafin, S., and D. Zardi, 2010b: Daytime heat transfer processes related to slope flows and turbulent convection in an idealized mountain valley. *J Atmos. Sci.*, **67**, 3739-3756.
- Serafin, S., and D. Zardi, 2010c: Daytime development of the boundary layer over a plain and in a valley under fair weather conditions: a comparison by means of idealized numerical simulations *J Atmos. Sci.*, **68**, 2128-2141.
- Shapiro, A., and E. Fedorovich, 2007: Katabatic flow along a differentially cooled sloping surface. *J. Fluid Mech.*, **571**, 149-175.
- Shapiro, A., and E. Fedorovich, 2008: Coriolis effects in homogeneous and inhomogeneous katabatic flows. *Quart. J. Roy. Meteor. Soc.*, **134**, 353–370.
- Shapiro, A., and E. Fedorovich, 2009: Nocturnal low-level jet over a shallow slope. *Acta Geophysica*, **57**, 950-980.
- Sharp, J., and C. F. Mass, 2004: Columbia Gorge gap winds: Their climatological influence and synoptic evolution. *Wea. Forecasting*, **19**, 970-992.
- Sievers, U., 2005: Das Kaltluftabflussmodell KLAM_21 - Theoretische Grundlagen, Anwendung und Handhabung des PC-Modells [The cold air drainage model KLAM_21 – Theoretical basis, application, and operation of the PC model]. *Berichte des Deutschen Wetterdienstes no. 227*, Offenbach am Main, Germany, 101pp.
- Simpson, J. E., 1999: *Gravity currents, 2nd Edition*. Cambridge Univ. Press, 259pp.
- Skyllingstad, E. D., 2003: Large-eddy simulation of katabatic flows. *Bound.-Layer Meteor.*, **106**, 217-243.
- Smith, C. M., and E. D. Skyllingstad, 2005: Numerical simulation of katabatic flow with changing slope angle. *Mon. Wea. Rev.*, **133**, 3065-3080.
- Smith, R., and Coauthors, 1997: Local and remote effects of mountains on weather: research needs and

- opportunities. *Bull. Amer. Meteor. Soc.*, **78**, 877-892.
- Soler, M. R., C. Infante, P. Buenestado, and L. Mahrt, 2002: Observations of nocturnal drainage flow in a shallow gully. *Bound.-Layer Meteor.*, **105**, 253-273.
- Spengler, T., J. H. Schween, M. Ablinger, G. Zängl, and J. Egger, 2009: Thermally driven flows at an asymmetric valley exit: Observations and model studies at the Lech Valley exit. *Mon. Wea. Rev.*, **137**, 3437-3455.
- Start, G. E., C. R. Dickson, and L. L. Wendell, 1975: Diffusion in a canyon within rough mountainous terrain. *J. Appl. Meteor.*, **14**, 333-346.
- Steinacker, R., 1984: Area-height distribution of a valley and its relation to the valley wind. *Contrib. Atmos. Phys.*, **57**, 64-71.
- Steinacker, R., and Coauthors, 2006: A mesoscale data analysis and downscaling method over complex terrain. *Mon. Wea. Rev.*, **134**, 2758-2771.
- Steinacker, R., and Coauthors, 2007: A sinkhole field experiment in the eastern Alps. *Bull. Amer. Meteor. Soc.*, **88**, 701-716.
- Stewart, J. Q., C. D. Whiteman, W. J. Steenburgh, and X. Bian, 2002: A climatological study of thermally driven wind systems of the US Intermountain West. *Bull. Amer. Meteor. Soc.*, **83**, 699-708.
- Stone, G. L., and D. E. Hoard, 1989: Low frequency velocity and temperature fluctuations in katabatic valley flows. *J. Appl. Meteor.*, **28**, 477-488.
- Stull, R. B., 1988: *An Introduction to Boundary Layer Meteorology*. Kluwer Academic, 670 pp.
- Sturman, A. P., and H. A. McGowan, 1995: An assessment of boundary-layer air mass characteristics associated with topographically-induced local wind systems. *Bound.-Layer Meteor.*, **74**, 181-193.
- Sturman, A. P., H. A. McGowan, and R. A. Spronken-Smith, 1999: Mesoscale and local climates. *Progress Physical Geography*, **23**, 611-635.
- Sturman, A. P., and Coauthors, 2003a: The Lake Tekapo Experiment (LTEX): An investigation of atmospheric boundary layer processes in complex terrain. *Bull. Amer. Meteor. Soc.*, **84**, 371-380.
- Sturman, A. P., and Coauthors, 2003b: Supplement to the Lake Tekapo Experiment (LTEX): An investigation of atmospheric boundary layer processes in complex terrain. *Bull. Amer. Meteor. Soc.*, **84**, 381-383.
- Sun, J., S. P. Burns, A. C. Delany, S. P. Oncley, T. W. Horst, and D. H. Lenschow, 2003: Heat balance in the nocturnal boundary layer during CASES-99. *J. Appl. Meteor.*, **42**, 1649-1666.
- Szintai, B., P. Kaufmann, and M. Rotach, 2010: Simulation of pollutant transport in complex terrain with a numerical weather prediction-particle dispersion model combination. *Bound.-Layer Meteor.*, **137**, 373-396.
- Taylor, J. R., M. Kossmann, D. J. Low, and P. Zawar-Reza, 2005: Summertime easterly surges in southeastern Australia: A case study of thermally forced flow. *Austr. Met. Mag.*, **54**, 213-223.
- Thompson, B. W., 1986: Small-scale katabatics and cold hollows. *Weather*, **41**, 146-153.
- Trachte, K., T. Nauss, and J. Bendix, 2010: The impact of different terrain configurations on the formation and dynamics of katabatic flows: Idealised case studies. *Bound.-Layer Meteor.*, **134**, 307-325.
- Triantafyllou, A. G., C. G. Helmis, D. N. Asimakopoulos, and A. T. Soilemes, 1995: Boundary layer evolution over a large and broad mountain basin. *Theor. Appl. Climatol.*, **52**, 19-25.
- Urfer-Henneberger, C., 1970: Neure Beobachtungen über die Entwicklung des Schönwetterwindsystems in einem V-förmigen Alpentale (Dischmatal bei Davos). [New observations of the development of a clear weather wind system in a v-shaped mountain valley (Dischma Valley near Davos)]. *Arch. Meteor. Geophys. Bioclimatol., Ser. B*, **18**, 21-42.
- Van de Wiel, B. J. H., A. F. Moene, O. K. Hartogensis, H. A. R. De Bruin, and A. A. M. Holtslag, 2003: Intermittent turbulence and oscillations in the stable boundary layer over land. Part III. A classification for observations during CASES-99. *J. Atmos. Sci.*, **60**, 2509-2522.
- Van den Broeke, M. R., 1997a: Momentum, heat and moisture budgets of the katabatic wind layer over a midlatitude glacier in summer. *J. Appl. Meteor.*, **36**, 763-774.
- Van den Broeke, M. R., 1997b: Structure and diurnal variation of the atmospheric boundary layer over a mid-latitude glacier in summer. *Bound.-Layer Meteor.*, **83**, 183-205.
- Van Gorsel, E., 2003: Aspects of flow characteristics and turbulence in complex terrain. Results from the MAP-Riviera project. Dissertation. University of Basel, Geography Department. ISBN 3-85977-247-1. 58 pp.
- Van Gorsel, E., A. Christen, C. Feigenwinter, E. Parlow, and R. Vogt, 2003a: Daytime turbulence statistics above a steep forested slope. *Bound.-Layer Meteor.*, **109**, 311-329.
- Van Gorsel, E., R. Vogt, A. Christen, and M. W. Rotach, 2003b: Low frequency temperature and velocity oscillations in katabatic winds. Ext. Abstr., Vol A, Int. Conf. Alpine Meteor. and MAP Meeting 2003. Publ. MeteoSwiss, No. 66, 251-254.
- Varvayanni, M., J. G. Bartzis, N. Catsaros, P. Deligianni, and C. E. Elderkin, 1997: Simulation of nocturnal

- drainage flows enhanced by deep canyons: The Rocky Flats case. *J. Appl. Meteor.*, **36**, 775-791.
- Vergeiner, I., 1983: Dynamik alpiner Windsysteme. [Dynamics of Alpine wind systems]. Bericht zum forschungsvorhaben "3556" des Fonds zur Forderung der wissenschaftlichen Forschung, Wien, Austria, 129 pp.
- Vergeiner, I., 1987: An elementary valley wind model. *Meteor. Atmos. Phys.*, **36**, 255-263.
- Vergeiner, I., and E. Dreiseitl, 1987: Valley winds and slope winds - observations and elementary thoughts. *Meteor. Atmos. Phys.*, **36**, 264-286.
- Vertacnik, G, I. Sinjur, and M. Ogrin, 2007: Temperature comparison between some Alpine dolines in winter time. ICAM 2007. http://www.cnrm.meteo.fr/icam2007/html/PROCEEDINGS/ICAM2007/extended/manuscript_95.pdf
- Viana, S., E. Terradellas, and C. Yagüe, 2010: Analysis of gravity waves generated at the top of a drainage flow. *J. Atmos. Sci.*, **67**, 3949-3966.
- Vosper, S. B., and A. R. Brown, 2008: Numerical simulations of sheltering in valleys: The formation of nighttime cold-air pools. *Bound.-Layer Meteor.*, **127**, 429-448.
- Vrhovec, T., 1991: A cold air lake formation in a basin - a simulation with a mesoscale numerical model. *Meteor. Atmos. Phys.*, **46**, 91-99.
- Wagner, A., 1932: Neue Theorie der Berg- und Talwinde [New theory of mountain and valley winds]. *Meteor. Z.*, **49**, 329-341.
- Wagner, A., 1938: Theorie und Beobachtung der periodischen Gebirgswinde. [Theory and observation of periodic mountain winds]. *Gerlands Beitr. Geophys. (Leipzig)*, **52**, 408-449. [English translation: Whiteman, C.D., and E. Dreiseitl, 1984: Alpine Meteorology: Translations of Classic Contributions by A. Wagner, E. Ekhardt and F. Defant. PNL-5141 / ASCOT-84-3. Pacific Northwest Laboratory, Richland, Washington, 121 pp].
- Weber, R. O., and P. Kauffmann, 1995: Automated classification scheme for wind fields. *J. Appl. Meteor.*, **34**, 1133-1141.
- Weber, R. O., and P. Kaufmann, 1998: Relationship of synoptic winds and complex terrain flows during the MISTRAL field experiment. *J. Appl. Meteor.*, **37**, 1486-1496.
- Weigel, A. P., 2005: On the atmospheric boundary layer over highly complex topography. Dissertation No. 15972, ETH, Zurich. [<http://e-collection.ethbib.ethz.ch/view/eth:27927>].
- Weigel, A. P., and M. W. Rotach, 2004: Flow structure and turbulence characteristics of the daytime atmosphere in a steep and narrow Alpine valley. *Quart. J. Roy. Meteor. Soc.*, **130**, 2605-2627.
- Weigel, A. P., F. K. Chow, M. W. Rotach, R. L. Street, and M. Xue, 2006: High-resolution large-eddy simulations of flow in a steep Alpine valley. Part II. Flow structure and heat budgets. *J. Appl. Meteor. Climatol.*, **45**, 87-107.
- Weigel, A. P., F. K. Chow, and M. W. Rotach, 2007: On the nature of turbulent kinetic energy in a steep and narrow Alpine valley. *Bound.-Layer Meteor.*, **123**, 177-199.
- Weissmann, M., F. J. Braun, L. Gantner, G. J. Mayr, S. Rahm, and O. Reitebuch, 2005: The Alpine mountain-plain circulation: Airborne Doppler lidar measurements and numerical simulations. *Mon. Wea. Rev.*, **33**, 3095-3109.
- Whiteman, C. D., 1982: Breakup of temperature inversions in deep mountain valleys: Part I. Observations. *J. Appl. Meteor.*, **21**, 270-289.
- Whiteman, C. D., 1986: Temperature inversion buildup in Colorado's Eagle valley. *Meteor. Atmos. Physics*, **35**, 220-226.
- Whiteman, C. D., 1990: Observations of thermally developed wind systems in mountainous terrain. In: W. Blumen, Editor, *AMS Meteorological Monographs*, **45** (23), 5-42.
- Whiteman, C. D., 2000: *Mountain Meteorology: Fundamentals and Applications*. Oxford University Press, New York, 355pp.
- Whiteman, C. D., and T. B. McKee, 1982: Breakup of temperature inversions in deep mountain valleys: Part II. Thermodynamic model. *J. Appl. Meteor.*, **21**, 290-302.
- Whiteman, C. D., and E. Dreiseitl, 1984: *Alpine Meteorology. Translations of Classic Contributions by A. Wagner, E. Ekhardt and F. Defant*. PNL-5141/ASCOT-84-3. Pacific Northwest Laboratory, Richland, Washington, 121 pp.
- Whiteman, C. D., and J. C. Doran, 1993: The relationship between overlying synoptic-scale flows and winds within a valley. *J. Appl. Meteor.*, **32**, 1669-1682.
- Whiteman, C. D., and X. Bian, 1998: Use of radar profiler data to investigate large-scale thermally driven flows into the Rocky Mountains. *Proc. Fourth Int. Symp. on Tropospheric Profiling: Needs and Technologies*, Snowmass, CO.
- Whiteman, C. D., and S. Zhong, 2008: Downslope flows on a low-angle slope and their interactions with valley inversions. I. Observations. *J. Appl. Meteor. Climatol.*, **47**, 2023-2038.

- Whiteman, C. D., K. J. Allwine, L. J. Fritschen, M. M. Orgill, and J. R. Simpson, 1989a: Deep valley radiation and surface energy budget microclimates. I. Radiation. *J. Appl. Meteor.*, **28**, 414-426.
- Whiteman, C. D., K. J. Allwine, M. M. Orgill, L. J. Fritschen, and J. R. Simpson, 1989b: Deep valley radiation and surface energy budget microclimates. II. Energy budget. *J. Appl. Meteor.*, **28**, 427-437.
- Whiteman, C. D., T. B. McKee, and J. C. Doran, 1996: Boundary layer evolution within a canyonland basin. Part I. Mass, heat, and moisture budgets from observations. *J. Appl. Meteor.*, **35**, 2145-2161.
- Whiteman, C. D., X. Bian, and J. L. Sutherland, 1999a: Wintertime surface wind patterns in the Colorado River valley. *J. Appl. Meteor.*, **38**, 1118-1130.
- Whiteman, C. D., X. Bian, and S. Zhong, 1999b: Wintertime evolution of the temperature inversion in the Colorado Plateau Basin. *J. Appl. Meteor.*, **38**, 1103-1117.
- Whiteman, C. D., S. Zhong, and X. Bian, 1999c: Wintertime boundary-layer structure in the Grand Canyon. *J. Appl. Meteor.*, **38**, 1084-1102.
- Whiteman, C. D., S. Zhong, X. Bian, J. D. Fast, and J. C. Doran, 2000: Boundary layer evolution and regional-scale diurnal circulations over the Mexico Basin and Mexican Plateau. *J. Geophys. Res.*, **105**, 10081-10102.
- Whiteman, C. D., S. Zhong, W. J. Shaw, J. M. Hubbe, X. Bian, and J. Mittelstadt, 2001: Cold pools in the Columbia Basin. *Wea. Forecasting*, **16**, 432-447.
- Whiteman, C. D., S. Eisenbach, B. Pospichal, and R. Steinacker, 2004a: Comparison of vertical soundings and sidewall air temperature measurements in a small Alpine basin. *J. Appl. Meteor.*, **43**, 1635-1647.
- Whiteman, C. D., B. Pospichal, S. Eisenbach, P. Weihs, C. B. Clements, R. Steinacker, E. Mursch-Radlgruber, and M. Dorninger, 2004b: Inversion breakup in small Rocky Mountain and Alpine basins. *J. Appl. Meteor.*, **43**, 1069-1082.
- Whiteman, C. D., T. Haiden, B. Pospichal, S. Eisenbach, and R. Steinacker, 2004c: Minimum temperatures, diurnal temperature ranges and temperature inversions in limestone sinkholes of different size and shape. *J. Appl. Meteor.*, **43**, 1224-1236.
- Whiteman, C. D., S. F. J. De Wekker, and T. Haiden, 2007: Effect of dewfall and frostfall on nighttime cooling in a small, closed basin. *J. Appl. Meteor.*, **46**, 3-13.
- Whiteman, C. D., and Coauthors, 2008: METCRAX 2006 – Meteorological experiments in Arizona's Meteor Crater. *Bull. Amer. Meteor. Soc.*, **89**, 1665-1680.
- Whiteman, C.D., S.W. Hoch, and G.S. Poulos, 2009: Evening temperature rises on valley floors and slopes: Their causes and their relationship to the thermally driven wind system. *J. Appl. Meteor. Climatol.*, **48**, 776–788.
- Whiteman, C. D., S. W. Hoch, M. Lehner, and T. Haiden, 2010: Nocturnal cold air intrusions into Arizona's Meteor Crater: Observational evidence and conceptual model. *J. Appl. Meteor. Climatol.*, **49**, 1894-1905.
- Wilczak, J. M., S. P. Oncley, and S. A. Stage, 2001: Sonic anemometer tilt correction algorithms. *Bound.-Layer Meteor.*, **99**, 127-150.
- Winkler, P., M. Lugauer, and O. Reitebuch, 2006: Alpines Pumpen [Alpine pumping]. *Promet* (Deutscher Wetterdienst), **32**, 34-42. [In German].
- Wong, R. K. W., and K. D. Hage, 1995: Numerical simulation of pollutant dispersion in a small valley under conditions with supercritical Richardson number. *Bound.-Layer Meteor.*, **73**, 15–33.
- Wotawa, G., and H. Kromp-Kolb, 2000: The research project VOTALP - general objectives and main results. *Atmos. Environ.*, **34**, 1319-1322.
- Wu, P., M. Hara, J.I. Hamada, M.D. Yamanaka, and F. Kimura, 2009: Why a large amount of rain falls over the sea in the vicinity of western Sumatra island during nighttime. *J. Appl. Meteor. Climatol.*, **48**, 1345–1361.
- Yang, K., T. Koike, H. Fujii, T. Tamura, X. Xu, L. Bian, and M. Zhou, 2004: The daytime evolution of the atmospheric boundary layer and convection over the Tibetan Plateau: Observations and simulations. *J. Meteor. Soc. Japan*, **82**, 1777–1792.
- Yao, W. Q., and S. Zhong, 2009: Nocturnal temperature inversions in a small enclosed basin and their relationship to ambient atmospheric conditions. *Meteor. Atmos. Phys.*, **103**, 195-210.
- Ye, Z., M. Segal, J. R. Garratt, and R. A. Pielke, 1989: On the impact of cloudiness on the characteristics of nocturnal downslope flows. *Bound.-Layer Meteor.*, **49**, 23-51.
- Ye, Z. J., J. R. Garratt, M. Segal, and R. A. Pielke, 1990: On the impact of atmospheric thermal stability on the characteristics of nocturnal downslope flows. *Bound.-Layer Meteor.*, **51**, 77-97.
- Yoshino, M. M., 1975: *Climate in a Small Area*. Tokyo, University of Tokyo Press, 549 pp.
- Zammett, R. J., and A. C. Fowler, 2007: Katabatic winds on ice sheets: A refinement of the Prandtl model. *J. Atmos. Sci.*, **64**, 2707–2716.
- Zängl, G., 2003: The impact of upstream blocking, drainage flow and the geostrophic pressure gradient on the persistence of cold-air pools. *Quart. J. Roy. Meteor. Soc.*, **129**, 117-137.

- Zängl, G., 2004: A reexamination of the valley wind system in the Alpine Inn Valley with numerical simulations. *Meteor. Atmos. Phys.*, **87**, 241 - 256.
- Zängl, G., 2005: Wintertime cold-air pools in the Bavarian Danube Valley Basin: Data analysis and idealized numerical simulations. *J. Appl. Meteor.*, **44**, 1950-1971.
- Zängl, G., 2008: The impact of weak synoptic forcing on the valley-wind circulation in the Alpine Inn Valley. *Meteor. Atmos. Phys.*, **105**, 37-53.
- Zängl, G., and J. Egger, 2005: Diurnal circulation of the Bolivian Altiplano. Part II: Theoretical and model investigations. *Mon. Wea. Rev.*, **133**, 3624-3643.
- Zängl, G., and S. G. Chico, 2006: The thermal circulation of a grand plateau: Sensitivity to the height, width, and shape of the plateau. *Mon. Wea. Rev.*, **134**, 2581-2600.
- Zängl, G., and S. Vogt, 2006: Valley-wind characteristics in the Alpine Rhine Valley: Measurements with a wind-temperature profiler in comparison with numerical simulations. *Meteor. Z.*, **15**, 179-186.
- Zängl, G., J. Egger, and V. Wirth, 2001: Diurnal winds in the Himalayan Kali Gandaki Valley. Part II. Modeling. *Mon. Wea. Rev.*, **129**, 1062-1080.
- Zardi, D., 2000: A model for the convective boundary layer development in an Alpine valley, *Proceedings, 26th Int. Conf. Alpine Meteor.* ICAM2000, Innsbruck, Austria, 11-15 September 2000. Österreichische Beiträge zur Meteorologie und Geophysik. Heft Nr. 23/ Publ. Nr. 362. ISSN 1016-6254.
- Zardi, D., R. Gerola, F. Tampieri, and M. Tubino, 1999: Measurement and modelling of a valley wind system in the Alps. *Proceedings of the 13th AMS Symposium on Boundary Layers and Turbulence*. 10-15 January 1999, Dallas, TX, 28-31.
- Zaremba, L. L., and J. J. Carroll, 1999: Summer wind flow regimes over the Sacramento Valley. *J. Appl. Meteor.*, **38**, 1463-1473.
- Zawar-Reza, P., and A. P. Sturman, 2006a: Numerical analysis of a thermotopographically-induced mesoscale circulation in a mountain basin using a non-hydrostatic model. *Meteor. Atmos. Phys.*, **93**, 221-233.
- Zawar-Reza, P., and A. P. Sturman, 2006b: Two-dimensional numerical analysis of a thermally generated mesoscale wind system observed in the MacKenzie Basin, New Zealand. *Aust. Meteor. Mag.*, **55**, 19-34.
- Zawar-Reza, P., H. McGowan, A. Sturman, and M. Kossman, 2004: Numerical simulations of wind and temperature structure within an Alpine lake basin, Lake Tekapo, New Zealand. *Meteor. Atmos. Phys.*, **86**, 245-260.
- Zhong, S., and J. Fast, 2003: An evaluation of the MM5, RAMS, and Meso-Eta models at subkilometer resolution using VTMX field campaign data in the Salt Lake Valley. *Mon. Wea. Rev.*, **131**, 1301-1322.
- Zhong, S., and C. D. Whiteman, 2008: Downslope flows on a low-angle slope and their interactions with valley inversions. II. Numerical modeling. *J. Appl. Meteor. Climatol.*, **47**, 2039-2057.
- Zhong, S., C. D. Whiteman, X. Bian, W. J. Shaw, and J. M. Hubbe, 2001: Meteorological processes affecting evolution of a wintertime cold air pool in the Columbia Basin. *Mon. Wea. Rev.* **129**, 2600-2613.
- Zhong, S., X. Bian, and C. D. Whiteman, 2003: Time scale for cold-air pool breakup by turbulent erosion. *Meteor. Z.*, **12**, 229-233.
- Zhong, S., C. D. Whiteman, and X. Bian, 2004: Diurnal evolution of three-dimensional wind and temperature structure in California's Central Valley. *J. Appl. Meteor.*, **43**, 1679-1699.
- Zoumakis, N. M., and G. A. Efstathiou, 2006a: Parameterization of inversion breakup in idealized valleys. Part I: The adjustable model parameters. *J. Appl. Meteor. Climatol.*, **45**, 600-608.
- Zoumakis, N. M., and G. A. Efstathiou, 2006b: Parameterization of inversion breakup in idealized valleys. Part II: Thermodynamic model. *J. Appl. Meteor. Climatol.*, **45**, 609-623.
- Zoumakis, N. M., G. A. Efstathiou, A. G. Kelessis, J. Triandafyllis, D. Papas, M. Chasapis, M. Petrakakis, P. Karavelis, 2006: A simple scheme for daytime estimates of surface energy budget in complex terrain. *Fresenius Environmental Bulletin*, **15**, 923-927.

TABLES:

Table 1. Observations of downslope flow on slopes of different inclination.

Angle (deg)	Inversion depth (m)	Inversion strength (K)	Max speed (m s^{-1})	Height of max speed (m)	Reference
21	4-8	5	1-2	0.6-2	Horst and Doran (1986)
9	16	4	1-2	6	Papadopoulos et al. (1997)
6.5	40-50	10	1.5	25	Horst and Doran (1986)
4	50	3	3.5 - 4	40	Monti et al. (2002)
1.6	25	7	4-6	15-20	Whiteman and Zhong (2008); Haiden and Whiteman (2005)

Table 2. Extreme minimum temperatures in selected basins. Data from most U.S. locations come from the U. S. National Climatic Data Center (NCDC).

Location	Temperature minimum	Date	Reference
Peter Sink, Utah	-56.3°C (-69.3°F)	Feb 1, 1985	Pope and Brough (1996)
West Yellowstone, Montana	-54°C (-66°F)	Feb 1933	NCDC
Taylor Park, Colorado	-51°C (-60°F)	Feb 1951	NCDC
Fraser, Colorado	-47°C (-53°F)	Jan 1962	NCDC
Stanley, Idaho	-48°C (-54°F)	Dec 1983	NCDC
Gruenloch Basin, Austria	-52.6°C (-63°F)	19 Feb - 4 Mar 1932	Aigner (1952)

Figure Captions

1. Diagram of the structure of the atmosphere above a mountain ridge . Adapted from Ekhardt (1948), © Société Météorologique de France. Used with permission.
2. Typical wind and temperature profiles through a) downslope and b) upslope flows on valley sidewalls. Shown are the typical depths and strengths of the temperature deficits or excesses, the heights and flow strengths of the wind maxima, and the slope flow depths. The TKE profile in a) follows that of Skillingstad (2003). Adapted from Whiteman (2000).
3. Observed (O) and theoretical (T) a) downslope and b) upslope wind profiles. Observations are from a slope on the Nordkette near Innsbruck, Austria. The theoretical curves come from Prandtl's (1942) model. Differences above the jet maximum between theory and observations are indicated by the dotted lines. Adapted from Defant (1949), © Springer-Verlag Publishing Co., Vienna, Austria. Used with permission.
4. Monte Carlo radiative transfer model simulations of direct (left) and diffuse (right) shortwave radiation fluxes under clear sky conditions over a 4 x 4 km domain encompassing Arizona's Meteor Crater at noon, 15 October 2006. From Sebastian Hoch.
5. Modeled propagation of shadows and extraterrestrial insolation across the Meteor Crater on October 15 at different times of day (MST). Shades of gray are insolation, with black indicating 0 and white indicating 1364 W m⁻². The horizontal scale is as in Fig. 4.
6. Normalized upslope mean wind component and temperature profiles over heated slopes, with indicated slope angles from 2° to 30°, as simulated using an LES model. H , v^* and θ^* are respectively the scaling values adopted to normalize the slope-normal coordinate n , the wind component $\langle u \rangle$ and the temperature $\langle T \rangle$. Error bars indicate standard deviations. The slope of the dry adiabatic lapse rate Γ_d is given for reference. Adapted from Schumann (1990), © Quarterly Journal of the Royal Meteorological Society. Reprinted with permission.
7. Vertical profiles of a) potential temperature, b) downslope wind speed component (m s⁻¹) and c) cross-slope wind speed component (m s⁻¹) at 1857 MST 8 October 2000 from four tethersondes running down a 1.6° slope at the foot of the Oquirrh Mountains. From Whiteman and Zhong (2008), © American Meteorological Society. Reprinted with permission.
8. Idealized picture of the development of daytime up-valley winds (upper panel) and nighttime down-valley winds (lower panel) in a valley-plain system with a horizontal floor. The red and blue curves are vertical profiles of the horizontal valley wind component at a location close to the valley inlet. Two columns of air are shown – one over the valley floor and one above the plain. Red and blue sections of the columns indicate layers where potential temperature is relatively warm (W) or cold (C). The free atmosphere is assumed to be unperturbed by the daily cycle at the tops of the columns. Adapted from Whiteman (2000).
9. (a) Comparison of different vertical profiles of potential temperature in an idealised valley-plain system (sketched in the insert). The profiles are taken along the valley axis (solid line) and over the plain (bullets) along the dashed vertical lines indicated in the insert at $t = 6$ h after simulated sunrise. (b) Difference between the two profiles at various heights. The horizontal dashed line at 1000 m indicates the sidewall ridge height. (Adapted from Rampanelli et al. 2004. © American Meteorological Society. Reprinted with permission).
10. Average up- and down-valley wind profiles obtained using all daytime and nighttime data from the four Alpine valley locations indicated. Adapted from Ekhardt (1944), © E. Schweizerbart Science Publishers (www.borntraeger-cramer.de). Used with permission.
11. A well known example of confluence between valleys (Wagner, 1938): the area north of the city of Trento, where the “Ora del Garda” wind, blowing from the Valle dei Laghi (A) through an elevated saddle (★), interacts with the up-valley wind blowing in the Adige Valley from South (B) (from de Franceschi et al. 2002). © American Meteorological Society. Reprinted with permission.
12. Temperature time series for surface-based temperature sensors at different heights on the sidewall of the Gruenloch Basin, Austria. Because the coldest air settles into the bottom of the basin, the lowest elevation sensors report the lowest temperatures and the highest elevation sensors report the highest temperatures.

13. Schematic depiction of disturbances to nocturnal temperature inversions in Austria's Gruenloch Basin as revealed in temperature traces from instruments located at different heights on the sidewalls (compare Fig. 12). The different forms of disturbances in the sub-figures can be compared to the first sub-figure in which an undisturbed temperature evolution is shown and a rough indication of the time and temperature scales for this and subsequent sub-figures is given. The disturbances are produced by strong background winds, shear at the top of the inversion, and variations in cloudiness and surface energy budget. From S. Eisenbach and B. Pospichal.

14. Schematic diagram of daytime circulations and temperature profiles above and alongside an elevated circular plateau, illustrating the daytime buildup of a baroclinic zone at the edges of the plateau that leads to a break-in of cold winds onto the plateau in the evening. The dry adiabatic lapse rate Γ_d is provided as a reference.

15. Diurnal flow patterns in the Central Colorado Rocky Mountains, looking northward from southern Colorado to the elevated basins of South Park, Middle Park and North Park. a) During daytime, upslope flows from inside and outside the basins converge over the basin rims. b) During late afternoon, cold air from the surroundings breaks into the basins across the rims. From Bossert and Cotton (1994a), © American Meteorological Society. Reprinted with permission.

FIGURES

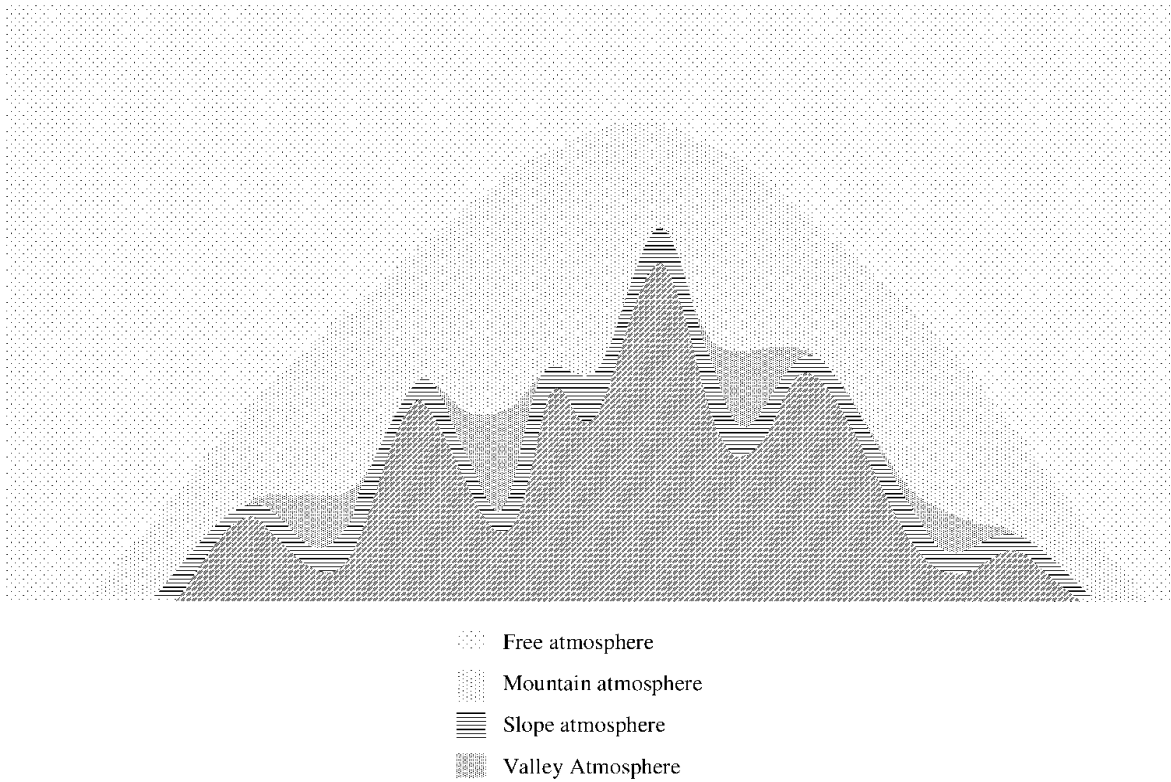


Figure 1. Diagram of the structure of the atmosphere above a mountain ridge. Adapted from Ekhart (1948). © Société Météorologique de France. Used with permission.

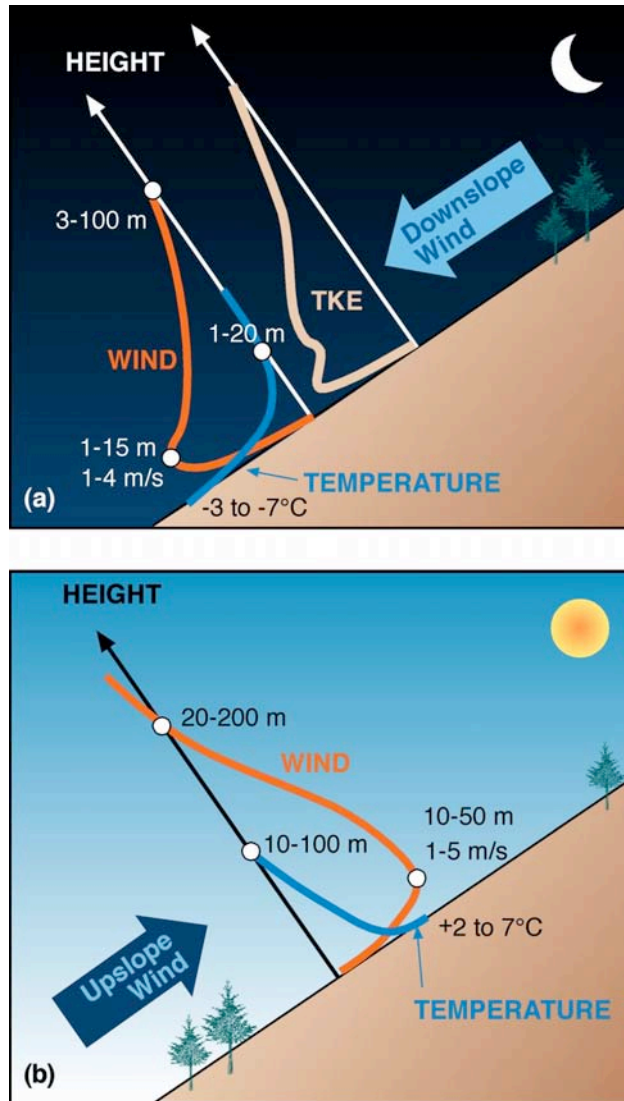
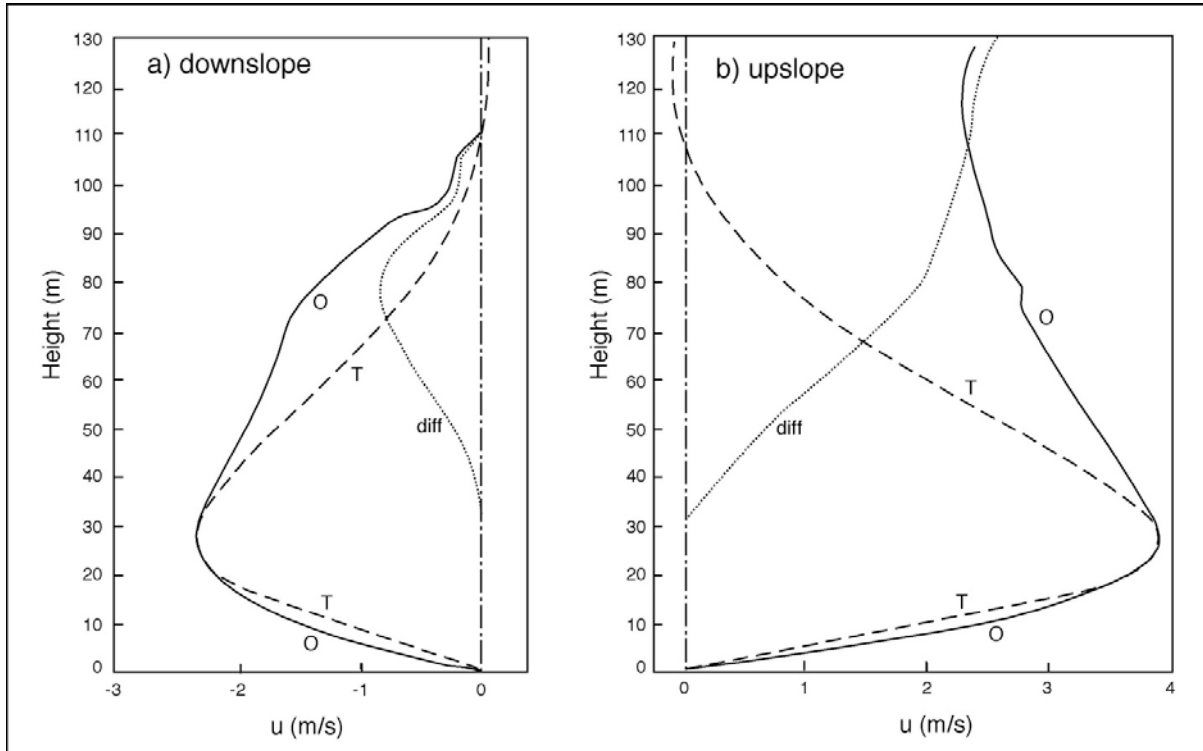


Figure 2. Typical wind and temperature profiles through a) downslope and b) upslope flows on valley sidewalls. Shown are the typical depths and strengths of the temperature deficits or excesses, the heights and flow strengths of the wind maxima, and the slope flow depths. The TKE profile in a) follows that of Skillingstad (2003). Adapted from Whiteman (2000).



3. Observed (O) and theoretical (T) a) downslope and b) upslope wind profiles. Observations are from a slope on the Nordkette near Innsbruck, Austria. The theoretical curves come from Prandtl's (1942) model. Differences above the jet maximum between theory and observations are indicated by the dotted lines. Adapted from Defant (1949), © Springer-Verlag Publishing Co., Vienna, Austria. Used with permission.

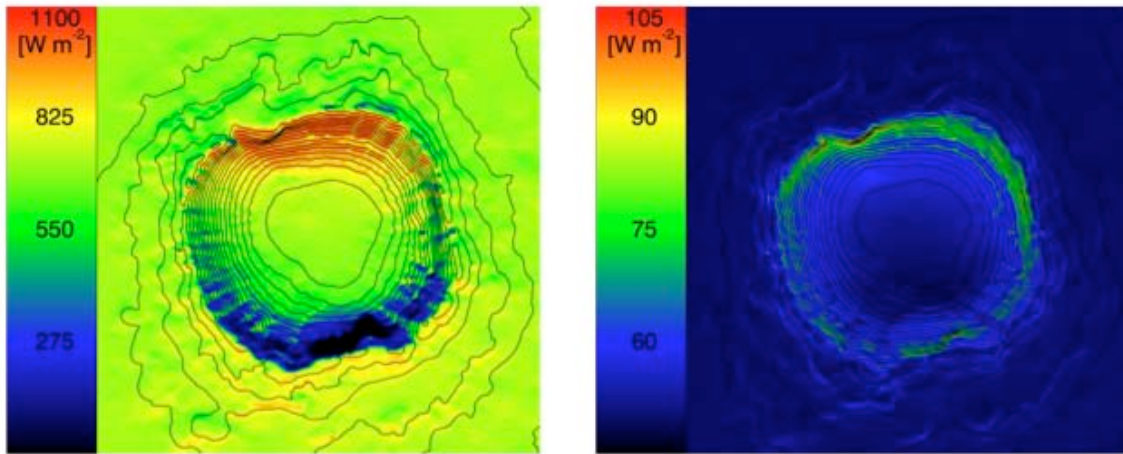


Figure 4. Monte Carlo radiative transfer model simulations of direct (left) and diffuse (right) shortwave radiation fluxes under clear sky conditions over a 4 x 4 km domain encompassing Arizona's Meteor Crater at noon, 15 October 2006. From Sebastian Hoch.

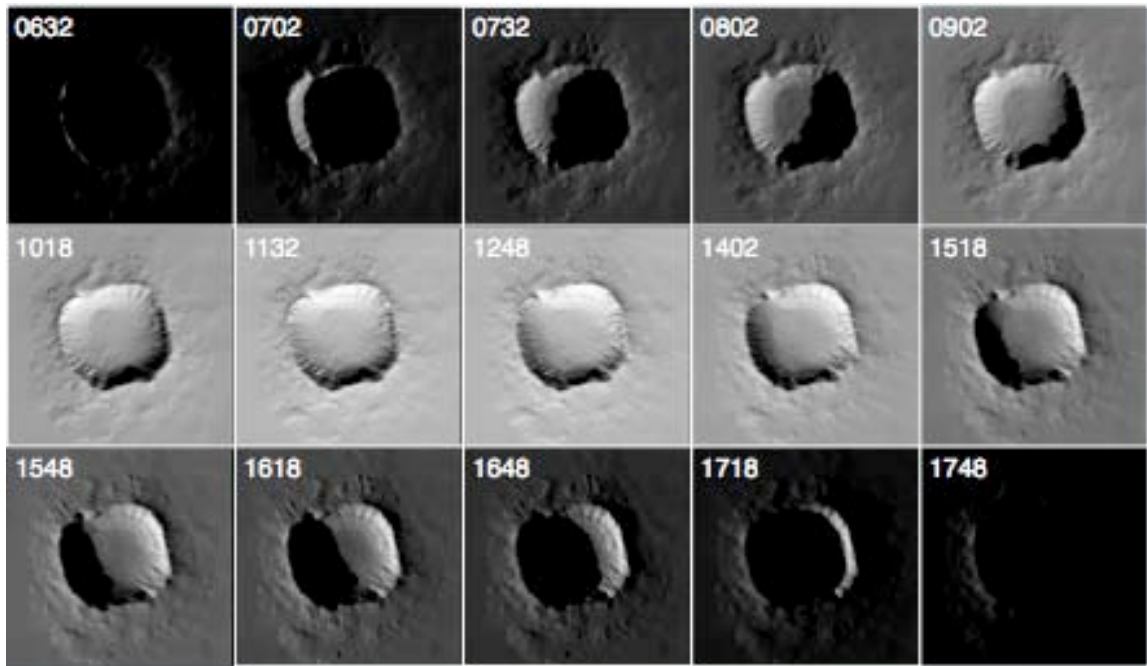


Figure 5. Modeled propagation of shadows and extraterrestrial insolation across the Meteor Crater on October 15 at different times of day (MST). Shades of gray are insolation, with black indicating 0 and white indicating 1364 W m^{-2} . The horizontal scale is as in Fig. 4.

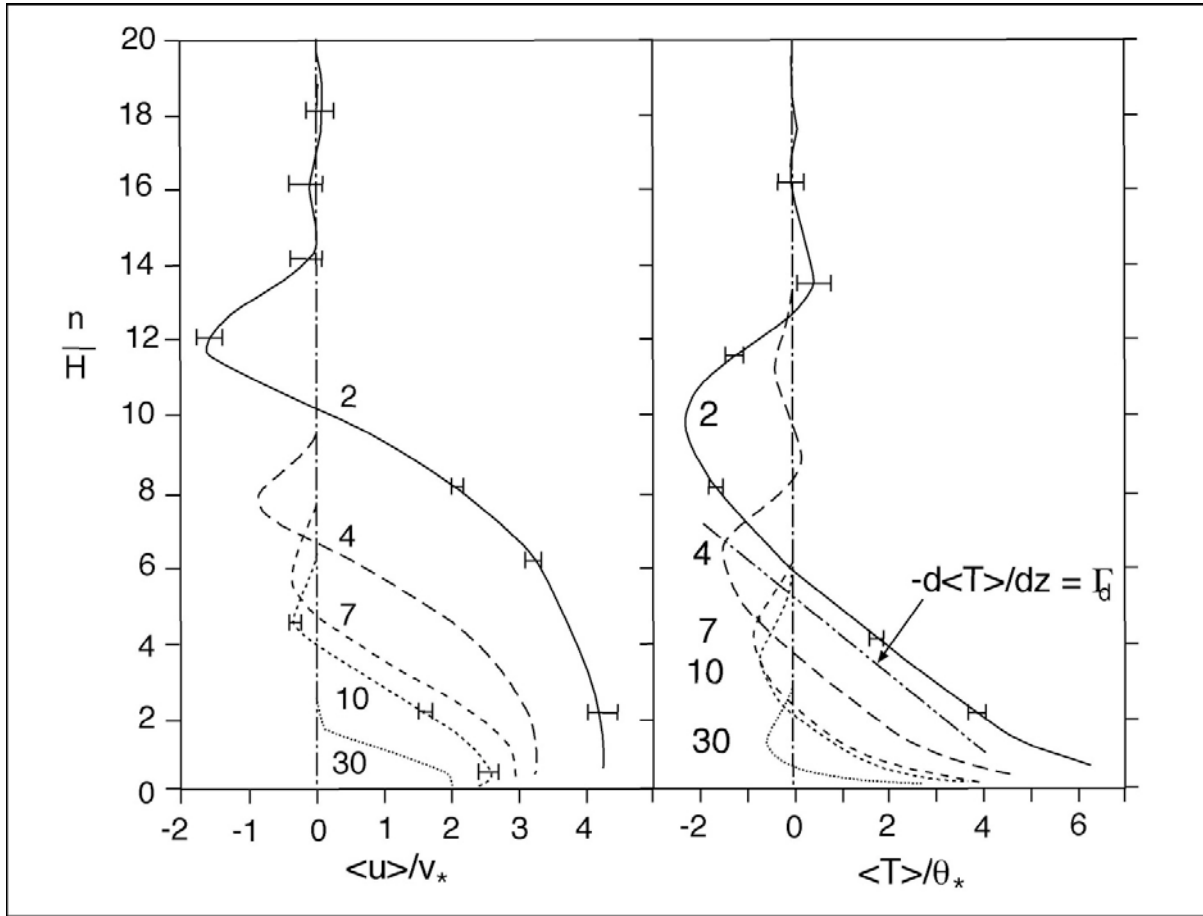


Figure 6. Normalized upslope mean wind component and temperature profiles over heated slopes, with indicated slope angles from 2° to 30°, as simulated using an LES model. H , v_* and θ_* are respectively the scaling values adopted to normalize the slope-normal coordinate n , the wind component $\langle u \rangle$ and the temperature $\langle T \rangle$. Error bars indicate standard deviations. From Schumann (1990), © Quarterly Journal of the Royal Meteorological Society. Reprinted with permission.

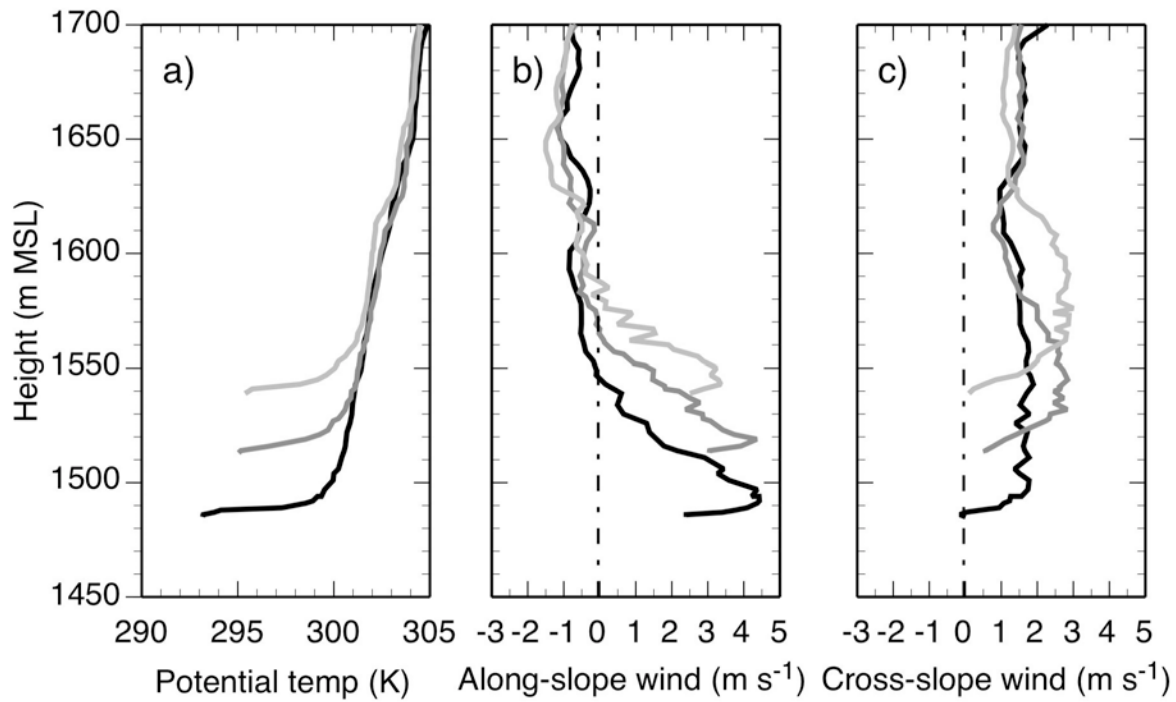


Figure 7. Vertical profiles of a) potential temperature, b) downslope wind speed component (m s^{-1}) and c) cross-slope wind speed component (m s^{-1}) at 2217 MST 8 October 2000 from four tether sondes running down a 1.6° slope at the foot of the Oquirrh Mountains at various distances from the top of the slope, namely 4200 m (light gray), 5100 m (dark gray), and 6200 m (black). From Whiteman and Zhong (2008), © American Meteorological Society. Reprinted with permission.

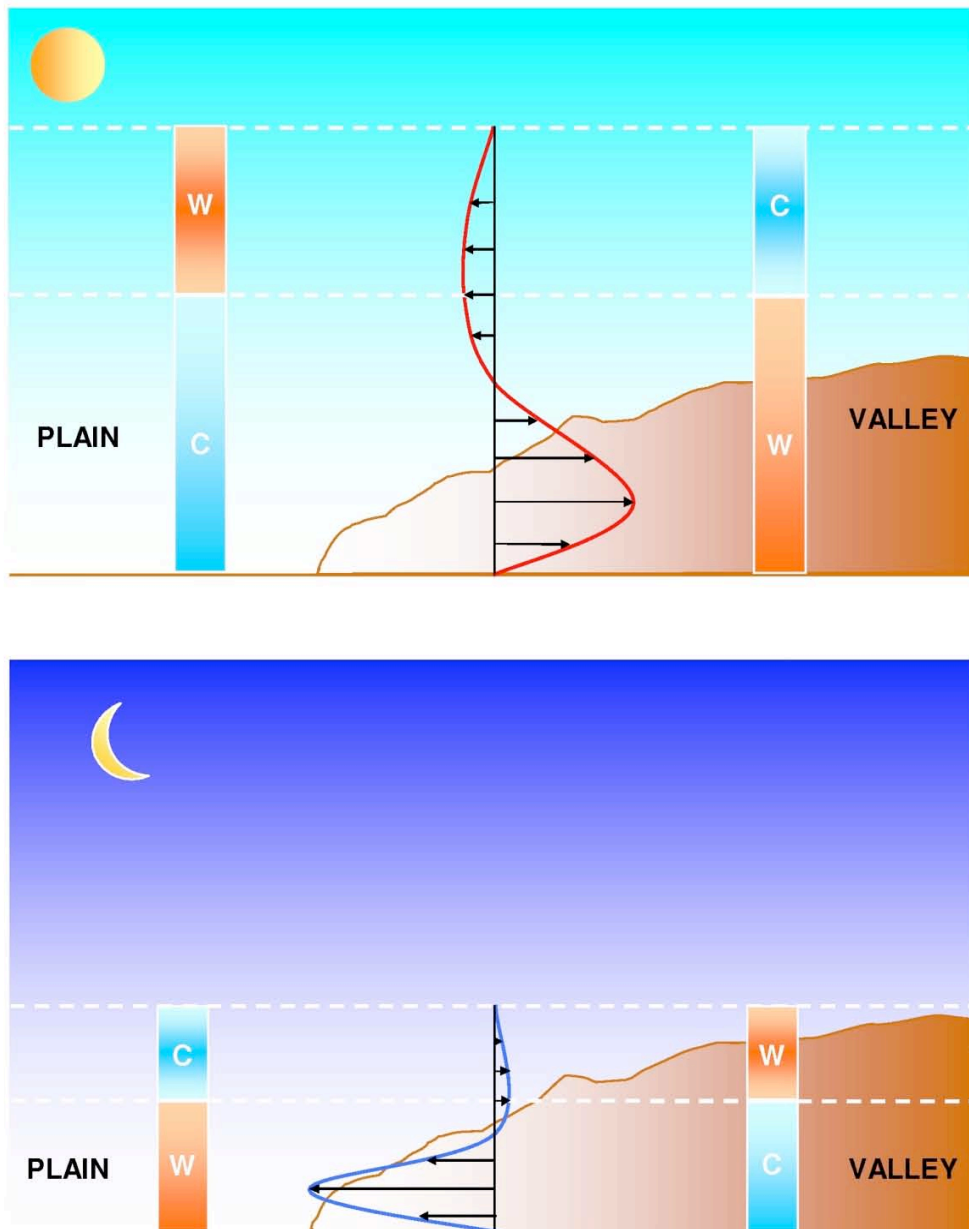


Figure 8. Idealized picture of the development of daytime up-valley winds (upper panel) and nighttime down-valley winds (lower panel) in a valley-plain system with a horizontal floor. The red and blue curves are vertical profiles of the horizontal valley wind component at a location close to the valley inlet. Two columns of air are shown – one over the valley floor and one above the plain. Red and blue sections of the columns indicate layers where potential temperature is relatively warm (W) or cold (C). The free atmosphere is assumed to be unperturbed by the daily cycle at the tops of the columns. Adapted from Whiteman (2000).

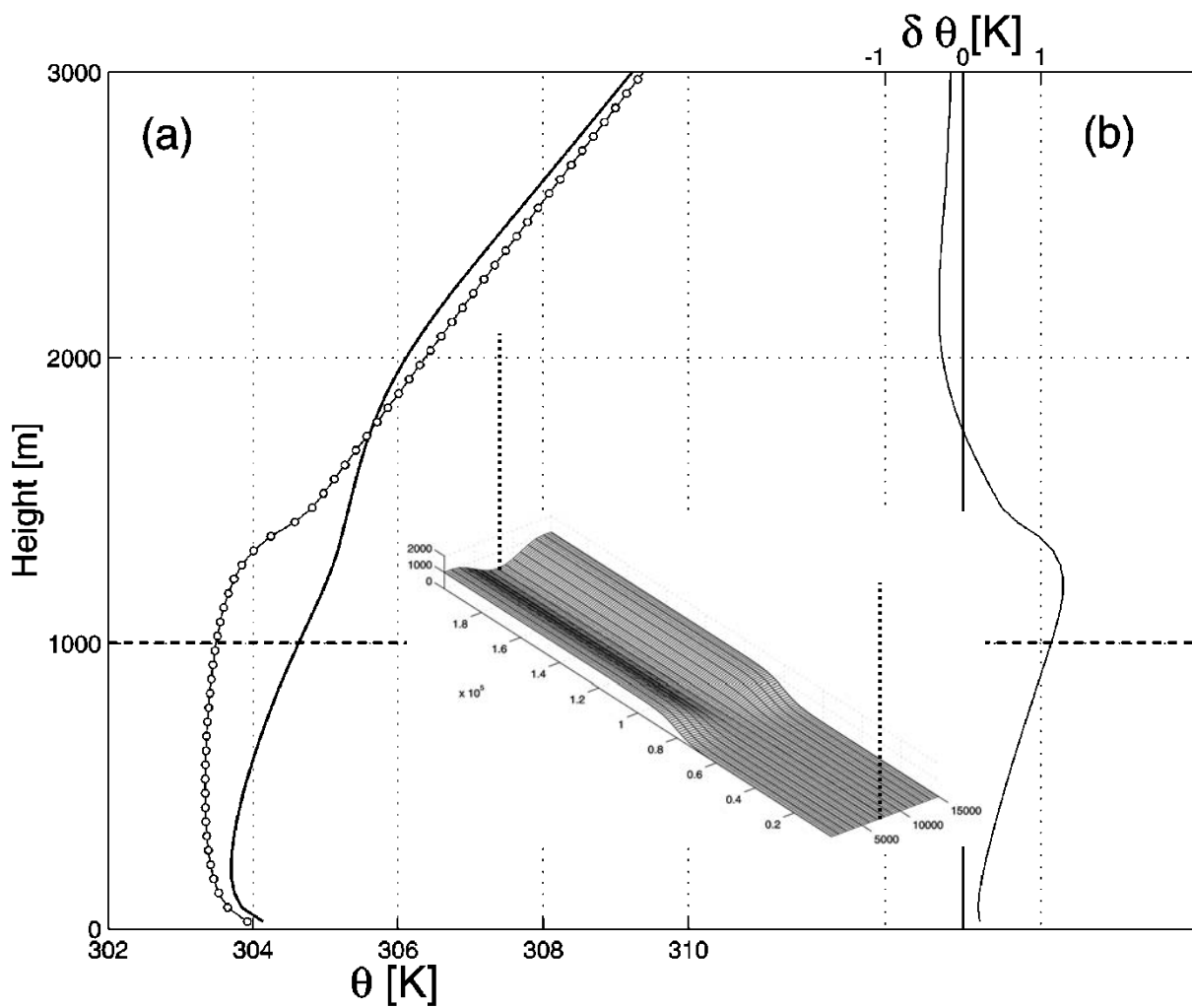


Figure 9. (a) Comparison of different vertical profiles of potential temperature in an idealized valley-plain system (sketched in the insert). The profiles are taken along the valley axis (solid line) and over the plain (line of circles) along the dashed vertical lines indicated in the insert at $t = 6$ h after simulated sunrise. (b) Difference between the two profiles at various heights. The horizontal dashed line at 1000 m indicates the sidewall ridge height. (Adapted from Rampanelli et al. 2004. © American Meteorological Society. Reprinted with permission).

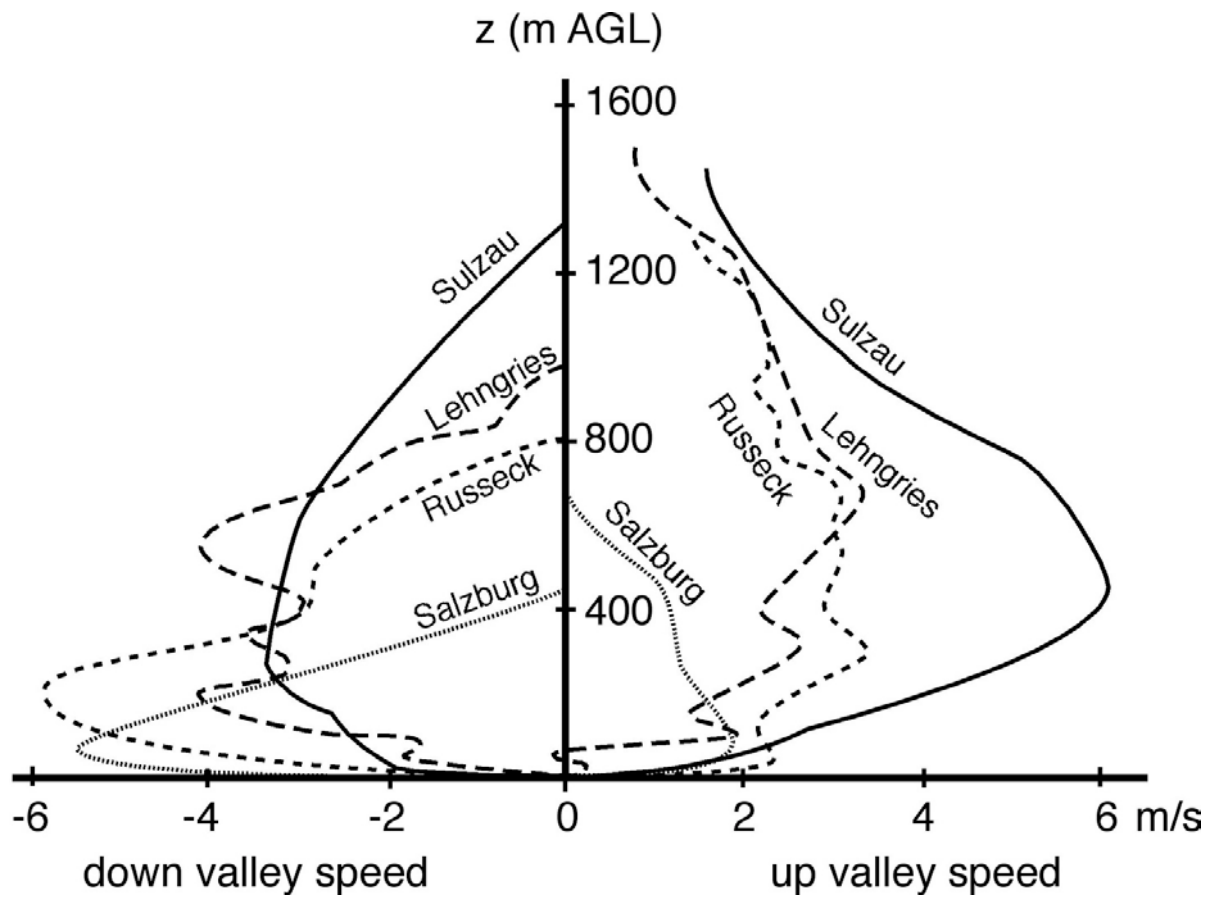


Figure 10. Average up- and down-valley wind profiles from four valleys using all daytime and nighttime data from the locations indicated (Ekhart 1944), © E. Schweizerbart Science Publishers (www.borntraeger-cramer.de). Used with permission.

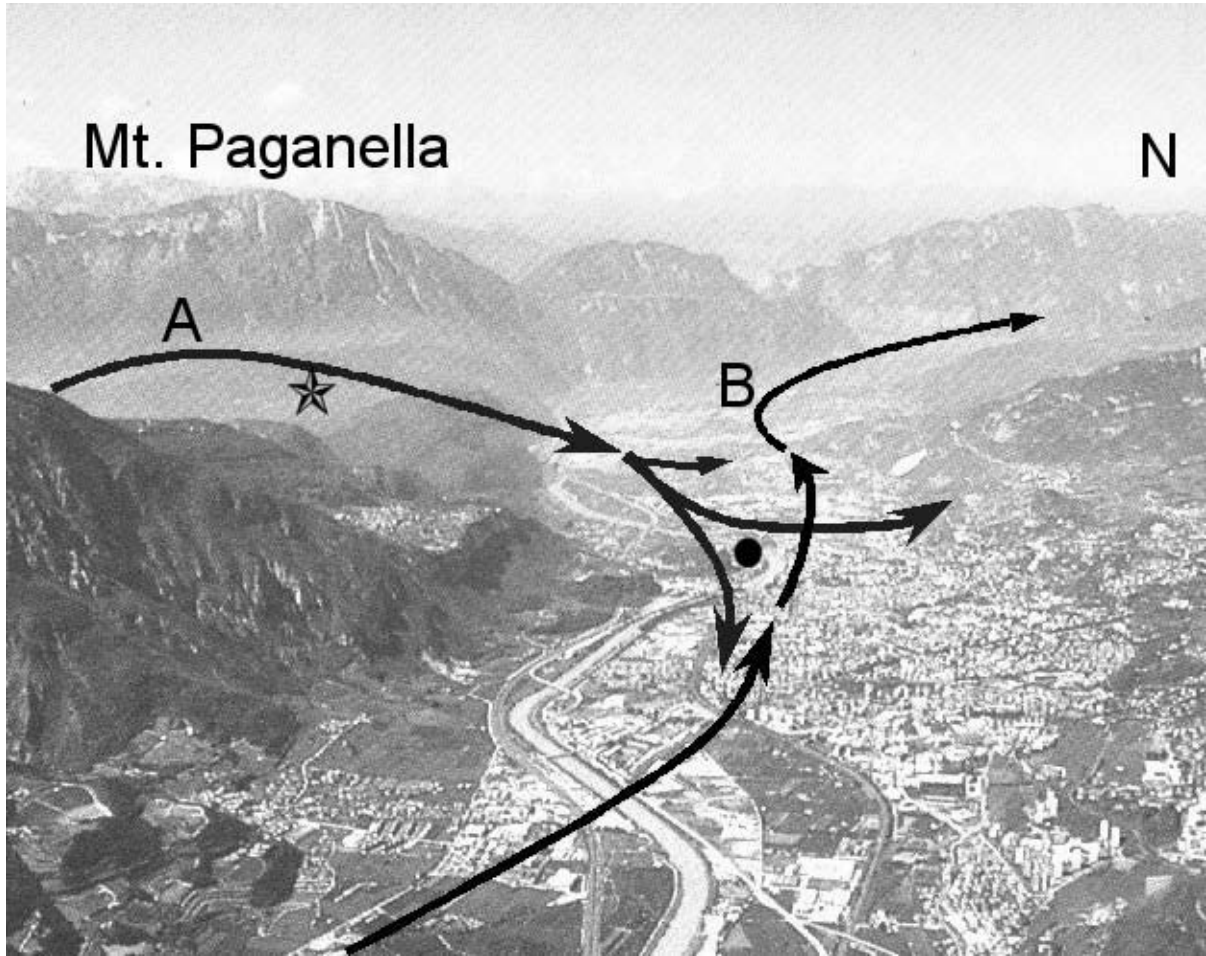


Figure 11. A well known example of confluence between valleys (Wagner, 1938): the area north of the city of Trento, where the “Ora del Garda” wind, blowing from the Valle dei Laghi (A) through an elevated saddle (★), interacts with the up-valley wind blowing in the Adige Valley from South (B) (from de Franceschi et al. 2002). © American Meteorological Society. Reprinted with permission.

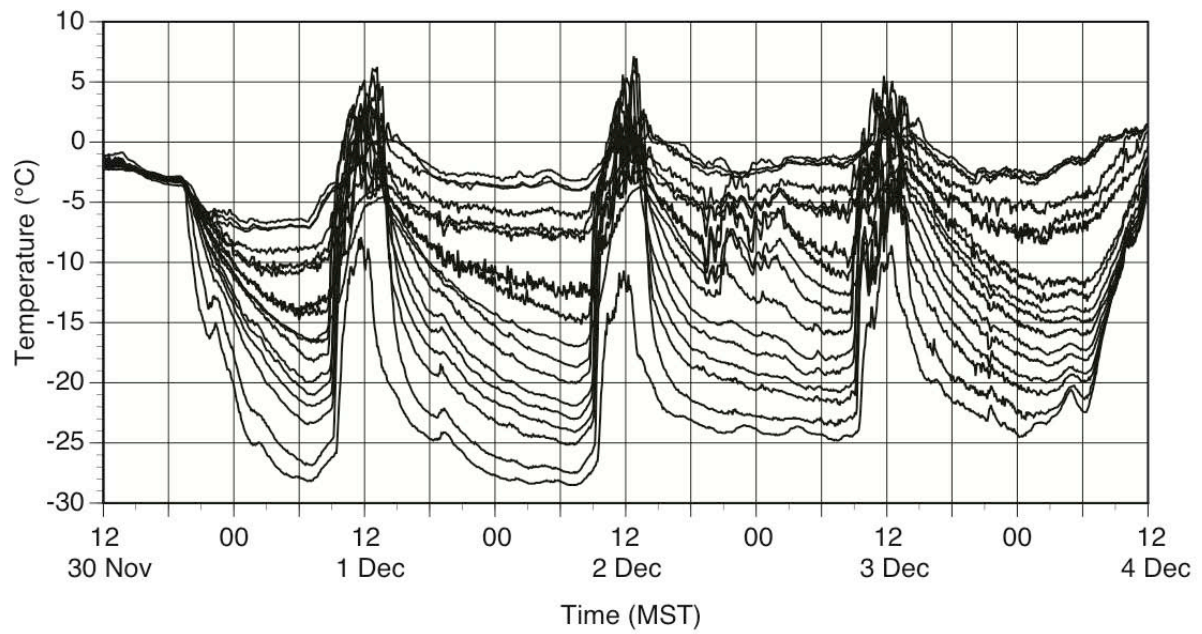


Figure 12. Temperature time series for surface-based temperature sensors at different heights on the sidewall of the Gruenloch Basin, Austria. Because the coldest air settles into the bottom of the basin, the lowest elevation sensors report the lowest temperatures and the highest elevation sensors report the highest temperatures.

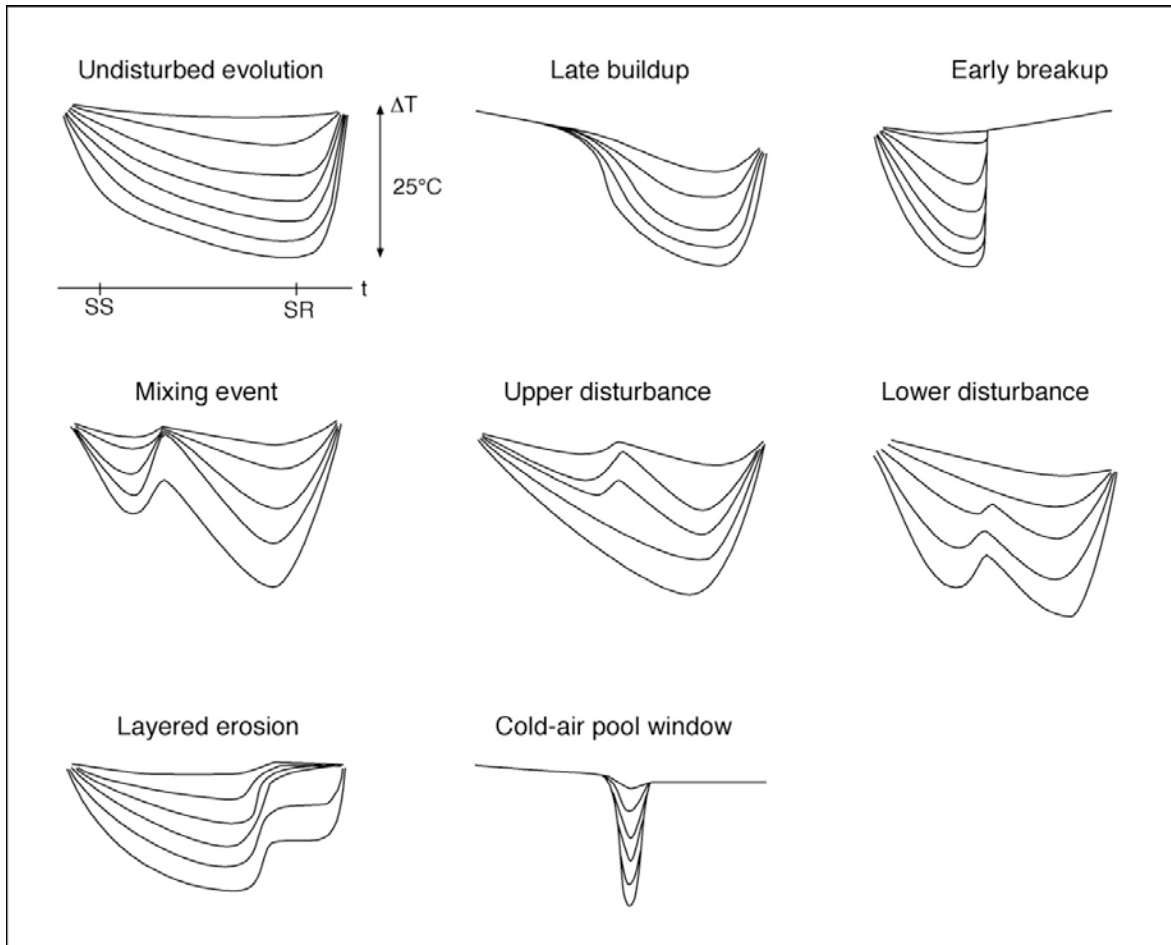


Figure 13. Schematic depiction of disturbances to nocturnal temperature inversions in Austria's Gruenloch Basin as revealed in temperature traces from instruments located at different heights on the sidewalls (compare Fig. 12). The different forms of disturbances in the sub-figures can be compared to the first sub-figure in which an undisturbed temperature evolution is shown and a rough indication of the time and temperature scales for this and subsequent sub-figures is given. The disturbances are produced by strong background winds, shear at the top of the inversion, and variations in cloudiness and surface energy budget. From Dorninger et al. (2011).

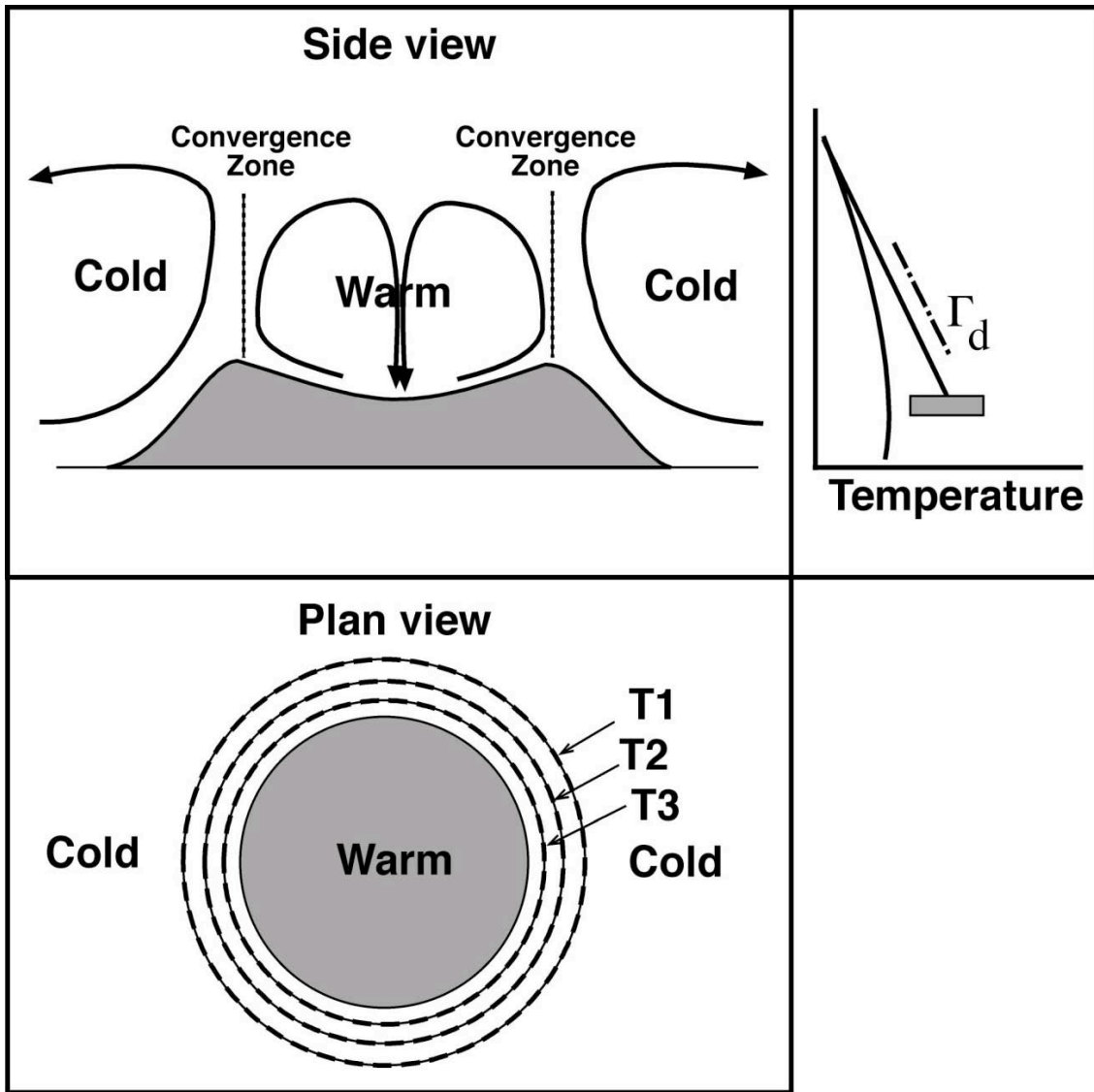
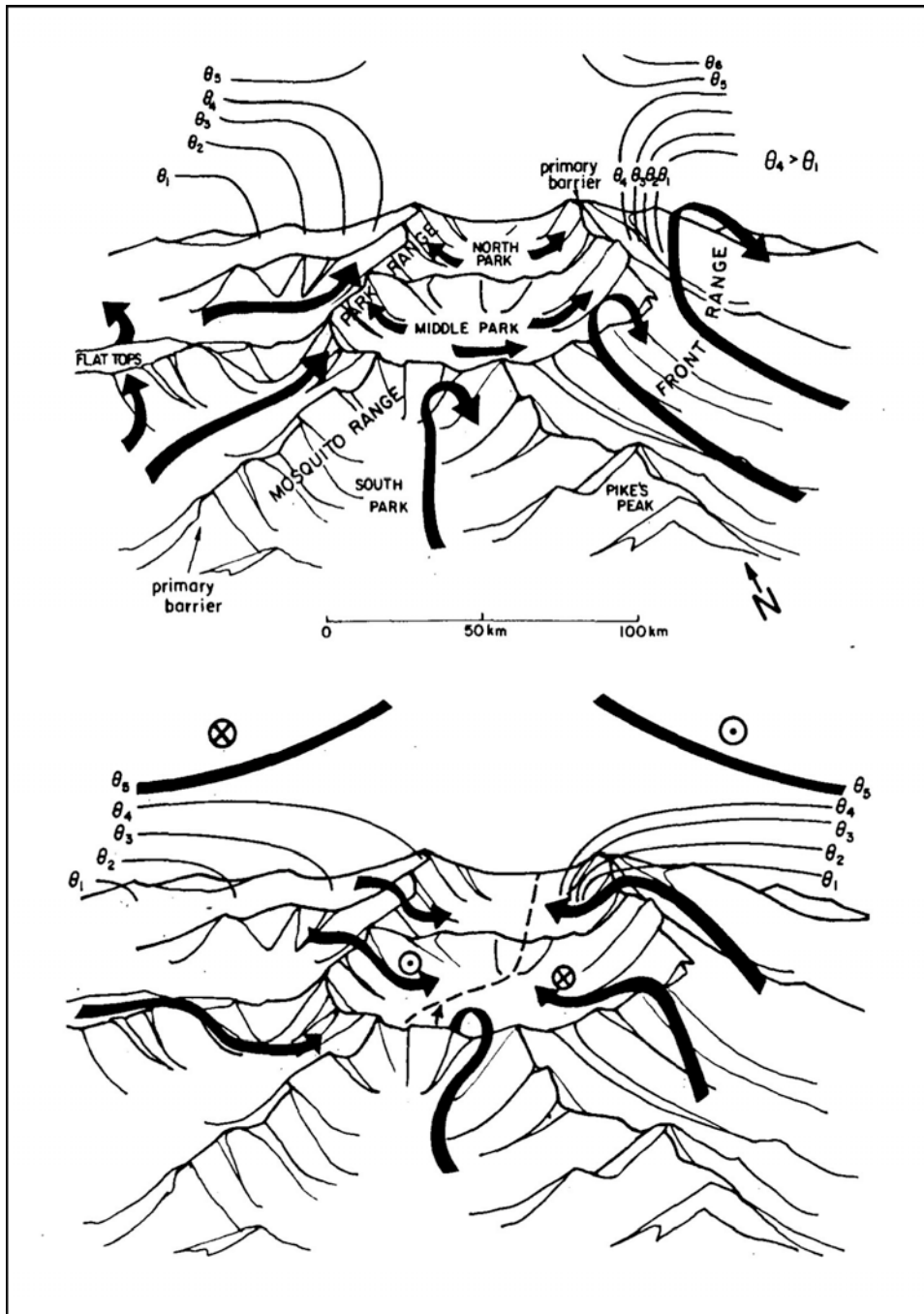


Figure 14. Schematic diagram of daytime circulations and temperature profiles above and alongside an elevated circular plateau, illustrating the daytime buildup of a baroclinic zone at the edges of the plateau that leads to a break-in of cold winds onto the plateau in the evening. The dry adiabatic lapse rate Γ_d is provided as a reference.



15. Diurnal flow patterns in the Central Colorado Rocky Mountains, looking northward from southern Colorado to the elevated basins of South Park, Middle Park and North Park. a) During daytime, upslope flows from inside and outside the basins converge over the basin rims. b) During late afternoon, cold air from the surroundings breaks into the basins across the rims. From Bossert and Cotton (1994a), © American Meteorological Society. Reprinted with permission.